VILNIUS GEDIMINAS TECHNICAL UNIVERSITY

Mantas GARNEVIČIUS

ADAPTIVE DEVELOPMENT OF A LIGHTWEIGHT COMPOSITE BEAM PROTOTYPE FOR A PEDESTRIAN BRIDGE

DOCTORAL DISSERTATION

TECHNOLOGICAL SCIENCES
CIVIL ENGINEERING (T 002)

Vilnius, 2023

The doctoral dissertation was prepared at Vilnius Gediminas Technical University in 2019–2023.

Supervisor

Dr Viktor GRIBNIAK (Vilnius Gediminas Technical University, Civil Engineering – T 002).

The Dissertation Defence Council of the Scientific Field of Civil Engineering of Vilnius Gediminas Technical University:

Chairman

Prof. Dr Darius BAČINSKAS (Vilnius Gediminas Technical University, Civil Engineering – T 002).

Members:

Assoc. Prof. Dr Tomas GEČYS (Vilnius Gediminas Technical University, Civil Engineering – T 002),
Dr Ina PUNDIENĖ (Vilnius Gediminas Technical University, Materials Engineering – T 008),
Prof. Dr Habil. Sigitas TAMULEVIČIUS (Kaunas University of Technology, Materials Engineering – T 008),
Dr. Carlos ZANUY SANCHEZ (Technical University of Madrid, Spain, Civil Engineering – T 002).

The dissertation will be defended at the public meeting of the Dissertation Defence Council of the Scientific Field of Civil Engineering in the SRA-1 Meeting Hall of Vilnius Gediminas Technical University at **10 a.m. on 15 January 2024**.

Address: Saulėtekio al. 11, LT-10223 Vilnius, Lithuania.
Tel.: +370 5 274 4956; fax +370 5 270 0112; e-mail: doktor@vilniustech.lt

A notification on the intended defence of the dissertation was sent on 14 December 2023.
A copy of the doctoral dissertation is available for review at the Vilnius Gediminas Technical University repository http://dspace.vgtu.lt and the Library of Vilnius Gediminas Technical University (Saulėtekio al. 14, LT-10223 Vilnius, Lithuania).

Vilnius Gediminas Technical University Book No 2023-051-M

doi: 10.20334/2023-051-M

mantas.garnevicius@vilniustech.lt

VILNIAUS GEDIMINO TECHNIKOS UNIVERSITETAS

Mantas GARNEVIČIUS

LENGVOS KOMPOZITINĖS PĖSČIŲJŲ TILTO SIJOS PROTOTIPO ADAPTYVUSIS KŪRIMAS

DAKTARO DISERTACIJA

TECHNOLOGIJOS MOKSLAI,
STATYBOS INŽINERIJA (T 002)

Vilnius, 2023

Disertacija rengta 2019–2023 metais Vilniaus Gedimino technikos universitete.

Vadovas

dr. Viktor GRIBNIAK (Vilniaus Gedimino technikos universitetas, statybos inžinerija – T 002).

Vilniaus Gedimino technikos universiteto statybos inžinerijos mokslo krypties disertacijos gynimo taryba:

Pirmininkas

prof. dr. Darius BAČINSKAS (Vilniaus Gedimino technikos universitetas, statybos inžinerija – T 002).

Nariai:

doc. dr. Tomas GEČYS (Vilniaus Gedimino technikos universitetas, statybos inžinerija – T 002),
dr. Ina PUNDIENĖ (Vilniaus Gedimino technikos universitetas, medžiagų inžinerija – T 008),
prof. habil. dr. Sigitas TAMULEVIČIUS (Kauno technologijos universitetas, medžiagų inžinerija – T 008),
dr. Carlos ZANUY SANCHEZ (Madrido technikos universitetas, Ispanija, statybos inžinerija – T 002).

Disertacija bus ginama viešame statybos inžinerijos mokslo krypties disertacijos gynimo tarybos posėdyje **2024 m. sausio 15 d. 10 val.** Vilniaus Gedimino technikos universiteto SRA-I Posėdžių salėje.

Adresas: Saulėtekio al. 11, LT-10223 Vilnius, Lietuva.
Tel. (8 5) 274 4956; faksas (8 5) 270 0112; el. paštas doktor@vilniustech.lt

Pranešimai apie numatomą ginti disertaciją išsiųsti 2023 m. gruodžio 14 d.

Disertaciją galima peržiūrėti Vilniaus Gedimino technikos universiteto talpykloje http://dspace.vgtu.lt ir Vilniaus Gedimino technikos universiteto bibliotekoje (Saulėtekio al. 14, LT-10223 Vilnius, Lietuva).

Abstract

The replacement of steel elements, solving the corrosion problem, describes the primary trend in the structural application of fibre-reinforced polymers (FRP). However, the relatively low modulus of elasticity of typical FRP materials raises the structural components' deformations. A possible solution to these problems is combining FRP composites with concrete elements. However, this fundamental improvement requires new design methodologies. Thus, this work introduces the adaptive design concept when the finite element (FE) modelling outcome defines the target reference of the design procedure. The iterative modification of the design solution, numerically identifying the disagreements between the experimentally verified model and physical test outcomes, stimulates the successive approach of the physical prototype to the reference numerical solution. Ultimately, this adaptive design concept diminishes the number of physical trials as correcting the FE model parameters helps identify the weakness of the physical prototype (without additional laboratory trials). Exemplifying the proposed adaptive design idea, this work employs a hybrid beam, which combines a polymeric fibre-reinforced concrete (PFRC) slab, a pultruded glass fibre-reinforced polymer (GFRP) profile, and a pultruded carbon fibre-reinforced polymer strip. The considered structural element utilises an efficient structural solution, which ensures the synergetic PFRC and pultruded GFRP profile effect by fixing the profile at the supports. This innovative structural solution contradicts the traditional concept of local bond improvement, e.g., employing GFRP profile perforation and mechanical anchorage systems. Furthermore, the proposed solution simplified the corresponding finite element model, ensuring the perfect bond assumption between the components. The physical tests proved the viability of the developed composite structure: the enhancement of the supports doubled the hybrid beam's flexural stiffness and load-bearing capacity regarding the reference bridge with weak supports.

The dissertation includes an introduction, three chapters, general conclusions, and a list of references. The First Chapter reviews the literature on the FRP manufacturing process, existing materials, physical characteristics, and structural design principles. The Second Chapter presents the adaptive design concept, considering the hybrid beam system's design example. The Third Chapter describes the experimental studies, verifying the proposed adaptive design concept. The author's list of publications on the topic of the dissertation consists of four journal articles (three with an Impact Factor from *Clarivate Analytics Web of Science*) and three conference presentations.

Reziumė

Pluoštu armuoti polimerai (FRP) vis plačiau naudojami statybos inžinerijoje. Dažniausiai jais keičiami plieniniai elementai, taip sprendžiant korozijos problemą, tačiau dėl mažo daugumos FRP medžiagų tamprumo modulio padidėja šių konstrukcinių elementų deformacijos. Galimas šios problemos sprendimas – sujungti FRP kompozitus su betoniniais elementais, tačiau šis sprendimas reikalauja naujų projektavimo būdų. Šiame darbe pateikiama adaptyvaus prototipavimo koncepcija, kai atsižvelgiant į eksperimentais patvirtinto baigtinių elementų (BE) modeliavimo rezultatą apibrėžiamas kompozitinio elemento komponavimo tikslas (kai neegzistuoja standartinis sprendimas). Iteracinis konstrukcinio elemento modifikavimas, atsižvelgiant į BE modelio ir fizinių bandymų rezultatų neatitikimus, leidžia fizinį prototipą laipsniškai priartinti prie etaloninio skaitinio modeliavimo rezultato, t. y. projektinio tikslo. Ši adaptyvaus prototipavimo koncepcija sumažina fizinių bandymų skaičių – BE modelio parametrų koregavimas padeda nustatyti fizinio prototipo trūkumus (be papildomų laboratorinių bandymų). Iliustruojant pasiūlytą adaptyvaus prototipavimo idėją, sukurta hibridinė sija, kuri sudaryta iš polimeriniu pluoštu armuoto betono (PFRC) pakloto plokštės, stiklo pluoštu armuoto polimero (GFRP) profiliuočio ir anglies pluoštu armuoto polimero juostos. Nagrinėjamai kompozitinei sijai suvienodintos betoninės plokštės ir GFRP profiliuočio deformacijos, fiksuojant FRP komponentes atramose. Šis inovatyvus konstrukcinis sprendimas prieštarauja tradicinei kompozitinių elementų komponavimo metodikai, kai perforacija ar mechaninės tvirtinimo priemonės užtikrino vietinį kompozito komponenčių sukibimą. Šis sprendimas taip pat supaprastino BE modelį užtikrinant komponenčių idealaus sukibimo modelio galiojimo sąlygą. Fiziniais bandymais įrodytas sukurtos kompozitinės konstrukcijos (t. y. adaptyvios prototipavimo koncepcijos) efektyvumas – atramų konstrukcijų modifikavimas be papildomo profiliuočio sukibimo gerinimo padvigubino kompozitinės sijos lenkiamąjį standį ir laikomąją galią, lyginant su analogu, turinčiu silpnas atramas.

Disertaciją sudaro įvadas, trys skyriai, išvados ir literatūros sąrašas. Pirmame skyriuje apžvelgiama literatūra apie FRP gamybą, medžiagų rūšis, jų savybes ir kompozitinių konstrukcijų projektavimo principus. Antrame skyriuje pristatoma adaptyvaus prototipavimo koncepcija bei etaloninio BE modelio kūrimas. Trečiame skyriuje pateikiami eksperimentiniai tyrimai, kuriais patikrinama pasiūlyta prototipavimo koncepcija. Autoriaus publikacijų disertacijos tema sąrašą sudaro keturi straipsniai (trys iš jų žurnaluose su *Clarivate Analytics Web of Science* cituojamumo rodikliu) ir 3 pranešimai konferencijose.

Notations

Abbreviations

BFRP – basalt fibre-reinforced polymer (liet. *basalto plaušu armuotas polimeras*);
CFRP – carbon fibre-reinforced polymer (liet. *anglies pluoštu armuotas polimeras*);
DIC – digital image correlation (liet. *skaitmeninio vaizdo koreliacija*);
FRP – fibre-reinforced polymer (liet. *plaušu armuotas polimeras*);
FE – finite element (liet. *baigtinis elementas*);
GFRP – glass fibre-reinforced polymer (liet. *stiklo pluoštu armuotas polimeras*);
LVDT – linear variable displacement transducer (liet. *kintamo poslinkio daviklis*);
PFRC – polymeric fibre-reinforced concrete (liet. *polimeriniu plaušu armuotas betona*s);
RC – reinforced concrete (liet. *gelžbetonis*).

Contents

Introduction

Problem formulation

Notwithstanding the modern industry's ability to produce composite materials with a wide range of mechanical properties applicable in medicine, aviation, etc, conservative design principles are predominant in the building industry. Innovative building technologies require new design concepts for developing materials with mechanical properties tailored for construction purposes. They oppose the current practice when standardised solutions are associated with applying existing materials with physical characteristics that imperfectly suit the structural requirements, leading to an inefficient increase in amounts of material for safety's sake.

Fibre-reinforced polymer (FRP) materials tend to replace steel in bridges and buildings, solving the corrosion problem. However, anisotropy of the mechanical performance of FRP complicates the connection problem; long-term effects, e.g., creep rupture, substantially reduce the material resistance. In addition, the relatively low deformation modulus of typical FRP materials raises the deformations of the structural components. Developing hybrid structures comprising compression-resistant concrete and high-performance in tension FRP profiles is essential. Although such hybrid systems are applicable for bridge engineering, the uncertainty of the inter-component bonding properties complicates further development of these innovative structures and design approaches. The typical solution focuses on local bond improvement. On the contrary, this research introduces an alternative solution, which combines the polymeric fibre-reinforced concrete slab and pultruded FRP profile fixed on the supports.

Relevance of the dissertation

This dissertation presents a novel design concept of the hybrid beam system comprising the polymeric fibre-reinforced concrete slab and pultruded FRP profile fixed on the supports. Connecting the FRP components to the supports solves the intercomponent bonding issue and simplifies the numerical model. The dissertation exemplifies the design of hybrid systems when the finite element (FE) modelling outcome defines the reference for the design procedure Agreement between the mechanical test results and predicted capacity reveals the adequacy of the physical prototype. Considering advanced composite materials, the modelling outcome determines the desired mechanical performance when the design guidelines are absent. The iterative modification of the design solution, numerically identifying the disagreements between the experimentally verified model and physical test outcomes (that diminishes the number of physical trials), stimulates the convergence of the prototype solution to the reference numerical outcome.

The proposed structural solution contradicts the traditional idea of local bond improvement. This dissertation demonstrates that the solution to the support problem (resulting from a low resistance of pultruded FRP profiles to transverse loads) improves the structural performance of the bridge prototype, doubling the structure's flexural stiffness and load-bearing capacity regarding the weak concrete supports' system.

Research object

The research object is the mechanical characteristics of a hybrid bridge prototype comprising the synthetic fibre-reinforced concrete slab and pultruded FRP profile fixed on the supports under a short-term mechanical load.

Aim of the dissertation

This dissertation aims to develop an adaptive design concept by creating an experimentally verified FE model of a hybrid beam as a reference solution for evaluating the prototyping efficiency when a standard solution does not exist. The design solution is altered to reach the reference numerical response if necessary.

Tasks of the dissertation

The following objectives helped to achieve the aim of the research:

1. To connect the beam components on the supports and ensure the composite action between the hybrid beam parts (i.e., concrete and FRP).
2. To develop the FE model using experimentally verified material laws and modelling concepts.
3. To develop a systematic design approach when the experimentally verified FE model describes the prototyping criteria and required parameters of the designed object, e.g., the load-bearing capacity and stiffness (which has no reference in the existing design codes).
4. To illustrate the adaptive design concept by developing a hybrid composite beam prototype.

Research methodology

The following *research methods* are chosen to investigate the *object*:

1. The theoretical analysis of the literature identifies efficient combination principles of hybrid structural elements.
2. The research objectives are clarified by summarising the FRP literature research's strengths, weaknesses, and gaps.
3. The literature research, numerical modelling, and physical experiments describe the solution to applying advanced structural materials and simplifying the theoretical model.
4. Physical tests of several hybrid beams verify the dissertation hypothesis and improve the design concept.
5. A comparative analysis of the literature results, numerical modelling, and physical tests ensure the formulation of conclusions.

The scientific novelty of the dissertation

The proposed design concept ensures a systematic relationship between materials engineering, structural engineering, and numerical methods. The possibility of considering an experimentally verified numerical model as a design reference provides an adaptive improvement of the prototype solution. Materials and design solutions are altered to reach the composite system's required (expected from numerical simulations) physical characteristics.

Practical value of the research findings

The proposed adaptive design concept includes the experimentally verified finite element model, which can be applied to different structural cases.

The proposed design methodology helps to develop FRP composites efficiently when the corresponding standard methods do not exist. The possibility of modifying the solution (regarding the reliable numerical model predictions) reduces the physical testing needs.

Fixing the FRP beam components at the supports ensures substantial simplification of the theoretical concept of the developed hybrid beam, which employs the perfect bond assumption between the composite components.

Defended statements

1. When an experimentally verified numerical model describes the design target, the proposed adaptive design concept demonstrates the practical example of enhancing the hybrid beam's flexural stiffness and load-bearing capacity by modifying the design solution.
2. The numerical identification of the disagreements between the experimentally verified model and physical test outcomes diminishes the number of physical trials as numerical modelling partially replaces the physical tests. After a reliable FE model is created, physical tests become unnecessary.
3. The experimentally verified FE model is an adequate reference for the proposed *adaptive* design of structural systems comprising advanced composite materials when the standard solution does not exist.
4. The hybrid beam in this research utilises an innovative design solution, fixing GFRP profiles at the supports, ensuring the bond between its components and, thus, the composite behaviour.

Approval of the research findings

Four articles were published on this research topic, three in scientific journals indexed in the *Clarivate Analytics Web of Science* databases with an Impact Factor. The author has made three presentations at three scientific conferences:

1. The First Olympiad in Engineering Science, 2023. Olympia, Greece. The presentation Gribniak, V., & Garnevičius, M. Developing an adaptive design concept for structural composites received the "Olympiad Medal"

Award (https://www.uis.no/en/about-uis/olympiad-in-engineering-science-summed-up).
2. The 13th *fib* International PhD Symposium in Civil Engineering, 2020. Paris, France (the Best Paper Award).
3. The 26th Annual International Conference on Composites/Nano Engineering, (ICCE-26), 2018. Paris, France.

Structure of the dissertation

The dissertation comprises three main chapters and an introduction. The introduction describes the research object, problem, relevance, aim, and methodology. It also formulates the research novelty and defended statements.

The First Chapter reviews the literature on FRP manufacturing, materials, physical characteristics, and structural design principles. An emphasis is put on the test procedures developed for these elements and corresponding modelling principles. The literature review revealed the efficient combination of composite materials of the hybrid beam prototype in this dissertation. The First Chapter concludes by formulating the main objective and tasks of the present investigation.

The Second Chapter presents an adaptive design concept when an experimentally verified FE model describes the design target. A nonlinear FE model of the hybrid concrete-FRP beam was created using the commercial software ATENA. The perfect connection between the components of the hybrid beam is assumed to simplify the model. The test results verified the reference model.

The Third Chapter describes the test results, verifying the adaptive design concept and four-point bending tests of the developed hybrid beam prototype. The disagreement between the experiment and modelling results raises the hypothesis of the insufficient capacity of the beam's support zones. The agreement results of the modified prototype proved the adaptive design concept.

General conclusions summarise the present dissertation, followed by a list of the literature references and publications by the author on the dissertation topic. The dissertation also features a reference list of the author's related publications. The dissertation comprises 113 pages, 65 figures, 8 tables and 83 references..

Acknowledgements

The author acknowledges the financial support from the European Regional Development Fund (Project No 01.2.2-LMT-K-718-03-0010) under a grant agreement with the Research Council of Lithuania.
The author also thanks VILNIUS TECH for the Junior Researcher position.

1

Fibre-Reinforced Polymer Composites in Construction

This chapter analyses fibre-reinforced polymer (FRP) materials and manufacturing techniques. It focuses on new construction opportunities and determines the advanced materials and those combinations to create an efficient hybrid beam structural prototype. The literature review describes test and simulation methods, design standards, and calculation principles of FRP-composing structures. The main research results of this chapter are published in the author's publications (Garnevičius & Gribniak, 2022; Garnevičius, Plioplys, Ng, Chu & Gribniak, 2020; Garnevičius, Plioplys, & Gribniak 2021a, 2021b; Gribniak et al., 2021; Sokolov et al., 2018).

1.1. Composite structures with fibre-reinforced polymer components

The materials engineering trends proposed developing efficient structural solutions (Gribniak, Sultani, Rimkus, Sokolov & Torres, 2021; Hou, Wang & Shi, 2022). As a result, there is a tendency to create new structural materials to change traditionally used concrete and steel (Gribniak, 2020). Many fibre-reinforced polymers have been developed, and different manufacturing methods have been invented (Kim, 2018; Potyrala, 2011). These materials have distinct mechanical properties (tensile strength, modulus of elasticity, etc.), resistances, and weaknesses (Liu, Liu & Feng 2020), and each of them need to be investigated to develop a reliable design methodology. All these different materials are easily mouldable and can take different geometric shapes. For this reason, the elements formed can be used in various ways, including the construction of bridges (Ghafoori et al., 2019; Siwowski, Piatek, Siwowska & Wiater, 2020; Siwowski, Rajchel & Kulpa, 2019). FRP composites are new materials made up of two or more different materials, using a polymer resin (matrix) and fibres (reinforcement) arranged in the element profile, thus creating a new material and an element analogous to reinforced concrete. New materials and new ways of producing FRP profiles are developed. These profiles can be combined with a wide range of other materials. Alternatives to traditional reinforced concrete and metal bridges are sought.

Nowadays, FRP composites are increasingly used in buildings and bridges: bridge beams, concrete and steel are strengthened with carbon fibre strips (Ghafoori et al., 2019; Issa & Kmeid, 2005; Keller, 2018; Siwowski et al., 2020; Thorhallsson, Hinriksson & Snæbjörnsson, 2017). Columns can also be retrofitted with FRP reinforcement (Modak, Sivasankar, Southararajan, Gunaselvi, 2020). Glass fibre-reinforced (GFRP) profiles replace metal beams of composite bridges (Koaik, Bel & Jurkiewiez, 2017; Mendes et al., 2011).

FRP can completely replace various bridge elements: bridge decks can be made from GFRP, replacing timber, steel, and concrete slabs (Keller, 2018; Lee, Hong & Park, 2010). Bridge deck steel reinforcement can be replaced with FRP grids, avoiding corrosion (Brunton, Bank & Oliva, 2016). FRP decks are easily assembled and disassembled, requiring no adhesive bonding or welding in poor conditions (Ali et al., 2020; Lee et al., 2010). FRP cables can also replace metal cables of cable-stayed bridges, reducing maintenance costs (Liu, Gu, Liu & Tafsirojjaman, 2022; Yang, Wang & Wu, 2020). Hybrid structures are also created by combining different materials with FRP: wood (Thorhallsson et al., 2017), steel (Ghafooriet et al., 2019), and concrete (Koaik et al., 2017; Muc, Stawiarski & Chwal, 2020; Siwowski, Kulpa, Rajchel & Poneta, 2018; Zou, Lin, Feng, Bao & Wang, 2020).

Steel corrosion is a problem for bridges worldwide because of design errors or inadequate maintenance. It affects structural performance and reduces the service life of bridges. Annually, maintenance, rehabilitation, and replacement of corrosion-damaged elements require tremendous investments (Ali et al., 2020; Zou et al., 2020). Especially vulnerable are reinforced and prestressed concrete bridges. Their deterioration was accelerated by the use of deicing salts (Hollaway

& Head, 2000). On top of that, the increasing cost of maintenance work, heavy use, and a more frequent need for infrastructure renewal in aggressive environments have forced engineers to look for more durable bridge materials (Bakis et al., 2002). That is why fibre-reinforced polymers were researched and applied in bridge structures. They are durable and resistant to corrosion and marine and industrial environments (Ali et al., 2020; Hollaway & Head, 2000).

The literature focuses on researching FRP elements combined with concrete. This synergetic combination gives the additional composite value regarding the sum of the contribution of the separate counterparts. For instance, pultruded components often face transverse loads regarding the pultrusion pathway; moreover, the pultruded details must resist bolt removal-induced local stresses (Naito, 2022; Preinstorfer, Huber, Reichenbach, Lees & Kromoser, 2022). Therefore, the smooth unidirectional roving and mats protect the longitudinal filaments, complicating the internal reinforcement structure of the FRP material (Correia, 2013). At the same time, this additional protection can be insufficient for developing FRP structures (Malakhov, Polilov, Li & Tian, 2021; Mosallam, 2011; Zhu, Zhu & Gribniak, 2022). In addition, the relatively low deformation modulus of typical FRP materials raises the deformations of the structural components. Together with the self-weight reduction increasing the kinematic displacements (Kim, 2018), the latter issue necessitates developing hybrid structures comprising compression-resistant concrete and high-performance in tension FRP profiles. Although hybrid composite systems are applicable for bridge engineering (Ali et al., 2020; Juozapaitis, Sandovič, Jakubovskis & Gribniak, 2021; Kim, 2018), the uncertainty of the intercomponent bonding properties complicates the development of these innovative structures. The typical solution focuses on local bond improvement, employing FRP profile perforation and mechanical anchorage systems, e.g., Mendes et al. (2011) and Zhang et al. (2021).

After thoroughly investigating available articles, it was decided to adapt the idea of a stress-ribbon structural system (Gribniak, Arnautov & Rimkus, 2021; Juozapaitis et al., 2021) in this dissertation to develop an efficient hybrid beam structure. A PFRC slab and FRP beam will be combined. The FRP beam will transfer the stresses to massive foundations, while the PFRC slab will be a lightweight deck. The combined FRP-PFRC will increase the hybrid beams' shear resistance and lower kinematic displacements. The FRP beam will be fixed in these concrete foundations to help avoid stress concentration in the profile (Jaruševičiūtė, 2021).

1.1.1. Fibre-reinforced polymer materials and testing approaches

This section reviews the literature on the structural application of FRP materials and common FRP types, their properties, and the experimental characterisation of FRP structural elements with particular attention to bridge structures. The literature (Bakis et al., 2002; Naito, 2022; Potyrala, 2011; Preinstorfer et al., 2022; Salzano et al., 2019) specified the most common FRP components of glass, basalt, and aramid fibres. These FRP composites have many subtypes with matrices of different materials, fibre orientation, and fibre content.

Glass fibre is a particular form of processed glass that consists of several oxides (silica) and other purified materials (limestone, fluorine, clay). It is commonly used in structures as single filaments or fabrics. This material has a low modulus of elasticity, low resistance to alkalis, low moisture resistance, and a lower long-term strength than other FRP materials (Hollaway & Head, 2000; Potyrala, 2011). A so-called alkali-resistant (AR) fibre (also known as CemFil fibre) with a higher zirconium oxide content has been developed to make it suitable for use with concrete (Potyrala, 2011). Long-term effects, e.g., creep rupture, substantially reduce the material resistance. In addition, the relatively low deformation modulus of GFRP raises the deformations of the structural components. At the same time, most other disadvantages have been overcome by changing the constituent materials of the glass fibres and can easily be used to form differently shaped profiles. Glass fibre is most commonly used to make decking (Lee et al., 2010) and beams (Dongdong, Yaru, Qilin & Feng, 2019), and it can also be used for composite bridges (Siwowski & Rajchel, 2019).

Another widely used FRP material is carbon fibre. It is produced by controlled pyrolysis. The properties and cost-effectiveness of the reinforcement filament will depend on the type of material used to crystallise the carbon during pyrolysis. This type of fibre has a high elastic modulus, is resistant to fatigue, and can have a very high material strength (Potyrala, 2011).

Due to its high cost, carbon fibre is less commonly used to make individual profiles but can be shaped similarly to glass fibre products if required. It is widely used to reinforce existing structures, and prestressed carbon fibre can reduce tensile stresses in bridge girders by up to 50% (Ghafoori et al., 2019). The most commonly used carbon fibre is carbon fibre strips and sheets. Due to its high material strength, carbon fibres can be used to make cables for cable-stayed or suspension bridges (Keller, 2018). These elements are fixed on existing bridge structures using various fixing devices (Li, Li, Lu & Shen, 2019; Siwowski et al., 2020). Carbon fibre elements can also be prestressed, further strengthening the system and reducing buckling. This technique can reinforce timber beams with basalt or glass fibre (Thorhallsson et al., 2017). A disadvantage of carbon fibres is that the level of reinforcement depends on the geometry of the bridge itself. In addition, there must be sufficient space to install carbon fibre strips and fixings on the bridge elements. Another major disadvantage of carbon fibre elements is that it takes much energy to generate the high temperatures needed to form the material, making it very expensive and uneconomical to produce profiles. However, the maintenance and repair of carbon fibre-reinforced polymer (CFRP) elements are cheaper than traditional materials (Ali et al., 2020). The advantages of carbon fibre are its high elastic modulus, strength, and fatigue resistance compared to glass fibre. Regarding service life, studies show that carbon fibre-reinforced polymers have more potential than aramid and glass fibres (Potyrala, 2011).

Aramid fibre is the second typical material for fibre-reinforced polymers. It is obtained by extruding an aromatic polyamide material between –50 ^{0}C and –80 ^{0}C into a cylinder heated to 200 ^{0}C. The fibres remaining after this process are stretched for strength and stiffness. Still, aramid fibres are also difficult to cut and otherwise machine (Potyrala, 2011). The disadvantages of aramid fibre are low compressive strength (500–1000 MPa), low long-term strength, and sensitivity to ultraviolet radiation. On the other hand, like carbon fibre, it has high strength and resistance to static and dynamic fatigue (Potyrala, 2011). However, aramid material is less widely used for economic reasons. Like carbon fibre, aramid materials in sheets and strips are used in bridge structures for refurbishment and strengthening (Ghafoori et al., 2019; Modak et al., 2020; Siwowski et al., 2020).

After analysing the researched articles, a chart was created representing the distribution of publications depending on the FRP reinforcement material **(**Fig. 1.1**)**. About half of the works research GFRP elements.

Flexural tests are the most common (Ascione et al., 2015; Aydin & Saribiyik, 2013; Koaik et al., 2017; Muttashar, Manalo, Karunasena & Lokuge, 2016), but shear tests are also carried out since FRP materials are susceptible (Siwowski et al., 2018). There is a smaller amount of other various tests done with FRPs ranging from tensile (El-Wazery, El-Elamy & Zoalfakar, 2017; Naito, 2022), compression (Yuana, Yao, Niu, Liu & Wuyun, 2019), heat resistance (Ghadimi, Russo & Rosano, 2017) to dynamic (Chróścielewski et al., 2018; Votsis, Stratford, Chryssanthopoulos & Tantele, 2017) and seismic testing (Mahboubi & Shiravand, 2019). They are carried out on structural elements (composite bridge deck slabs, beams) (Hollaway & Head, 2000; Lee et al., 2010; Li, Zhang, Zhao & Deng, 2015; Zhang, Li, Shao & Fan, 2018). In some cases, tests are carried out on existing structures (Ghafoori et al., 2019; Li et al., 2019; Rossini, Spadea & Nanni, 2019; Siwowski et al., 2019; Votsis et al., 2017) to assess how closely they match the design calculations and numerical models, but they are never carried out to failure. Loads may be added in various ways, but the most common are using compression apparatus or weights in laboratory conditions and loaded vehicles on sites.

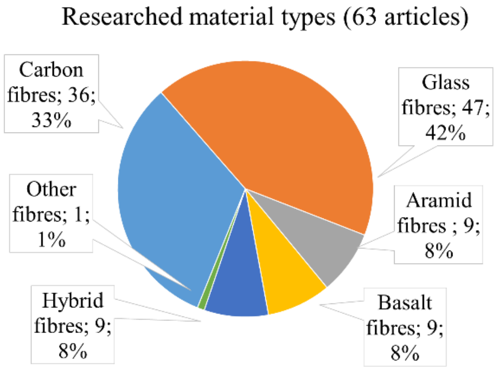

Fig. 1.1. Article distribution depending on the reinforcement material (data from 63 literature sources) (made by the author)

Tests on FRP bridges or bridges built, including FRP elements, can also be carried out after they have been constructed to verify the agreement between the numerical models and design calculations (Ghafoori et al., 2019; Li et al., 2019; Rossini et al., 2019; Siwowski et al., 2019; Votsis et al., 2017). Testing of these bridges is usually carried out immediately after construction. An example is testing a new hybrid FRP/concrete car bridge in Poland (Siwowski et al., 2018); testing is completed using trucks (Siwowski et al., 2019). It is a 22 m bridge with composite beams of glass and carbon fibre FRPs (Siwowski et al., 2018).

This test determined the deflections and stiffness of the bridge, evaluated the overall performance of the hybrid bridge elements, and performed a dynamic analysis. The analysis showed that the bridge serves better than the finite element model, meaning the design and modelling methodology must be improved (Siwowski et al., 2019).

Laboratory tests are usually carried out on bridge sections or separate elements, such as beams, decking, and columns (Hollaway & Head, 2000; Lee et al., 2010; Li et al., 2015; Zhang et al., 2018). They are carried out to ascertain these elements' stiffness, load-bearing capacity, and structural behaviour. The most common test is four-point bending (Aydin & Saribiyik, 2013; Fahmy, Sayed, Farghal & Ahmed, 2019; Keller, Schaumann & Vallee, 2007; Koaik et al., 2017; Muttashar et al., 2016; Siwowski et al., 2018); sometimes, three-point bending is used (Tuwair, Drury, & Volz, 2019) to determine the bending strength and load-bearing capacity. Shear tests are also conducted (Koaik et al., 2017; Siwowski et al., 2018). A relevant laboratory test example is Siwowski et al. (2018). This work conducts four-point bending and shear tests of a composite beam.

After collecting and analysing all the articles, a chart plot was created, which presents the distribution of lab and field tests and the type of tests usually carried out regarding FRP composites (Fig. 1.2a, b).

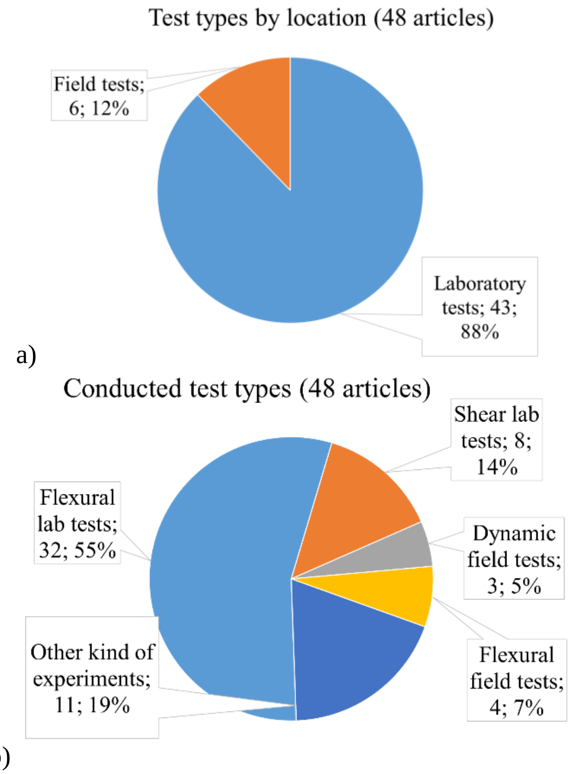

Fig. 1.2. Distribution of testing (data from 48 sources): (a) lab and field tests; (b) conducted test types (made by the author)

1.1.2. Manufacturing methods

Various methods of producing profiles from FRP materials are described in this section. The profiled section's mechanical properties depend on the manufacturing method (Liu et al., 2020; Potyrala, 2011). The profiles can also be easily damaged if they need additional machining to be adapted to the specific structure (Shi, Cui & Li, 2019), so they must be produced to the most accurate parameters possible. The most precise and cheapest method is mechanical pultrusion (Correia et al., 2013). Still, there are other methods of making FRP elements: hand forming, fibre wrapping, resin transfer forming, vacuum-assisted resin transfer moulding, and spray forming (Potyrala, 2011; Tamakuwala, 2020). Production methods are actively being developed and studied (Tackitt & Walsh, 2005; Tamakuwala, 2020).

The pultrusion method is fully automated and reliable. It produces FRP profiles with the most precise dimensions and consistent mechanical properties (Bakis et al., 2002). The pultruded elements also have the highest fibre volume ratio (Goh, Yap, Agarwala & Yeong, 2018). The process involves drawing the reinforcing fibre without stopping, distributing it accurately over the area of the profile to be produced via a distributor, injecting a resin matrix to impregnate the fibre using a processing machine, and then heating the shape in a heater until it hardens and forms its final geometry. Ultimately, the profile is cut with a saw to the required length (Correia, 2013; Potyrala, 2011).

A good fibre distribution is critical, as the quality and performance of the profile depend on its arrangement across the profile cross-section. The fibres used in this process are aramid, carbon, or glass fibre, and the resin matrix is usually polyester. The profiles produced by this method do not require any further processing. Any components and elements can be made this way (Ali et al., 2020; Potyrala, 2011). The pultrusion direction and reinforcement filament distribution coincide, ensuring the mechanical performance of the structural FRP (Correia, 2013; Dang & Phan, 2021; Obaidat, 2020) and can be virtually moulded into any shape (Liu et al., 2020). Pultruded objects have a high fabrication rate, fibre content, and large volume at a low operating cost (Correia, 2013).

After analysing all the articles, a chart plot was drawn to show the distribution, depending on the manufacturing method used to produce the researched elements (Fig. 1.3). The articles found and analysed included the most common FRP manufacturing processes. The cheapest and most efficient method is the pultrusion method, an automated method that is the most widely used and the most accurate (Bakis et al., 2002; Potyrala, 2011). All other methods are either more expensive or less cost-effective.

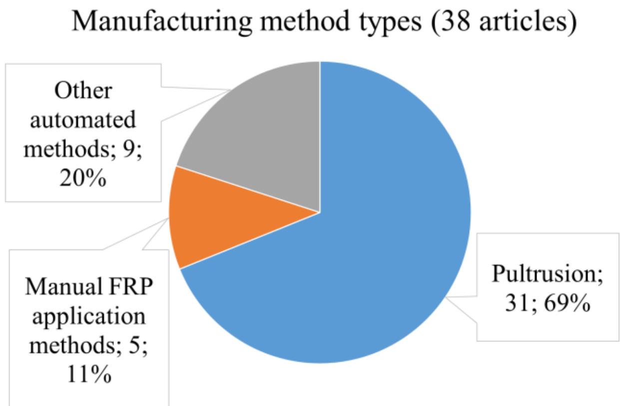

Fig. 1.3. Articles' distribution considering the FRP manufacturing method (data from 38 sources) (made by the author)

1.1.3. Design principles

This section reviews the articles and literature on the existing codes and standards for FRP structures and materials. One of the problems encountered in the research and application of this relatively new material is that there are not enough standards and design codes (Canning & Luke, 2016). Strengthening bridges with FRPs describes the typical literature analysis object. However, there is little information about the bridge design and practically nothing about hybrid bridge design. The profiles made from FRP have different material properties in the respective directions depending on how the fibres are oriented in the composite material. For the same reason, there are also various problems in joining these elements with other FRPs or different materials (concrete, steel, etc.). A common cause of failure in hybrid bridges using FRP composites is the disintegration of the bonding material and the separation of the FRP from the rest of the structure. This occurs because FRP joints are designed the same way as steel joints, even though the mechanical properties of these materials differ significantly.

FRP bridges cannot be safely and confidently designed using methods and standards used for traditional materials; the design of such structures lies beyond the standard regulation field. Bridges with FRP elements are often wastefully designed due to their different material properties (lower modulus of elasticity, lower ductility, and orthotropic material) and different failure mechanisms (Bakis et al., 2002; Potyrala, 2011). Elements made of FRP materials have been reliably used to reinforce or renovate existing structures for more than ten years (Ghafoori et al., 2019; Siwowski et al., 2020). However, no widely accepted guidelines exist for designing FRP elements except for retrofitting (Ali et al., 2020).

To make this structure more attractive to designers, new design methods, codes, and standards must be developed, or existing ones must be modified to quickly adapt to this relatively new material. The area where most of the current codes and standards are concentrated is the retrofitting and repairing structures with CFRP and AFRP; they are also used to improve the seismic performance of bridges. Most of the strengthening standards are developed in Canada, The United States, Japan, and Europe (Bakis et al., 2002).

These standards and codes still need to be improved because many types of FRP with different fibres and matrices (Keller, 2018) react differently when exposed to various environmental influences or loads. Furthermore, element properties from these materials can even be influenced by the methods used to manufacture them (Liu et al., 2020) and the additional machining applied to them (Shi et al., 2019). Therefore, no universally accepted design norms or procedures exist (Potyrala, 2011). Many companies producing all-FRP structures ensure their use on the market by issuing specific recommendations and design guidelines (FIBERLINE, 2003), as exemplified by the Fiberline company, which adapts itself to the German DIN norms and European standards and obtains certificates for the materials they use, which ensure the reliability of the elements they produce, according to the given minimum requirements for the quality, tolerances, strength, stiffness, and surface of structural profiles for load-bearing purposes (Table 1.1).

Table 1.1. Minimum FRP material properties to ensure class

Property	Units	Test method	Minimum properties	
			E23 Grade	E17 Grade
Full section test	GPa	Annex D, EN 13706-2:2002	23	17
Tension modulus-axial	GPa	EN ISO 527-4	23	17
Tension modulus-transverse	GPa	EN ISO 527-4	7	5
Tension strength-axial	MPa	EN ISO 527-4	240	170
Tension strength-transverse	MPa	EN ISO 527-4	50	30
Pin-bearing strength-axial	MPa	Annex D, EN 13706-2:2002	150	90
Pin-bearing strength-transverse	MPa	Annex D, EN 13706-2:2002	70	50
Flexural strength - axial	MPa	EN ISO 14125	240	170
Flexural strength - transverse	MPa	EN ISO 14125	100	70
Interlaminar shear strength-axial	MPa	EN ISO 14130	25	15

Most of the literature discusses specific design methods (Rossini et al., 2019; Zhang et al., 2018) for the particular structures considered in those articles. The papers apply old calculation methods to FRP composite structures, modify existing calculations, simplify them, and apply them to new systems, such as the spatial decking trusses composed of the orthotropic plate, aluminium, and glass fibre tubes (Zhang et al., 2018). The stiffness of this complex structure could be calculated using the proposed method for hybrid deck-truss systems, which is based on the rules of classical structural mechanics (Li et al., 2015). Still, it would be very complex and unsuitable for the design application. Therefore, a simplified version is proposed, simplifying this complex structure and modifying the formulae accordingly, resulting in a more acceptable design for engineers for this type of structure.

More research has to be completed with FRPs and their elements because, so far, a portion of these bridges designed with FRPs can resist up to 18 times their design strength, which makes their design uneconomical and very conservative. In addition, very little has been done on the shear transfer mechanisms of hybrid bridges made of FRP and concrete, how they are affected by dynamic effects, and the effect temperature has on these connections between concrete and FRP elements (Zou et al., 2020). This work is focused on short-term loading conditions.

There are some design guides for all FRP elements. Examples are the ASCE design guides for plastics and FRP elements (American Society of Civil Engineers, 1984; American Society of Civil Engineers, 1985; Mosallam, 2011). First, a manual describing the properties of plastic materials has been developed (ASCE, 1984), and then a guide to assist the engineer in selecting the appropriate combinations of plastic materials that will have the required material properties for the required structures and the calculation of these structures (ASCE, 1985). More detailed design guides are now developed to describe the design of FRP joints and elements. Their most recent principle covers the design of pultruded FRP joints and components, the calculation and design of various joints, the code suitable for modelling these joints, and the studies carried out on them (Mosallam, 2011). However, these manuals are only applicable to all FRP elements and structures. Guidance is lacking for hybrid components and structures.

The distribution of articles depending on the design methods and standards mentioned is presented below (Fig. 1.4). Standards and design guides are developed and updated based on research, but this slow process takes years. Most of the existing standards are currently produced by the companies involved in producing FRP composites, such as Fiberline or Strongwell, and all current standards belong to local manufacturers. Most national design standards have been developed for bridge repairs and retrofitting (Bakis et al., 2002). However, none of these current guidelines or standards are accepted universally (Potyrala, 2011). Many new design guides are still being developed (Canning & Luke, 2016; Bakis et al., 2002). As there is very little design guidance and many different types of FRP hybrid beams, only the material parameters of the FRP elements will be taken from the company FIBERLINE provided certificates.

The absence of the design reference complicates the development of innovative structures. Therefore, this dissertational work extends the adaptive design concept (Rong, Zhao, Feng & Xie, 2022). This concept is typical for theoretical analysis (Rong et al., 2022) and architectural design (Xie, 2022). However, to the best of the author's knowledge, it was not used for structural problems.

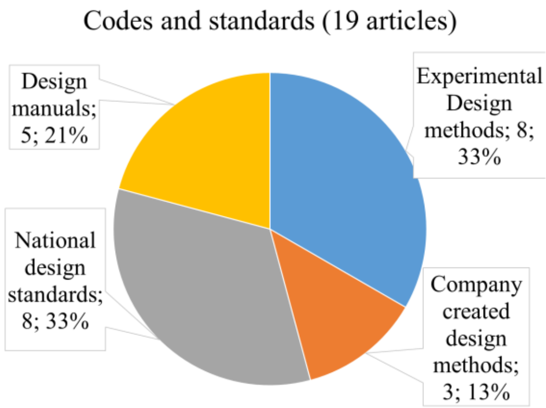

Fig. 1.4. Distribution of articles regarding design methods and standards (data from 19 sources) (made by the author)

1.1.4. Development perspective

Even though FRP composites have been used for decades, they still have several disadvantages. Unfortunately, these disadvantages stop FRP composites from replacing traditional materials even more and taking their place alongside them.

For this type of composite to become more widely accepted, more research has to be done into the material itself; because material properties depend on the orientation of the fibre reinforcement and the fibre quantity, it is hard to separate the material from the structure, so the manufacturer trying to design the material has to create the system as well (Potyrala, 2011).

There is a vast variety of FRP composites with different mechanical and material properties (Potyrala, 2011). Thus, the structural application of these composites requires experimental investigation with particular attention to developing reliable constitutive models (Ali et al., 2020). More research still needs to be done to determine long-term behaviour, fire resistance, sustainability, recycling, and life cycle costs (Bakis et al., 2002; Keller, 2018; Kim, 2018). The main reason for FRP structure failures is their connections, either joint between elements or bond failure, which is why they are the most overdesigned parts of the bridges. In general, there is still much unnecessary overdesigning of FRP-concrete structures, sometimes increasing the load-bearing capacity up to 18 times the required amount (Zou et al., 2020).

The analysed literature shows that more research is still required on FRP composites (Ali et al., 2020). In addition, more research on the material itself is needed. Because of this lack of research, there are not enough design norms. With no design norms, there is little trust in the material, and even the built bridges are highly conservative. These problems can only be solved by conducting more research and applying FRP composites more widely. They are already being used in many bridges; more testing and modelling are needed for more efficient use, creating better design methodology and profile geometry. The challenges faced by FRP composites are the same as those faced by traditional materials in the past, like steel (Ali et al., 2020).

1.2. Numerical modelling

This section reviews research publications dealing with the numerical modelling of FRP structural components; it analyses the modelling problems, software, and the choice of material models. Furthermore, the papers dealing with the bond between FRP and concrete are examined in detail, as this connection is typical for the structural application of FRP composites. Besides, it governs simulation results adequacy (Sun, Peng & Yu, 2017).

Numerical modelling works reported in the literature focus on two general purposes: (1) verification of constitutive models, using test results of laboratory specimens (Chen, Sun, Meng, Jin & Li, 2019; Dongdong et al., 2019; Eskandaria et al., 2019; Li et al., 2015; Siwowski et al., 2018; Thorhallsson et al., 2017; Zhang et al., 2018); (2) analysis of full-scale structural elements (He, Liu, Chen & Dai, 2012; Mahboubi & Shiravand, 2019; Muc et al., 2020; Votsis et al., 2017; Yang et al., 2020). Fig. 1.5a describes the selected papers' distribution structure regarding the simulation object. It can be observed that 24 out of 29 articles dealt with experimental specimens. These simulations account for load-bearing capacity, deformations (Dongdong et al., 2019; Keller & Schollmayer, 2004; Siwowski et al., 2018), dynamics (Siwowski et al., 2019; Votsis et al., 2017; Yang et al., 2020), accidental effects (e.g., fire resistance), long-term degradation of mechanical performance, and other aspects (Eskandaria et al., 2019; Mahboubi & Shiravand, 2019; Yuana et al., 2019). The literature analysis identified the following simulation targets: failure of FRP composites (Eskandaria et al., 2019), debonding of FRP components (Cai, Pan, & Zhou, 2017; Muc et al., 2020), and elastic simplification of structural behaviour (He et al., 2012; Keller & Schollmayer, 2004; Mahboubi & Shiravand, 2019; Mandal & Chakrabarti, 2017; Votsis et al., 2017; Yang et al., 2020; Yuana et al., 2019). The first two aspects are typical for analysing laboratory samples (Cai et al., 2017; Eskandaria et al., 2019; Muc et al., 2020). On the contrary, the elastic (or elastic–plastic) simplifications are characteristic of full-scale structural models (He et al., 2012; Mahboubi & Shiravand, 2019; Votsis et al., 2017; Yang et al., 2020). Reference (Siwowski et al., 2019) proves the elastic material assumption, highlighting relatively low stresses in structural components under the service load.

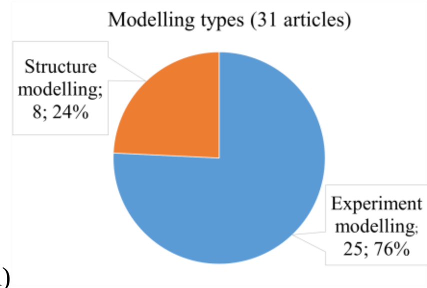

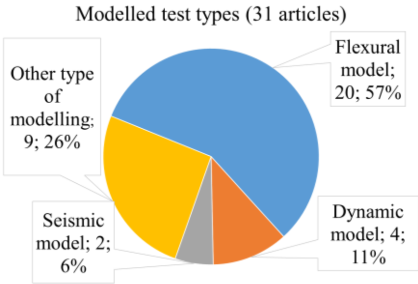

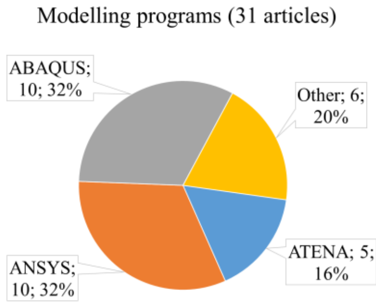

Fig. 1.5. Literature distribution (data from 31 sources): (a) by modelling object; (b) by modelling type; (c) by application (made by the author)

In some cases, shear failure (Eskandaria et al., 2019), bond behaviour of the composite components, and interlaminar slippage are among the modelling parameters (Cai et al., 2017; Chen et al., 2019; Eskandaria et al., 2019; Muc et al., 2020; Robinson & Melby, 2015;). The mentioned problems cause the essential difference between the simulation strategies of FRP composites and other structural materials, like steel or concrete. Nevertheless, the FRP modelling has similarities to the analysis of timber structures. Several studies investigated FRP-timber composites, revealing the structural efficiency of such a hybrid system (Issa & Kmeid, 2005; Thorhallsson et al., 2017). However, that is a rare exception as the typical simulation objects are the concrete reinforced with FRP bars, near surface-mounted strips, and external sheets (Cai et al., 2017; Mahboubi & Shiravand, 2019; Yuana et al., 2019). Fig. 1.5b describes the distribution of the articles depending on the modelling object test type. Bending tests are typically used to verify the numerical models (Dongdong et al., 2019; Papapetrou, Tamijani, Brown, & Kim, 2018). The references (Mahboubi & Shiravand, 2019; Yang et al., 2020) present examples of seismic analysis; references (Chróścielewski et al., 2018; Siwowski et al., 2019; Votsis et al., 2017) are current dynamic analysis examples. The appropriate software must be chosen to simulate dynamic and seismic loads and their structural response (Table 1.2).

Table 1.2. Capabilities of software used in the literature

Program	Bond modelling	Material parameter modelling	Seismic analysis	Dynamic analysis
ANSYS	Contact elements	linear/nonlinear for metals, rubber, foam, concrete	Simple assistant program ANSeismic	+
ABAQUS	Contact property assignment or adhesive joints	linear/nonlinear, UMAT, and VUMAT subroutines to create complex material models	Abaqus/Standard, Abaqus/Explicit seismic analysis by subjecting model to accelerogram	Implicit in Abaqus/Standard, explicit in Abaqus/Explicit
Sofistik	Perfect bond	linear/nonlinear for steel, concrete	+	+
OpenSees	A bond model	linear/uniaxial for steel, concrete, reinforcing steel	Subjecting a structural model to one (or more) ground motion records	-
NASTRAN	Surface contact function	linear/nonlinear for metals, rubber, user-specified materials	FEMAP + NX NASTRAN seismic analysis by subjecting the model to accelerogram	FEMAP + NX NASTRAN
ATENA	A bond model	linear/nonlinear for concrete, user-specified materials	+ AmQuake for masonry buildings	+

Fig. 1.5c shows the percentage distribution of the modelling software used in the literature for simulating FRP components. The most widely used software packages are ANSYS (Dongdong et al., 2019; He et al., 2012; Keller & Schollmayer, 2004; Li et al., 2015; Muc et al., 2020; Votsis et al., 2017; Yang et al., 2020; Zhang et al., 2018) and ABAQUS (Chen et al., 2019; Eskandaria et al., 2019; Mandal & Chakrabarti, 2017; Robinson & Melby, 2015; Yuana et al., 2019;), and the rarer software is ATENA (Cai et al., 2017; Chaiyasarn et al., 2021; Juozapaitis et al., 2021). Other packages are rarely applied (Mahboubi & Shiravand, 2019; Mendes et al., 2011; Papapetrou et al., 2018; Siwowski et al., 2019).

The analysed research shows a tendency to model FRP structures in a laboratory environment (Chen et al., 2019; Dongdong et al., 2019; Eskandaria et al., 2019; Li et al., 2015; Siwowski et al., 2018; Thorhallsson et al., 2017; Zhang et al., 2018) because most testing is also completed in such conditions. The most common modelled test is four-point bending (Fig. 1.5b) because the results can be easily compared to the experimental results. However, more research is required on modelling the bonding of FRP elements, especially its material properties, with a limited number of articles considering the heterogeneity of the mechanical properties intrinsic to FRP composites. Also, few literature publications about the support joints of such structures can be found.

1.2.1. Material models

The material models chosen for the FE modelling are essential for the modelling. In addition, various problems require a different complexity of the constitutive models, with specific research requiring exact definitions for adequate modelling results. Laboratory tests (He et al., 2012; Muc et al., 2020; Siwowski et al., 2019) and manufacturers' certificates (FIBERLINE, 2021; Votsis et al., 2017; Yang et al., 2020) define the material properties; these material properties are typically modelled as elastic (Fig. 1.6a). Table 1.3 summarises the mechanical properties assumed in the selected literature sources. In this table, E determines the modulus of elasticity, and V_f is the fibre content. A considerable variation of material properties (moduli of elasticity and tensile/compression strength) is observed. Furthermore, various filament materials, e.g., CFRP, BFRP, GFRP, or combinations of these fibres, are used in the literature.

The advanced simulations attempt to represent the heterogeneity of the mechanical properties of FRP. Typically, the difference in the elasticity moduli specified in different directions simulates the material parameters' anisotropy (Chen et al., 2019; Eskandaria et al., 2019; Muc et al., 2020; Papapetrou et al., 2018; Robinson & Melby, 2015;).

The material model problem relates to the limited ability of software to describe anisotropic material properties. Still, often, there is no need to use advanced calculations to solve deformation problems and analyse the beams or bridge structures under service conditions. Table 1.2 specifies the programs considered in the literature and their capabilities, specifying nonlinear material models.

Fig. 1.5 shows that numerical models typically simulate pedestrian, vehicular, and dead loads (Dongdong et al., 2019; He et al., 2012; Keller & Schollmayer, 2004; Muc et al., 2020; Siwowski et al., 2019; Votsis et al., 2017), assessing FRP parts' load-bearing capacity and deformations; other loads, such as seismicity or dynamics, are less frequent (Siwowski et al., 2019; Yang et al., 2020). Most selected papers used concentrated and uniformly distributed loads to simulate the loading conditions. Distributed loads simulated pedestrians; point-loads model vehicular effects (Muc et al., 2020).

References (Eskandaria et al., 2019; Yuana et al., 2019; Mandal & Chakrabarti, 2017; Zhu et al., 2022) describe the specific examples of numerical analyses. The research article (Yuana et al., 2019) investigated the stability of FRP specimens under compressive load: articles (Eskandaria et al., 2019; Mandal & Chakrabarti, 2017; Zhu et al., 2022) analysed failure mechanisms of FRP structural elements and their connections. Rare literature sources considered modelling the effects of wind loads or temperature (Ghadimi et al., 2017) on FRP elements.

Dynamic parameters, such as the oscillation shape, damping coefficients, and accelerations of the structure, are essential for modelling FRP elements because of such structures' high deformability and low self-weight. The dynamic bridge assessment is much more complex than static calculations and requires a more sophisticated model (Chróścielewski et al., 2018; Siwowski et al., 2019). Therefore, such simulations require ensuring adequate determination of the bridge geometry and material parameters (Siwowski et al., 2019; Votsis et al., 2017). Moreover, the bridge parameters can change over time (Votsis et al., 2017). Even parapets, sidewalks, or ballast influence the dynamic response (Siwowski et al., 2019; Votsis et al., 2017) and alter the structure's stiffness (Chróścielewski et al., 2018).

The analysed research papers choose the material model based on the research objectives. For example, suppose modelling is done with FRP components in the service load state (He et al., 2012; Siwowksi et al., 2019) or for solving deformation problems (Chróścielewski et al., 2018; Siwowski et al., 2019; Votsis et al., 2017). In that case, the anisotropy is not considered. Still, for dynamic assessments (Chróścielewski et al., 2018; Siwowksi et al., 2019) and advanced material simulations (Chen et al., 2019; Eskandaria et al., 2019; Muc et al., 2020; Papapetrou et al., 2018; Robinson & Melby, 2015), the material model has to describe FRP materials' heterogeneity and be as accurate as possible to be in good agreement with the experimental results.

Table 1.3. Mechanical properties of FRP materials reported in the literature

Reference	Material	E, GPa	Strength, f_t/f_c, MPa	Element type	V_f
(Dongdong et al., 2019)	GFRP	59.2	1320/560	Tubes	80%
(Siwowski et al., 2019)	CRFRP	115.8	1150/464	Girder from laminates	x
(Siwowski et al., 2018)	GFRP	24.0	450/280	Hybrid girder from laminates	x
	CFRP	125	1270/360	Hybrid girder from laminates	x
(Li et al., 2015)	GFRP	31.5	1000/560	Tubes	x
(Yang et al., 2020)	CFRP	153	1950	Hybrid cable	x
	BFRP	52.0	1521	Hybrid cable	x
(Papetrou et al., 2018)	GFRP	45.3	830	Hybrid girder from laminates	x
	CFRP	114	1370	Hybrid girder from laminates	x
(Robinson & Melby, 2015)	GFRP	27.6	378	Tubes	x
(Chen et al., 2019)	GFRP	40.0	500	Laminate	68%
	CFRP	120	2200	Laminate	68%
	BFRP	33.1	560	Laminate	68%
(Eskandaria et al., 2019)	GFRP	150	2323	Laminate	x
(Yuana et al., 2019)	CFRP	200	1831	Laminate	50%
(Mahboubi & Shiravand, 2019)	CFRP	241	3710	CFRP strip	x
(Mandal & Chakrabarti, 2017)	CFRP	140	2200/1600	Joint	x
(Cai et al., 2017)	BFRP	45.0	1090	Rebar	x

The description of the bonding parameters in the models also depends on the research target. For service loads and deformation behaviour, the bond parameters in the models are described as perfect. Specific bond parameters are usually provided for advanced simulations and articles researching bond properties. Research on FRP elements is ongoing; the number of publications is equally distributed between those with and without specified bonding parameters (Fig. 1.6b).

1.2.2. Engineering problems

A few problems occur while modelling FE models with FRP components. Assumptions are made to simplify these models, but these assumptions can be unacceptable, depending on the research object.

The bond problem complicates structural analysis and numerical modelling (Zou, Feng, Bao, Wang & Xin, 2020; Zou et al., 2020). Still, studies (He et al., 2012; Obaidat, 2020; Papapetrou et al., 2018; Siwowski et al., 2018, 2019) describe the typical analysis examples, neglecting the bond problem. References (Cai et al., 2017; Chen et al., 2019; Malakhov et al., 2021; Muc et al., 2020; Nerilli &Vairo, 2018; Robinson & Melby, 2015) defined the cases when the bond parameters were among the research subjects. For instance, Chen et al. (2019) focused the research on the FRP laminate bonding properties. Four remaining works consider the FRP-concrete bond performance of the hybrid structural systems, which describe the research object of this dissertation. Dang and Phan (2021) and Cai et al. (2017) investigated concrete's FRP bar bonding performance. Robinson and Melby (2015) studied the mechanical resistance of the concrete-filled GFRP tube, and Muc et al. (2020) simulated the composite deck slab. However, a rare publication considers the support joint's resistance of the FRP profiles, e.g., Zhang et al. (2020).

A few different functions can affect the bond modelling results: by creating a surface-to-surface interaction, assigning it to the appropriate surfaces and choosing the required contact properties, or by creating an adhesive joint, connecting two components with a glue-like material with a finite thickness (ABAQUS) (Chen et al., 2019; Robinson & Melby, 2015) and using contact elements (ANSYS) (Muc et al., 2020). An empirical bond model determines the mechanical contact in ATENA (Cai et al., 2017). Of the 29 articles about modelling, only fourteen of them consider bond modelling problems (Fig. 1.6b).

FRP elements are classified as "shell" elements for bridge deck panels in the references (He et al., 2012; Votsis et al., 2017), and beam elements in the article (Dongdong et al., 2019), no unified methodology exists yet. Modelling with FRP elements is carried out in the same way as with conventional materials. There is practically no difference in modelling this type of structure at low loads. However, when modelling these structures at high stresses, particular care must be taken in describing their connections with other elements and specifying the appropriate bond parameters, as these structures often fail at their joints (Eskandaria et al., 2019; Mandal & Chakrabarti, 2017; Zhu et al., 2022). It is also necessary to identify these materials as anisotropic in the software due to their different nature of disintegration compared to conventional materials to assess the exact failure mode of the modelled element. However, most articles apply linear material parameters (Fig. 1.6a). The perfect connection assumption and linear-elastic material parameters will be used in the hybrid beam structure modelling to determine whether these assumptions for deformation problem solving are correct and how well they correspond with the composite beam experimental results. The smeared reinforcement model, developed for concrete mesh reinforcement (Cervenka, 2002) adapted to FRP (Gribniak et al., 2021), will be applied in the modelling. The fibre volume fraction must also be determined to evaluate the amount of fibre reinforcement area in the cross-section (Gribniak, Kaklauskas, Kwan, Bačinskas & Ulbinas, 2012). This will allow the creation of a reliable FE model, a reliable reference for the physical experiments. A moment-curvature diagram can evaluate hybrid beam deformations (Gribniak, 2009).

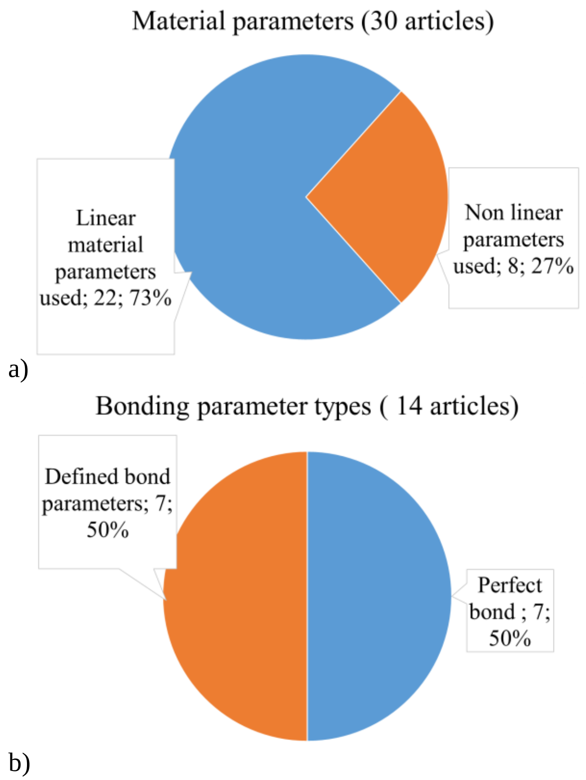

Fig. 1.6. Literature distribution (data from 30 and 14 sources):
(a) by material parameters; (b) by adhesion parameters (made by the author)

1.3. Conclusions of the First Chapter and formulation of the dissertation's tasks

Based on the literature analysis, FRP elements are increasingly developed and characterised, making these materials acceptable for various structural applications. Regarding bridges, many such structures have been built or repaired in the Czech Republic, Switzerland, the United States of America, Poland, South Korea, with the main load-bearing and secondary elements made of FRP materials. FRP materials (typically carbon fibre sheets, cables, and strips) are widely used to retrofit existing structures. This material type is low in weight and has a similar or higher strength than traditional materials, making them attractive for constructing temporary bridges.

1. The market is dominated by the three most common FRP components: glass, carbon, and aramid fibres. These materials are also used in combination, producing hybrid elements. The cement-based composite materials have also been developed with glass, polymer, and carbon fibres to improve cracking resistance and deformation ductility. These materials are typically used for bridge deck slabs, cables, and load-bearing components.
2. Pultrusion is the most frequent manufacturing method, ensuring precise dimensions of FRP components, fast industrial manufacturing, and a high fibre content in the matrix (about 75%) compared to other manufacturing methods (hand moulding, fibre wrapping, resin transfer moulding, injection moulding).
3. Various numerical simulations have been conducted with different FRP materials and components, including beam, truss, cable-stayed, and suspension bridges. However, problems arise when describing the material and connection (bond) models, accounting for the anisotropy of FRP materials.
4. Application of FRP components in relatively long-span structures (e.g., 10—15 m long bridges) faces a significant challenge because of excessive deflections and vulnerability to dynamic loads. The research must focus on the shear resistance of FRP components and their bonding performance with concrete. In addition, there is a gap in knowledge about the dynamics of FRP components, fatigue, and fire resistance. Consequently, tests on existing bridges demonstrate unreasonably high safety reserve, with some structures withstanding up to 18 times higher loads than the design requirement.

5. Due to the lack of globally accepted design norms and manufacturing standards, FRP elements are used more exclusively in constructing pedestrian bridges, platforms, architectural details, facades, pipelines, and chemical containers.
6. The four-point bending is the most widespread test and modelling determining mechanical performance. Physical beam prototypes must be produced after completing the model to verify the finite element (FE) modelling results.

Therefore, this dissertation aims to develop an adaptive design concept when the experimentally verified numerical model describes the design reference. Based on the analysed articles, the following research objectives are formulated:

1. The hybrid beam structure describes the adaptive design object. It composes a pultruded GFRP I profile and CFRP strip in the tension zone to increase the beam tension resistance and limit deformations and polymer fibre-reinforced concrete (PFRC) slab. The polymeric fibres enhance the ductility and cracking resistance of the concrete. In addition, the PFRC deck slab could withstand the excessive deformations of the bridge, ensuring the overall stiffness of the hybrid system. For the development of this hybrid beam, the FRP components should be fixed in relatively rigid supports.
2. Material laws were experimentally determined for the development of the FE model. However, the models typically assume the perfect bond model between the composite components.
3. A literature gap exists in the systematic computer-aided design approach for FRP-composing structures when the experimentally verified FE model describes the design target. Moreover, the existing design approaches are far too conservative because of a lack of reliable models and design standards. Therefore, the produced constitutive models and prototypes determine the efficiency of the proposed adaptive design concept.
4. A hybrid beam for a pedestrian bridge was created to exemplify the proposed adaptive design concept. The beam was compared to the verified FE model. If necessary, the beam modification ensures agreement with the model predictions.

2

Adaptive Design of Hybrid Structural Systems

This chapter introduces the adaptive design concept, employing a hybrid beam prototype (Fig. 2.1) to exemplify the design principles. This structural element combines the polymeric fibre-reinforced concrete (PFRC) slab, pultruded glass fibre-reinforced polymer (GFRP) profile, and pultruded carbon fibre-reinforced polymer strip distributed in the tensile zone of the profile; the reasoning for the combination is provided in the literature review. The main research results of the chapter are published in the author's publications (Gribniak et al., 2021; Garnevičius et al., 2020, 2021a; Garnevičius & Gribniak, 2022) and conference presentations (Sokolov et al., 2018; Garnevičius et al., 2021b). The chapter describes the adaptive design concept, assuming existing experimentally verified material models and modelling principles. The Third Chapter experimentally proves the modelling assumptions.

2.1. Adaptive design concept

This section describes the adaptive design concept when the finite element (FE) modelling outcome determines the reference result, describing the system's efficiency and, hence, the modification reference of the developed prototype. Although such hybrid designs apply to bridge engineering and replacing steel with

GFRP components is the key to the corrosion problem, the uncertainty of the GFRP bonding performance with concrete complicates the hybrid system (Mendes et al., 2011; Zhang et al., 2021).

The designed beam comprises the polymeric fibre-reinforced concrete (PFRC) slab, resisting the compression force from the support joints and fixing the glass-fibre-reinforced profile (GFRP, 120×60/6/6 mm I-profile by FIBERLINE, Denmark). The preliminary simulations determined the support block's geometry (Jaruševičiūtė, 2021). In addition, a carbon-fibre-reinforced polymer (CFRP, 10 × 1.4 mm by S&P C-Laminate, UK) strip strengthens the most tensioned face of the GFRP profile. Fig. 2.2 demonstrates the composite beam's schematic and anticipated cross-sections. This structural scheme (Fig. 2.1) employs the stress-ribbon bridge concept (Gribniak et al., 2021; Juozapaitis et al., 2021) to develop the hybrid element. This way, the concrete provides a reliable connection with the GFRP profile on the supports. In addition, FE modelling checks the proposed concept's viability when the smeared reinforcement approach (Gribniak et al., 2021) describes the mechanical performance of FRP components, the physically nonlinear material model (Garnevičius et al., 2020) defines the PFRC behaviour, and the perfect bond model represents the contact problem. After the hybrid beam geometry was decided, it was modelled in the commercial software ATENA.

As shown in the interaction between the concept ("1") and the verified FE model ("2"), it produces the preliminary solution under the assumed design constraints. The predicted output determines the objective reference for further physical tests ("3"), verifying the efficiency of the concept "1" (i.e., "Verification 1"). Under-performing the referenced outcome, an engineer modifies the design concept ("4"). The iterative adaptation continues until an acceptable agreement between the results of physical tests and numerical simulations (i.e., "Verification 2").

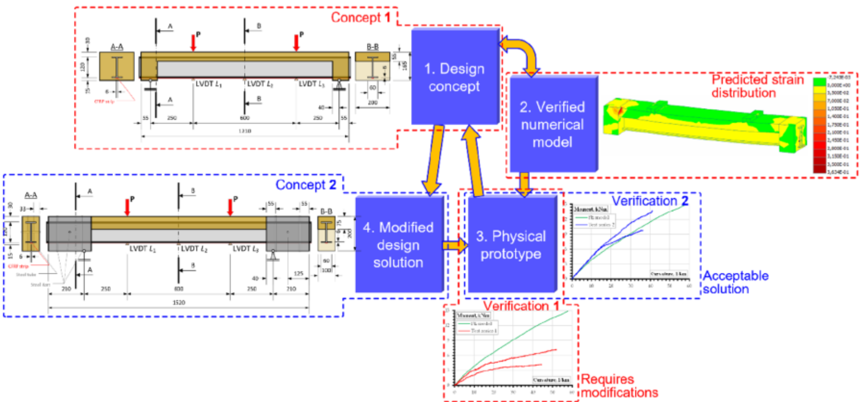

Fig. 2.1. Adaptive design concept (made by the author)

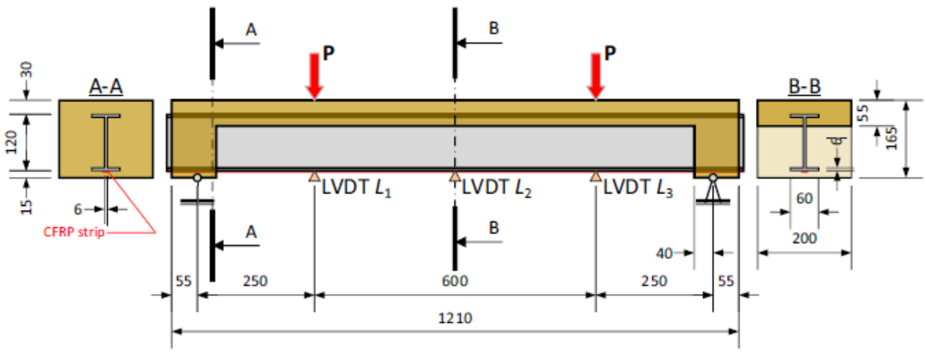

Fig. 2.2. Hybrid beam schematic and anticipated cross-sections (made by the author)

Advanced computational procedures can replace expert opinion-based optimisation, making the proposed concept efficient for adaptive computer-aided design. Moreover, the FE outcomes can provide excessive information for optimising the materials parameters and structural solutions. The analysis consists of three steps: verifying material models and modelling procedures, developing the reference numerical model of the composite system, and adapting the physical prototype design and manufacturing technology. Thus, the experimental verification at the first stage guarantees the adequacy of the reference model. This section assumes the numerical models that are verified to simplify the presentation structure. The Third Chapter proves this assumption.

2.2. Stage 1: Verifying material models for numerical analysis

This Section presents the research and tests to determine the material parameters of PFRC and GFRP. The parameters were applied to the FE modelling to verify the model, which will be used as a reference for evaluating the results of the prototype beam tests. The PFRC mixture proportions are also provided in this Section.

2.2.1. Pultruded glass fibre-reinforced polymer profile modelling

A GFRP square hollow section (SHS) profile in the market (FIBERLINE, Denmark) was chosen and investigated to obtain material parameters and verify the FE model. After receiving the material parameters, a verified material model was created that can be applied to any geometrical shape. Section 3.2.1 describes the experimental part of this investigation.

This section introduces the finite element (FE) modelling approach to the mechanical analysis of GFRP pultruded profiles. The modelling ensures acceptable adequacy with the maximal allowable mesh size. This principle complies with the current structural modelling trends when the finite element numbers' limitation determines the model optimisation objective. Furthermore, the proposed modelling concept allows for estimating the fibre reinforcement efficiency, understood as the ability to resist mechanical load proportional to the dry filaments' content and experimental elastic moduli of the GFRP constituents.

A three-point bending test determines the mechanical performance of the profiles. The experiment is discussed in the Third Chapter in more detail. The FE model is developed based on the smeared reinforcement concept (Fig. 2.3) to predict the stiffness and load-bearing capacity of the profiles. An efficient balance between the prediction accuracy and computation time characterises the developed FE approach that does not require specific descriptions of reinforcement geometry and refined meshes necessary for modelling the discrete fibres. The proposed FE approach also analyses the fibre efficiency in reinforcing the polymer matrix. The efficiency is understood as the model's ability to resist mechanical load proportional to the dry filaments' content and experimental elastic modulus value.

The straight fibres have no specific geometry as the volume percentage and orientation (regarding the global coordinate system) describe the mechanical properties of the reinforcement having perfect contact with the matrix (i.e., no slip between the filament and finite elements is allowed). The fibres are not resistant to axial compression. The solid finite elements can include several reinforcement systems (layers) smeared in different directions to represent a complex filament architecture characteristic of particular FRP pultruded components.

In this research, the 3D solid finite elements describe the polymer matrix, assuming the fracture mechanic principles for tensile failure and the plasticity approach to compressive failure. Fig. 2.4 shows the softening law in compression related to a linear descending branch of the diagram. In this figure, f_c is the compressive strength; f_{c0} is the onset of nonlinear compressive behaviour; ε_{cp} is the plastic strain at the compressive strength; ε_d is the compressive ductility. The plastic displacement and crack band size ratio define the strain ε_d. The crack band determines a fictitious crushing zone related to the finite element size. The principal compressive stresses describe the failure plane normal to the stress direction; the post-peak compressive strain localises in this plane. Such formulation reduces the FE mesh dependency of the model (Cervenka, 2002).

A layer of the smeared reinforcement models the glass filaments. In such a way, a separate 1D material model, coinciding with the pultrusion direction, describes the reinforcement. A perfectly elastic-brittle constitutive law defines the tension failure of the fibres, which do not resist the compression stresses.

The absence of material tests (Table 2.1) essential for the proposed FE approach makes the FIBERLINE profile analysis only illustrative. Fig. 2.4 shows the corresponding numerical model built using 3D isoparametric brick eight-node finite elements with eight integration points and an average size of 5 mm. The modelled steel plates preserve the GFRP SHS profile from stress concentration at the supports and load application point. Figs. 2.5b and 2.5c show that the FIBERLINE profile model has no geometry imperfections and ignores the corner roundness of the SHS profile (Fig. 2.5b) because of the engineering simplification. The 3D solid finite elements describe the polymer matrix; smeared reinforcement represents the glass filaments (Fig. 2.3). The respective constitutive model of the GFRP material employs the polyester resin and E-glass fibre properties obtained from the literature (El-Wazery et al., 2017; FIBERLINE, 2021) and presented in Table 2.1.

Table. 2.1. Material properties of the GFRP composite constituents

Property	Resin (Isophthalic polyester)[1]	E-glass filament[1]
Tensile strength [MPa]	90	3445
Elastic modulus [GPa]	3.23	73.0
Poisson's ratio	–	–
Density [g/cm^3]	1.35	2.58

[1]Properties adapted from the literature (El-Wazery et al., 2017; FIBERLINE, 2021)

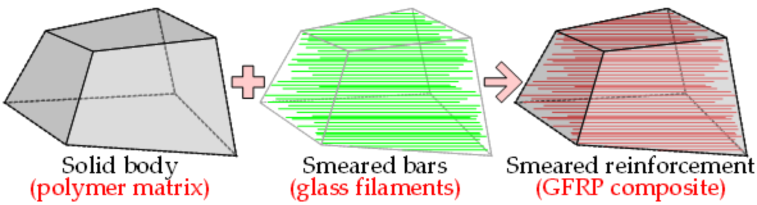

Fig. 2.3. Adopting the smeared reinforcement concept (Cervenka, 2002)

Table 2.2 provides experimental values of all material parameters necessary for the numerical modelling of the FIBERLINE profile. Therefore, simulations of this profile illustrate the proposed fibre efficiency concept and the limitations of the standard testing procedures. The material parameters in Table 2.1 describe the elastic constitutive models of the isophthalic polyester resin and smeared reinforcement in all simulations. Equal compressive and tensile strength values were assumed for the polymer. Several FE simulations were conducted, varying only the supposed fibre content V_f. Table 2.3 summarises the parameters of the numerical models.

Two FE simulations were carried out, assuming different fibre volume fractions. *Model 1* considers a profile with the 56.2% filament content estimated from the mass fraction obtained in the burning tests (a detailed description of this test is in the Third Chapter) to determine the fibre content. *Model 2* assumes the fibre volume fraction of 44.0%, which corresponds to the manufacturer-specified nominal mass fraction (60%) transformed by Equation (2.1) and the constituent material densities ρ_m and ρ_f defined by FIBERLINE (2021):

$$V_f = \frac{w_f \cdot \rho_m}{w_f \cdot \rho_m + \left(1 - w_f\right) \cdot \rho_f}, \tag{2.1}$$

where ρ_f and ρ_m are the fibre and matrix densities (Table 2.1), and w_f is the mass percentage of fibres determined in the heating tests. The above parameter is necessary for the numerical modelling to describe the fibre reinforcement area in the cross-section (Gribniak et al., 2012, 2021).

Table. 2.2. Material properties of the FIBERLINE GFRP composite

Property	FIBERLINE[1]
Tensile strength [MPa]	250
Elastic modulus [GPa]	22
Poisson’s ratio	0.29

[1]Properties adapted from the literature source (FIBERLINE, 2021)

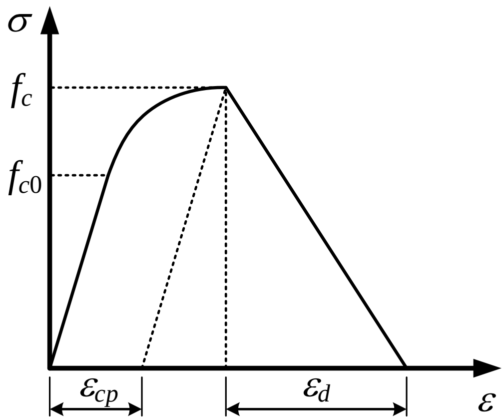

Fig. 2.4. Constitutive model of the polymer matrix in compression (Gribniak et al., 2021)

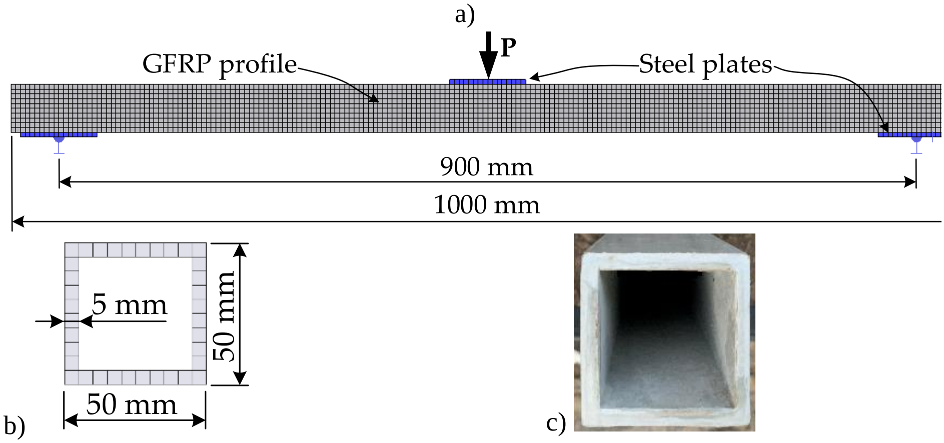

Fig. 2.5. Flexural FIBERLINE profile: (a) FE model; (b) the modelled cross-section; (c) Actual cross-section imperfection (Gribniak et al., 2021)

Fig. 2.6 compares the numerical prediction and the experimentally measured vertical displacements at the mid-span. The FE simulations consider the load increments applied in small (0.4 mm) steps.

Table 2.4 describes the accuracy of numerical predictions in the flexural stiffness *EI* and ultimate load P_u terms. The first three models represent the Ugira profile, and the FIBERLINE SHS sample was the modelling object of the remaining two simulations. The identical profile models had the same geometry, FE mesh, and material parameters; the volumetric fibre content was only the difference. The elastic analysis defines the flexural stiffness as follows:

$$EI = \frac{\mathrm{P} \cdot l^3}{48 \cdot u}, \tag{2.2}$$

where P and u define the load and corresponding vertical displacement; l is the loading span (= 0.9 m, Figs. 2.7 and 2.5a). The elastic behaviour of the flexural profiles (Fig. 2.8) makes the above simplification possible: the stiffness *EI* was calculated for the experimentally determined P-u pairs at all ascending load stages. Table 2.4 shows the *EI* and P_u values averaged for the identical profiles. The difference between the predicted and experimental outcomes divided by the test value defines the prediction error.

Table. 2.3. Parameters of the numerical models

Parameter	FIBERLINE	
	Model 1	*Model 2*
Fibre content V_f [%]	56.2	44.0
Tensile strength of fibre $f_{t,f}$ [MPa]	3445	
Elastic modulus of fibre E_f [GPa]	73.0	
The ultimate strain of fibre ε_u	0.047	
Compressive strength of polymer matrix f_c [MPa]	90	
Nonlinear behaviour onset of the polymer matrix in compression f_{c0} [MPa]	85.7	
Elastic modulus of polymer matrix E_m [GPa]	3.23	
Plastic strain at compressive strength of polymer matrix ε_{cp}	0.027	
Compressive ductility of polymer matrix ε_d	0.10	
Finite element size [mm]	5	

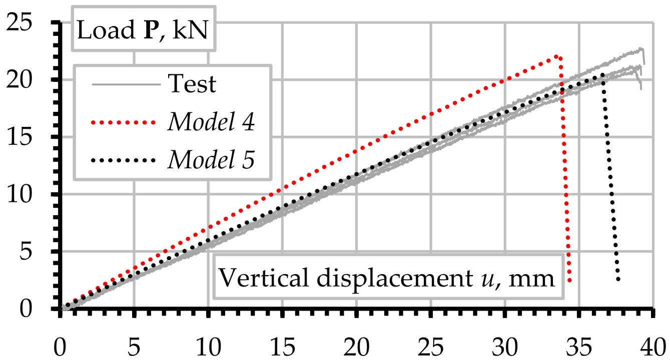

Fig. 2.6. Comparison of measured and numerically predicted load-vertical displacement diagrams at the FIBERLINE profile mid-span (Gribniak et al., 2021)

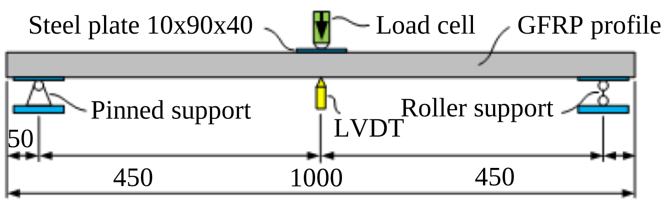

Fig. 2.7. Three-point bending test loading scheme (Gribniak et al., 2021)

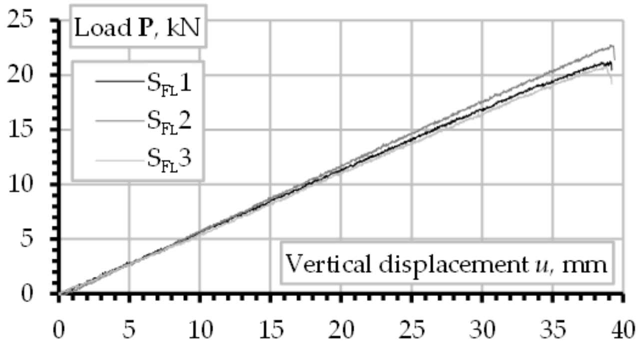

Fig. 2.8. Three-point bending test results of the FIBERLINE profiles (Gribniak et al., 2021)

Table. 2.4. Accuracy analysis of numerical models

<table>
<tr><th rowspan="2">Analysis</th><th rowspan="2">V_f [%]</th><th colspan="3">Flexural stiffness EI [kN·m^2]</th><th colspan="3">Ultimate load P_u [kN]</th></tr>
<tr><th>Test</th><th>Model</th><th>Error [%]</th><th>Test</th><th>Model</th><th>Error [%]</th></tr>
<tr><td>Model 1</td><td>56.2</td><td rowspan="2">8.62 ± 0.29</td><td>10.49</td><td>21.8</td><td rowspan="2">21.61 ± 1.04</td><td>22.16</td><td>2.5</td></tr>
<tr><td>Model 2</td><td>44.0</td><td>8.92</td><td>3.5</td><td>20.42</td><td>–5.5</td></tr>
</table>

The modelling results (Table 2.4) demonstrate that the assumed fibre volume V_f affects the predictions. The analysis of the FIBERLINE predictions identifies that an inadequate V_f assumption increases the EI prediction error from 3.5% (*Model 2*) to 21.8% (*Model 1*). However, the opposite tendency in the ultimate load prediction exists as the fibre content increase remedies the P_u predictions. This can result from the additional fibres identified during the heating tests regarding the manufacturer's specified content.

An efficient balance between the prediction accuracy and computation time characterises the developed FE approach that does not require specific descriptions of reinforcement geometry and refined meshes necessary for modelling the discrete fibres (Garnevičius et al., 2020). The ATENA software also allows smearing the reinforcement in different directions to represent the complex fibre architecture in GFRP profiles (Correia, 2013). The testing procedure is detailed in Section 3.2.1 of this dissertation.

2.2.2. Fibre-reinforced concrete

The proposed design concept requires verifying the FE model because of its fundamental role in developing an adequate design solution. In other words, a preliminary modelling result can make the optimisation process impossible under wrong assumptions. In the considered case (Fig. 2.1), the three essential parts compose the physically nonlinear FE model: the PFRC deck and supports, the fibre-reinforced polymer (FRP) profile and strip, and the bond between the components. So, a punching-shear test was completed to verify the FE model. Section 3.2.2 describes the physical test procedures. Juozapaitis et al. (2021) developed the considered PFRC to withstand substantial deformations in the stress-ribbon deck. The polymeric fibres make possible crack closure after removing the load. This dissertation adopts this concrete mixture to develop the beam prototype.

This section also includes the punching-shear test results using the 550 × 550 × 40 mm PFRC plates and the fibre pull-out test results and modelling. The following mix proportions for an m^3 were used: 356 kg of cement CEM I 42.5 R, 201 l of water, 177 kg of limestone powder, 890 kg of 0/4 mm sand, and 801 kg of 4/16 mm crushed aggregates. The concrete included a superplasticiser (2.6% of the cement weight) and 3.5 kg of the admixture SCP 1000 OPTIMIZER. The mixture also had 4.2 kg of *Durus EasyFinish* synthetic macro-fibres (40 × ∅0.7 mm, tensile strength = 500 MPa; modulus of elasticity = 6.0 GPa) and 0.6 kg of synthetic micro-fibres (13 mm × ∅22 μm, tensile strength = 380 MPa).

The plate samples simply supported through the perimeter were subjected to the vertical load localised at 100 × 100 mm in the centre. One part of the support line was modelled as pinned. The steel plate was divided into 3 mm finite elements, and the concrete plate was divided into 15 mm FE elements. In every modelling step, the load increased by 0.5 kN. Fig. 2.9 shows the loading scheme and setup; Fig. 2.10 shows the FE model and simulated and experimental cracking results, demonstrating good agreement. In addition, the load-bearing capacity prediction error did not reach 10%. So, together with the previous verification results in Section 2.2.1, these outcomes make the developed FE model (Fig. 2.1) reliable.

The previous studies (Garnevičius, 2020, 2021a, 2021b) developed and optimised the proportions of polymeric fibre-reinforced concrete (PFRC) used for producing the hybrid beam. This section verifies the material model of PFRC. Two tests are used for this purpose: synthetic fibre pull-out and PFRC slab punching shear. Section 3.2.2 describes the experimental details; this section focuses on the numerical modelling aspects.

Strength and stiffness are the key parameters characterising the bond performance of fibres in concrete. This research employs pull-out tests to investigate the bond behaviour of synthetic macro-fibres. Garnevičius et al. (2020) investigated two types of macro-fibres, but this section considers only one polymeric fibre type

(DURUS EASYFINISH) used for producing PFRC. The pull-out tests (Section 3.2.2) deemed two embedment lengths (i.e., 10 mm or 20 mm). The load-displacement diagrams from pull-out tests (Fig. 2.11) demonstrate the bond performance characterised by the strength and deformation modulus. In the second stage, further experimentation of the feasibility of improving the bond performance of the chosen fibre was explored.

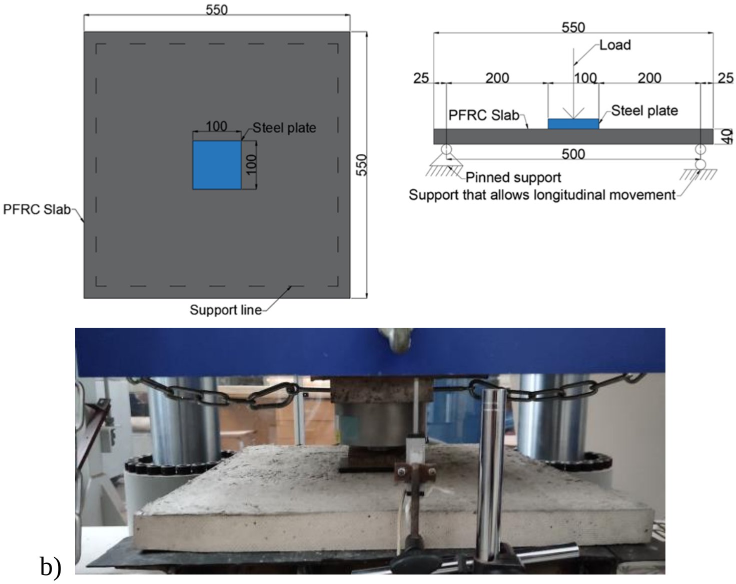

a)

b)

Fig. 2.9. Plate testing: (a) The plate schematic; (b) test setup (made by the author)

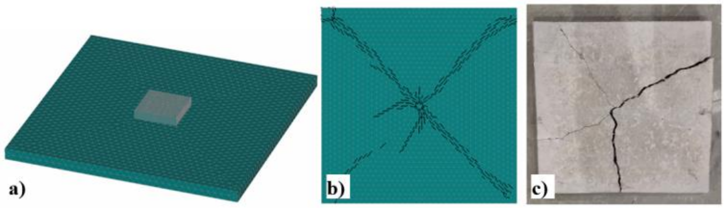

Fig. 2.10. Punching-shear test: (a) FE model, (b) simulated, and (c) experimental results (made by the author)

To verify different numerical modelling aspects, this section also describes the development of the numerical model suitable to predict the deformation response of a synthetic macro-fibre. The continuous pulling-out behaviour of the fibres is considered (i.e., failure of fibres was not modelled). The deformation problem is solved in the 3D formulation. Isoparametric tetrahedral elements with

10 degrees of freedom and four integration points are used. A rectangular shape replaced the round cross-section of the fibre, simplifying the FE model's development. The producer specified the 0.9 mm equivalent diameter of the fibre. The simplified geometry was calculated to represent the area and perimeter of the rectangle identical to the original dimensions. The 0.25×2.58 mm equivalent cross-section was obtained.

The pull-out tests of the synthetic fibres were a part of the research project that developed PFRC for the stress-ribbon bridge prototype (Juozapaitis et al., 2021). The 100 mm concrete cube represents the test sample. After testing the concrete specimens, the concrete compressive strength was determined to be from 48.0 MPa to 57.7 MPa. A detailed discussion of the results is given in the published article (Garnevičius et al., 2020). The 10 mm and 150 mm global sizes of finite elements with 100 times refinement at the bond contact satisfying the mesh comparability condition were assumed for the fibre and concrete. The resultant number of FE was approximately equal to 4000. Fig. 2.12 shows the FE models of different embedment lengths.

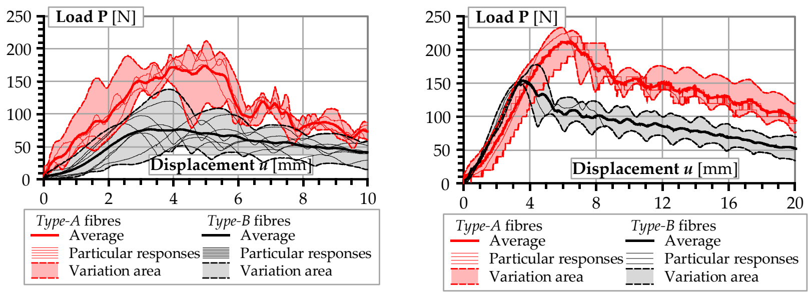

a) b)

Fig. 2.11. Load-displacement diagrams of the pull-out tests (Considered fibre: Type-A): (a) fibres with embedment length 10 mm; (b) 20 mm (made by the author)

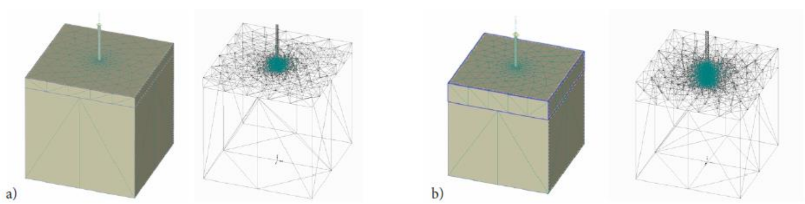

Fig. 2.12. FE models of different bonding lengths: (a) 1 cm embedded fibre; (b) 2 cm embedded fibre (made by the author)

The prescribed deformations were applied to the free end of the fibre in a step-wise manner. The loading step = 0.25 mm was chosen. Thus, the 10 mm and 20 mm embedment lengths simulations included 50 and 100 loading steps. The movements of the bottom surface of the specimen (Fig. 2.12) were fixed in all directions. The solution to the deformation problem employed the Newton-Raphson iteration procedure, assuming 40 iterations at each loading step.

The pull-out test results of the fibres having a 20 mm embedment length were used to verify the adequacy of the identified parameters of the bond model (Table 2.5). Fig. 2.13 demonstrates the results of this modelling. The specified bond model was found suitable to represent the deformation behaviour of synthetic macro-fibres. The prediction errors corresponding to the 10 mm and 20 mm simulation results do not exceed 4%. The developed model is suitable for simulating the averaged deformation behaviour of synthetic fibres characteristic of advanced mesoscopic models. A more detailed analysis of the modelling is provided in the published article (Garnevičius et al., 2021a).

Table. 2.5. Parameters of the concrete and bond models

Bond model	
Normal stiffness K_{nn}	1500 [GN/m^3]
Tangential stiffness K_{tt}	1500 [GN/m^3]
Tensile strength f_t	15.0 [MPa]
Cohesion factor C	7.0 [MPa]
Friction coefficient μ	0.20 [–]

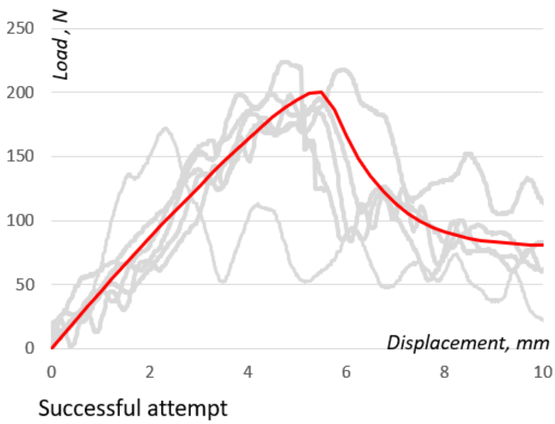

Fig. 2.13. Load-displacement diagrams of the 1 cm bonding length, the results (grey), and predictions (red) using the bond parameters described in Table 2.8
(made by the author)

2.3. Stage 2: Development of the finite element model

The ATENA software helps analyse deformation response and predict the load-bearing capacity of the hybrid beam by simulating a four-point bending test. The material models verified in the previous works (Gribniak et al., 2021; Garnevičius et al., 2020) describe the mechanical behaviour of PFRC and FRP components. The tetrahedral mesh generates the finite element (FE) model, shown in Fig. 2.14. The plates of perfectly elastic material protect the concrete on the load application points (Fig. 2.14a) and have a 15 mm FE mesh size. The monolithic concrete part of the beam (Fig. 2.14b) has a 30 mm mesh size; the CFRP strip and GFRP profile have a 7.5 mm finite element size. This mesh was dense enough to ensure the accuracy of the calculations. The model monitoring results are vertical displacements at the midspan and load application points.

The Nonlinear Cementitious material model (Garnevičius et al., 2020) with 55 MPa compressive strength, established in Section 2.2.2, determines the deformation behaviour and failure mechanism of PFRC. An elastic-plastic model (elasticity modulus = 170 GPa and tensile strength = 2.8 GPa) determines the material behaviour of the 10 × 1.4 mm CFRP strip (Gribniak et al., 2021).

The 3D solid finite elements describe the polymer matrix of the GFRP profile, assuming the fracture mechanic principles for tensile failure and the plasticity approach to compressive failure. Gribniak et al. (2021) adapted the smeared reinforcement model, which is described in Section 2.2.1, initially developed for reinforced concrete elements with structural mesh reinforcement (Cervenka, 2002), to represent the glass filaments and verified this numerically efficient solution, simulating the three-point-bending tests of FRP profile fabricated by the same manufacturer as in this dissertation. The verification (Gribniak et al., 2021) demonstrated the FE model's ability to predict the profile's load-bearing capacity and deformation response. An elastic-brittle constitutive law defines tension failure of the fibres oriented in the pultrusion direction. The same burning tests, detailed in the Third Chapter, were completed with the FIBERLINE I profile used in the hybrid beam prototypes. Similarly, as mentioned in Section 2.2.1, the V_f was determined to be 63.4%. The polymer matrix has an elastic modulus of 3.23 GPa and a tensile strength of 90 MPa. The E-glass fibres (smeared reinforcement) have a 73 GPa elastic modulus and a 3445 MPa tensile strength; the filaments do not resist compression stresses. The perfect connection was assumed between all the model components.

The first loading stage considers the self-weight of the beam. Two concentrated loads were applied in succeeding increments, resulting in a 0.125 kNm moment increase at each successive increment on the 600 mm pure bending zone (Fig. 2.2). The model was then calculated, and results were obtained.

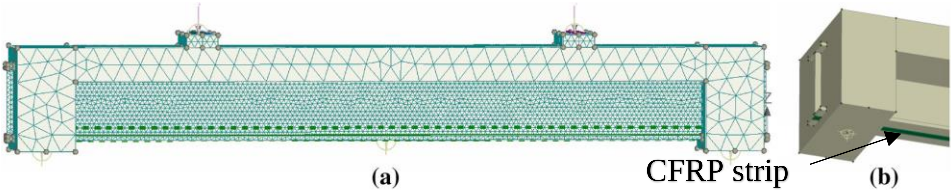

Fig. 2.14. Finite element model of the hybrid beam: (a) FE discretisation; (b) support view (made by author)

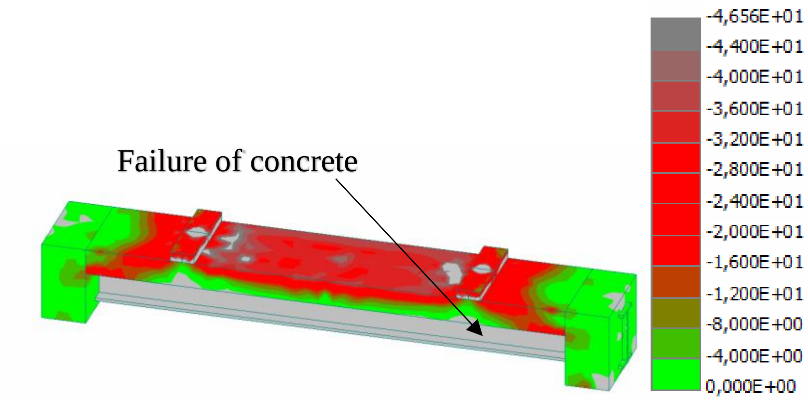

Fig. 2.15. Compression stress prediction results of the first series beam (in MPa) (made by the author)

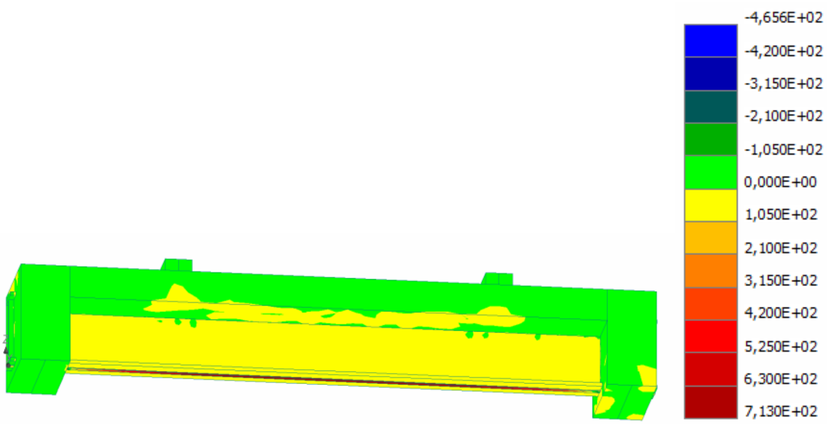

Fig. 2.16. Normal stresses in the preliminary hybrid beam model (in MPa) (made by the author)

Fig. 2.15 shows the compression stresses in the PFRC part of the beam and the supports. The failure occurred in the compressed concrete near the support at the 17.25 kNm bending moment or 138 kN load; the calculated vertical displacement at the mid-span was equal to 10.4 mm. This was the most considerable deflection of the beam. Fig. 2.16 shows the stresses in the beam in the longitudinal direction. The CFRP strip is the most affected component, bearing the maximum tension stresses (713 MPa).

After gaining the results from the monitoring points selected during the FE modelling, the moment-curvature diagram was formed. The moment-curvature response describes the adequate measure of the global deformation behaviour of the composite beams (Gribniak, 2009; Gribniak et al., 2021, 2021). The curvature was calculated in the pure bending zone from the deflections, assuming the circular deformation shape of the beam:

$$\kappa = \frac{8 \cdot \delta}{l_b^2 + 4 \cdot \delta^2}, \delta = L_2 - (L_1 + L_3)/2, \tag{2.3}$$

where l_b is the length of the pure bending zone (= 600 mm); L_1, L_2, and L_3 are the monitoring point readings.

After calculating the curvature, a graph was created with the results (Fig. 2.17). This graph will be compared to the physical test results and used as a reference point. The physical tests in Sections 3.3 and 3.4 verify the model's adequacy.

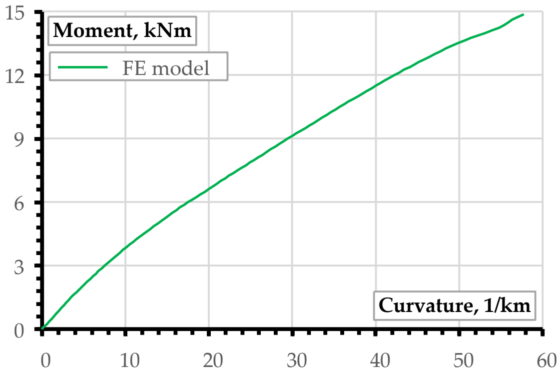

Fig. 2.17. Modelled moment-curvature diagram sets the design reference (the perfect FRP connection to the supports) (made by the author)

2.4. Stage 3: Design adaptation

Following the proposed adaptive design concept (Fig. 2.1) and using the FE model verified in Section 2.3, the reference design solution is calculated for the hybrid beam prototype, shown in Fig. 2.2. The design adaptation refers to physical tests of the corresponding beam prototype. This section presents the physical test results, while Section 3.3 describes the testing procedure.

The moment and curvature diagrams were created using Eqn. 2.3 presented in the previous chapter. Instead of monitoring point readings, during the physical tests, linear variable displacement transducers (LVDTs) were used to capture the vertical displacements at the beam mid-span and below the load application points. A detailed description of the preparations, concrete casting, and the physical tests themselves is given in the Third Chapter.

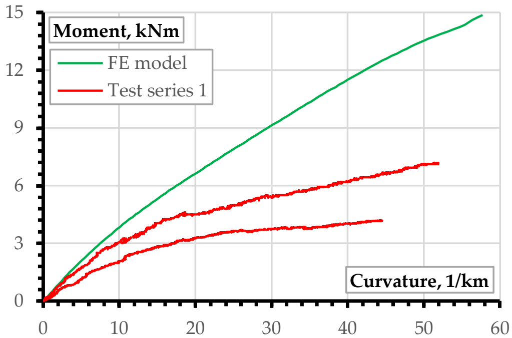

Fig. 2.18. Comparison of the FE modelling and the first series testing moment-curvature relationships (made by the author)

The diagrams from the modelling and the first series of physical tests are compared in Fig. 2.18. This figure shows the corresponding moment–curvature diagrams from the first test series results and numerical simulations. In this research, the FE modelling outcomes define the reference for developing an efficient hybrid beam system. As described in Section 1.3, efficiency is understood as the ability of the physical prototype to outperform the numerical prediction results.

The first design stage considers the results shown in Fig. 2.18. The insufficient strength and stiffness of the beam (Fig. 2.2) are evident. It was hypothesised that disagreement between the test and modelling outcomes results from an inadequate resistance of the support joints. Therefore, it was arbitrarily decided to reduce the bond strength (10 Pa) between the FRP components (GFRP profiles and CFRP strips) and concrete supports to predict the same beam stiffness, as observed experimentally. Fig. 2.19 shows the compression stresses in the PFRC part of the beam and the supports. The failure of the concrete supports occurred at the 5.75 kNm bending moment or 46 kN load; the calculated vertical displacement at the mid-span was equal to 7 mm. This was the most significant deflection of the beam, with a weak connection in the supports between the concrete and the GFRP and CFRP. Fig. 2.20 shows the normal stress distribution. The CFRP strip is still the most affected component, bearing the maximum tension stresses (205 MPa) just like in the perfectly connected model before. Fig. 2.21 shows the corresponding simulation results and the test outcomes. This figure shows the experimental results of nominally identical beam samples in red lines. The observed diversity could result from the geometry differences, which significantly affect the deformation performance of the test samples. On the contrary, the numerical model (green line) assumes the averaged geometry characteristics.

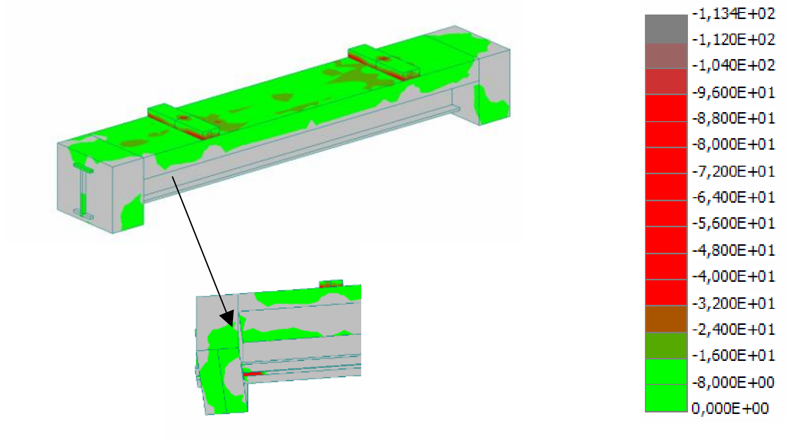

Fig. 2.19. Compression stress prediction results of the first beam series with a weak connection at supports (in MPa) (made by author)

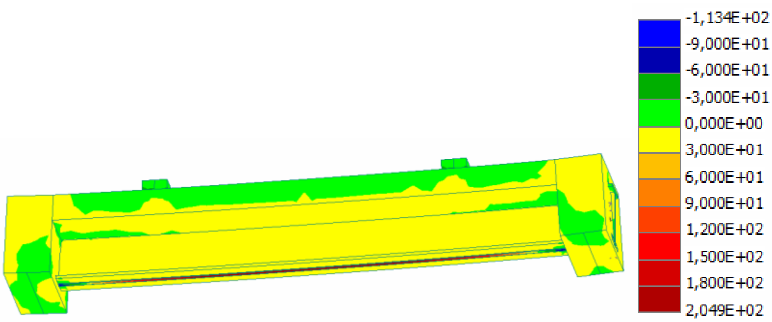

Fig. 2.20. Normal stresses in the preliminary hybrid beam model with a weak connection at supports (in MPa) (made by author)

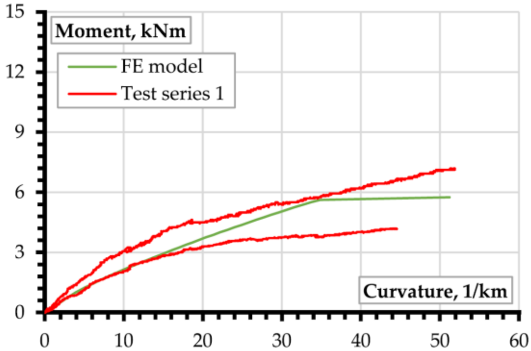

Fig. 2.21. Comparison of the moment–curvature from the FE modelling with a weak contact between the GFRP profile and concrete supports and the first series test results (made by the author)

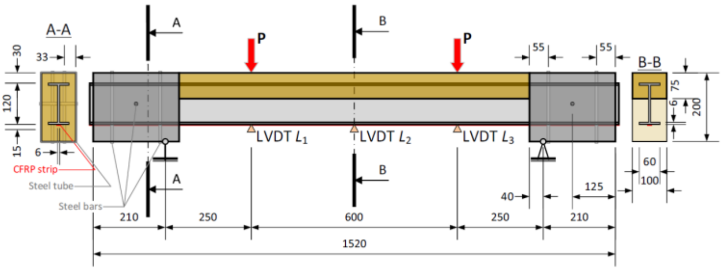

Fig. 2.22. Updated hybrid beam schematic and modified cross-sections (made by the author)

A modification of the support blocks was needed, so our beam schematic was redesigned (Fig. 2.22), and a second beam series was produced and tested. This section presents only the physical test results to simplify the comparative analysis, while Section 3.4 describes the testing procedure. The blue lines in Fig. 2.23 illustrate the deformation response of the second beam series. The test outcomes reveal noticeable agreement with the FE model, considered an efficient reference, assuming the perfect bond between all composite parts of the hybrid beam and an increase in the 107.5% load-bearing capacity regarding the first series of hybrid beams. Moreover, the second series of beams had no perforation of the GFRP profile.

Fig. 2.23 exemplifies the proposed design philosophy when an experimentally verified numerical model describes the target reference. In this figure

(Fig. 2.23), blue lines show the second test series experimental outcomes of two nominally identical beam samples.

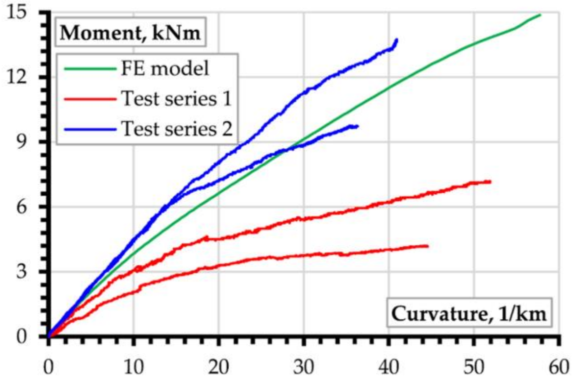

Fig. 2.23. Experimental moment–curvature relationships of the hybrid beams (both series) compared with the numerical prediction (made by the author)

The detailed analysis requires additional tests (to ensure the reliability of the numerical estimations). However, the differences between the alternative solutions shown in Figs. 2.18 and 2.21 are apparent, illustrating the concept's efficiency. Thus, the results of the second beam series (Fig. 2.23) allow for a relationship between the improvement of the structural performance and the proposed modification of the support joints, anchoring the GFRP profile. In addition, this solution simplifies the numerical model as the perfect bond assumption solves the modelling problems reported in the literature (Muc et al., 2020), making the FE approach acceptable for designing the hybrid systems considered in this dissertation.

After the preliminary tests (Series 1 and 2), the mechanical performances of the PFRC and FRP hybrid, reinforced concrete (RC), and steel-concrete composite beams were compared. These elements had the same flexural stiffness (EI = 0.310 MPa·m^4). The steel-concrete beam included the 50 × 25 mm S355 steel I-profile with 3 mm thickness, and the RC beam was reinforced with three 16 mm bars of B500 steel. The concrete strength was identical (C55) for all samples. All the beams were modelled using the FE software ATENA. A four-point bending simulation was carried out, adding two 0.5 kN loads per step. All elements had the 600 mm pure bending zone and 250 mm shear spans. Table 2.6 compares the load-bearing capacity, relative weight, and deflections of the beams. The cross-sections of the steel-concrete composite and RC beams are provided in Fig. 2.24. The hybrid beam was 25.8% lighter than the RC beam, as shown in Table 2.6. However, the steel-composite beam was of similar weight (Steel-concrete =

17.93 kg, FRP-PFRC = 18,44 kg) but had only half of the load-bearing capacity of the hybrid FRP-PFRC beam (Steel-concrete = 67 kN, FRP-PFRC=138 kN). Thus, the efficiency of the proposed hybrid beam system is apparent compared to other composites.

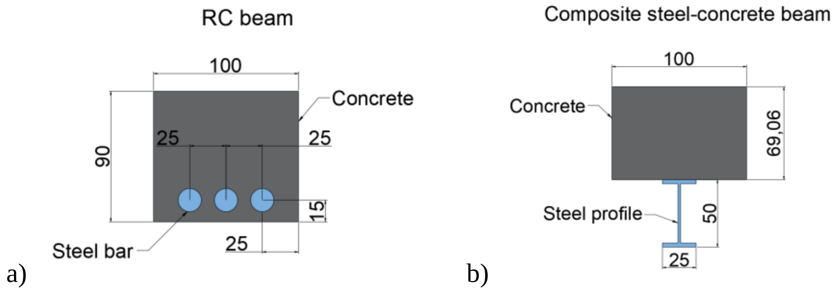

Fig. 2.24. Composite beam cross-sections: (a) RC beam; (b) steel–concrete composite beam (made by the author)

Table. 2.6. Beam load-bearing capacity and weight comparison

Beam type	Load-bearing capacity/max displacement	Relative weight, kg/m
FRP-PFRC	138 kN/10.4 mm	18.44
Steel-concrete	67 kN/52.0 mm	17.93
Reinforced concrete	106 kN/56.0 mm	24.85

2.5. Large-scale beam design

This section extends the proposed prototyping concept (Fig. 2.1) to the large-scale hybrid beam. The preparations and testing details are provided in Section 3.5. Fig. 2.25 shows the preliminary solution of the 3 m long prototype accounting for the modified design of the support joints (Fig. 2.22). As Fig. 2.25 shows, the GFRP profile height increased from 120 mm to 200 mm (I-profile by FIBER-LINE, Denmark) regarding the prototype in Fig. 2.22. This increment increases the size of the concrete part and supports. Simultaneously, the CFRP strip dimensions (10 mm × 1.4 mm by S&P C-LAMINATE, UK) and concrete proportions remained the same. As in the previous cases, the simulation employs the software ATENA and the same material models as for the preliminary tests (Section 2.3). The load increment was two 0.5 kN loads per step.

Figs. 2.26 and 2.27 show the FE model and the normal stress distribution corresponding to the ultimate load. The predicted load-bearing capacity is 105 kN, and this load induces the 29.4 mm displacement at the mid-span. The failure was due to the crushing of the concrete in the pure bending zone (the red-filled area in Fig. 2.27).

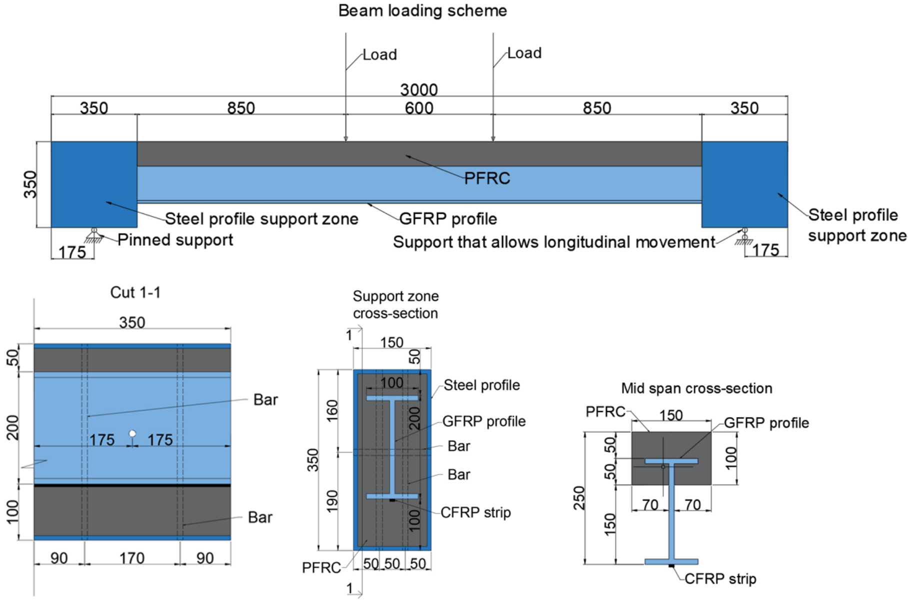

Fig. 2.25. Hybrid beam schematic and cross-sections of the support and mid-span zones (dimensions in mm) (made by the author)

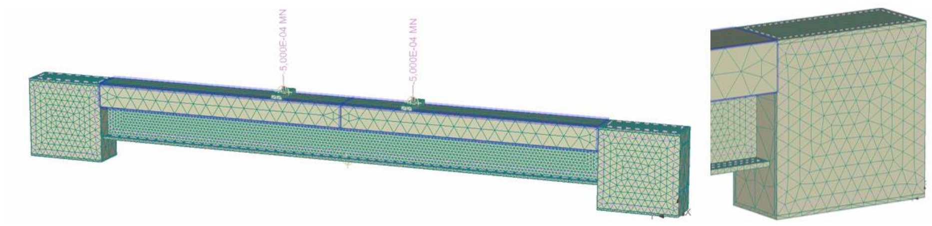

Fig. 2.26. Finite element model of the large-scale hybrid beam (made by the author)

The developed beam's deformation performance was expected to correspond to the predicted one. However, that was not the case for this beam. For example, Fig. 2.28 compared the vertical displacements measured at the mid-span (the black line) and predicted numerically (the red diagram). The difference between these graphs is evident.

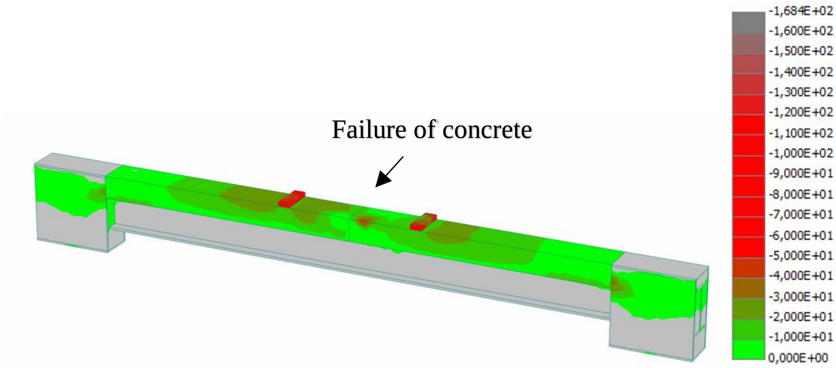

Fig. 2.27. Compressive stress distribution (MPa) in the large-scale beam FE model) (made by the author)

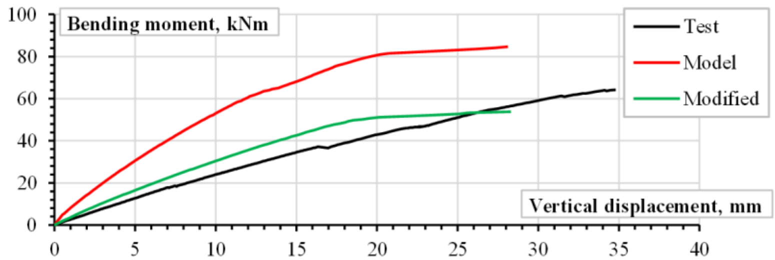

Fig. 2.28. Comparison of experimentally measured and modelled deformation results (made by the author)

Analysis of the modelling results identified the substantial stresses localised in the CFRP strip (distributed on the tension surface of the GFRP profile). Therefore, to overcome the apparent difference between the mechanical performance of the physical object and the numerical model, Fig. 2.28 includes the prediction results of the beam, excluding the mechanical contact between the CFRP strip and concrete on the supports (the green graph).

Remarkably, the typical monitoring devices did not capture the integrity loss of the hybrid system. Still, modifying the numerical reference model defined the manufacturing hybrid beam's technological drawback (i.e., insufficient bonding performance of the supports). The previous research (Garnevičius & Gribniak, 2022) obtained a similar outcome at the first production stage, proclaiming the vital role of the quality of the supports for the proposed structural system, which increases with increasing the hybrid beam dimensions. This result defines the further improvement object.

After the last beam (S-6) was tested with larger support joints and low prestress in the CFRP, the load-bearing capacity of this beam was close to that of the modelled beam, with perfect connections between the CFRP and GFRP. The difference was lower than 14%. The failure mode and location were similar to the model predictions (Fig. 2.29).

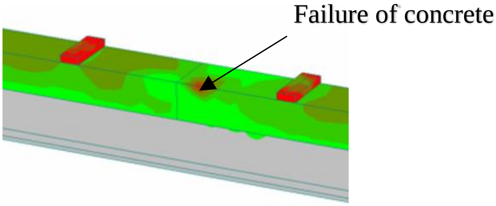

a)

b)

Fig. 2.29. Comparison of FE model and S-6 beam: (a) failure of FE model with perfect connection with the CFRP, (b) failure that occurred during testing (made by the author)

2.6. Conclusions of the Second Chapter

This chapter determines an adaptive design concept when the numerically predicted outcome modifies the design target. Considering advanced composite materials, the modelling outcome determines the desired mechanical performance because of a lack of design guidelines. Physical tests verified the FE model (GFRP and PFRC materials and bond models). The pilot tests checked the viability of the developed composite structure, providing the engineer with an apparent solution to the support problem resulting from a low resistance of pultruded FRP profiles to transverse loads regarding the pultrusion direction. Thus, the supports' quality controls the hybrid beam stiffness and load-bearing capacity without the additional FRP bond improvement with concrete. Although the formal solution requires further tests to ensure the result's reliability, the apparent difference between the alternative solutions and the ability to control the design outcome proves the proposed adaptive design concept.

1. The adaptive design modification improved the test outcomes of the second beam series, revealing noticeable agreement with the FE model and doubling the stiffness and load-bearing capacity of the hybrid beam system regarding the first series results. The physical prototype change moved the hybrid beams' mechanical properties to the predicted FE modelling results, diminishing the need for additional physical tests. Therefore, the numerical model can be regarded as an efficient reference: the supports' enhancement doubled the beam's flexural stiffness and load-bearing capacity regarding the reference bridge with typical weak supports without the additional GFRP bond improvements.
2. By fixing the FRP components in the rigid supports, the numerical model is simplified, i.e., the perfect bond assumption solves the modelling problems reported in the literature, making the FE approach acceptable for designing the hybrid systems considered in this dissertation. The longitudinal strain distribution was observed during the physical testing to verify the correctness of the perfect bond assumption between the model components, identifying no noticeable slip. This result proves the ideal bond modelling assumption.
3. An adaptive design concept can be considered for practical applications when an experimentally verified numerical model describes the desired structural design of an FRP-concrete hybrid beam. This concept can include advanced optimising algorithms that can double the structure's flexural stiffness and load-bearing capacity, even if the concrete support system is weak. Nevertheless, it is imperative to conduct further tests to ensure the results' reliability and optimise the support blocks' geometry.
4. The verified model was also compared to other composite beams (steel-concrete, reinforced concrete). It was found that the hybrid FRP-PFRC beam was 25.8% lighter than the RC beam. However, the steel-composite beam was of similar weight but had only half of the load-bearing capacity of the hybrid beam.

3

Experimental Programme of the Adaptive Design Concept

The chapter discusses the experimental programme completed to acquire material parameters of the glass and carbon fibre-reinforced polymer (GFRP and CFRC) materials, the physical tests of the prototype hybrid beams, and the large-scale beams. Longitudinal strain distribution in the hybrid beams is also discussed in this chapter, revealing strain compatibility of the hybrid cross-section components. The results of this chapter were published in journal articles (Gribniak et al., 2021; Garnevičius et al., 2020, 2021a; Garnevičius & Gribniak, 2022) and conference presentations (Sokolov et al., 2018; Garnevičius et al., 2021b).

3.1. Experimental programme

This section describes the proposed design concept when the verified finite element (FE) model describes the adaptive design reference. The physical tests were carried out in three stages, and two nominally identical beams were produced for each series. First, the specimens were poured using the same mix proportions with a target 55 MPa compressive strength, as considered in the previous studies (Gribniak et al., 2021; Garnevičius et al., 2020). The Second Chapter specifies the concrete mix proportions and structural schemes for all three series of tests (Figs. 2.2, 2.22, and 2.25).

The physical testing was conducted after the adaptive design concept was devised, and a preliminary design scheme of the hybrid beam sample was created. The first series of tests showed that the initial design concept required modification. Analysing the numerical model outcomes, i.e., modifying the FE model to represent the test's outcome, revealed the concrete supports' insufficient strength. The second test series was conducted after changing the design solution of the hybrid beam's supports. The second series of test results agreed with the reference FE modelling results, proving the adaptive design concept. Lastly, a large-scale beam test was conducted to verify the proposed adaptive design concept with a larger beam span.

3.2. Verifying material models

As mentioned in Section 2.2.2, the proposed design concept requires verification of the FE model. The fibre-reinforced polymer (FRP) profile verification tests have been described in Section 3.2.1. In addition, Section 3.2.2 describes the punching-shear slab test and fibre pull-out test for verifying the polymeric fibre-reinforced concrete (PFRC) constitutive model.

3.2.1. Pultruded glass fibre-reinforced polymer profile tests

This section employs the results of the GFRP profiles tested by Gribniak et al. (2021). It describes the internal structure analysis results of the I-shaped profile (FIBERLINE, Denmark) employed in the hybrid beam prototype. This analysis is necessary to quantify the fibre content and develop the finite element (FE) model (Section 2.3). In addition, the mechanical (bending) test of a square hollow section (SHS) profile verifies the adequacy of the FE model in Section 2.2.1. The geometrical shape of the profile is irrelevant to the determination of the material properties; the results can be easily applied to any profile shape, including I profiles. Polyester and vinyl ester resins reinforced with continuous E-glass filaments compose the FIBERLINE profile; the manufacturers' provided fibre mass percentages were 60 ± 5% (FIBERLINE, 2021).

The SEM analysis identified that the GFRP samples have a visually dense structure, few tiny pores, and good adhesion between the fibre and the matrix (Fig. 3.1a). The filaments have a diameter of approximately 21–25 μm. In addition, several layers have been identified in the GFRP material, showing a complex fibre alignment (Fig. 3.1b). The profiles manufactured by FIBERLINE employ a more sophisticated pultrusion method, ensuring higher mechanical properties. However, Fig. 3.2 shows a microstructure corresponding to the cut-side surface consistent with the pultrusion direction of the FIBERLINE profile. Numerous damaged filaments result from such a cut. This figure also demonstrates the bond damages of the separate fibres (Fig. 3.2b). Similar surfaces define the boundaries of the specimens for determining the effective fibre fraction V_f. The filament damages (Fig. 3.2a) explain the reinforcing efficiency losses in the material verification testing phase. Perforation of FRP profiles can result in a decrease in mechanical properties. Avoiding unnecessary perforation would avoid such a decrease.

Heating (matrix evaporation) tests also determined the fibre content in GFRP. The standard ISO 1172:1996 "Textile-glass-reinforced plastics. Prepregs, moulding compounds, and laminates. Determination of the textile-glass and mineral-filler content. Calcination methods" defines the test procedure requirements. An electric furnace SNOL 7.2/1100 (SNOL, Lithuania) was used for these tests. For that purpose, small fragments (≈ 10 g), cut from the walls and flange joints of the profiles, were dried until the constant weight at 105 ± 5 °C (the drying time = 24 h). After that, the specimens were heated at 625 ± 5 °C until the polymer evaporated. The heating regime: 2 h to reach a temperature of 625 °C and 3 hours to achieve a constant weight. The heating procedure determines the mass percentage of fibres w_f and Eqn. 2.1 defines the volume fraction V_f. This parameter is necessary for the numerical modelling to describe the fibre reinforcement area in the cross-section (Gribniak et al., 2012, 2021).

The analysis results of three GFRP wall and flange joint samples had 71% fibre content on average. This demonstrates that the estimated fibre content exceeds the mass fraction declared by FIBERLINE (60 ± 5%). The neglecting of the weight of the heat-resistant aggregates cannot explain such a big difference that can be a consequence of the complex reinforcement architecture if the manufacturer specifies only longitudinal fibre content.

FIBERLINE design manual (FIBERLINE, 2003) states that various types of roving and intricate weaves and mats compose the reinforcement system of the pultruded structural profiles. Unfortunately, detailed information about the fibre percentage and orientation is missing in the FIBERLINE datasheets. Similarly, tests were conducted with the I-shaped profile used for the hybrid beams, and the fibre volume fraction (V_f) was calculated to be 63.4%. The I-profiles also have almost identical fibre content in the wall and flange joint specimens. Thus, the current pultrusion technologies solved the resin localisation problems at the web-flange junction.

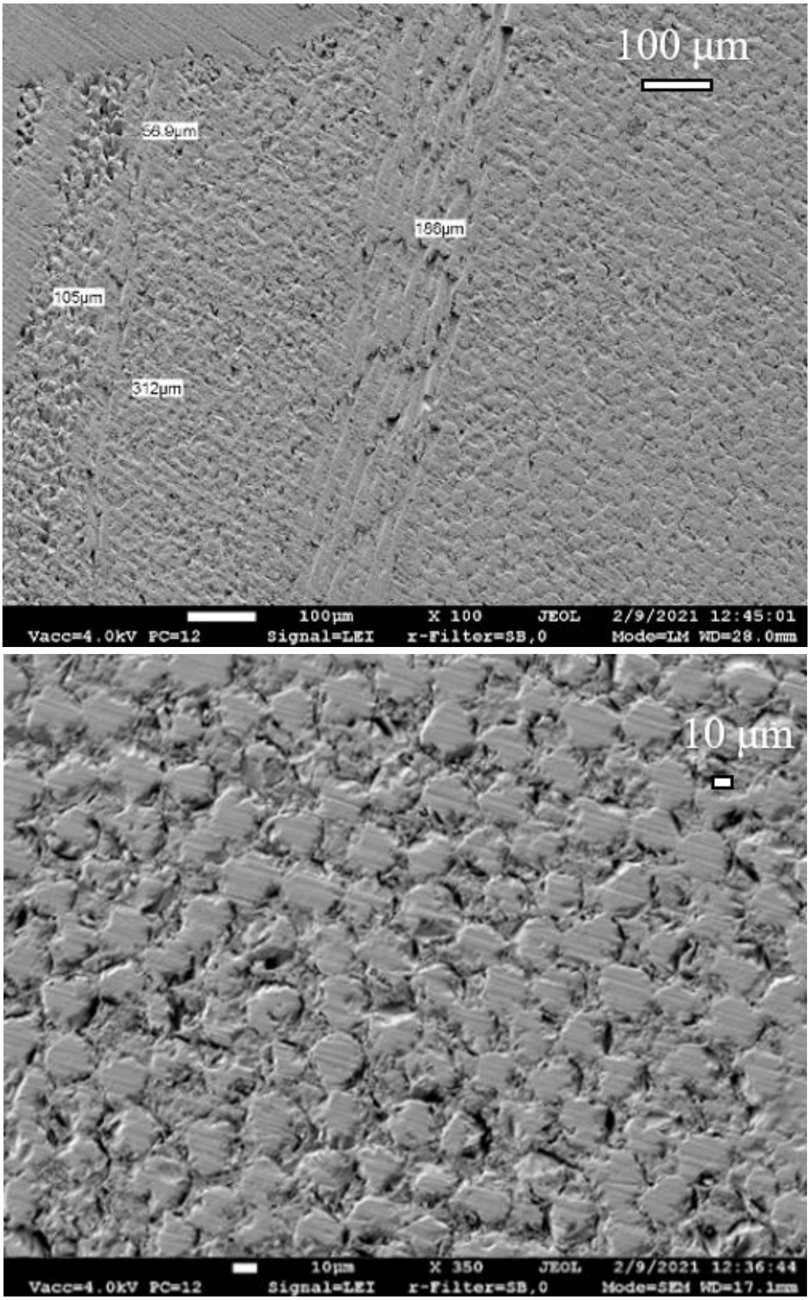

a)

b)

Fig. 3.1. SEM images of the GFRP I-shaped profile: (a) layered fibre distribution in the flange joint (x100 magnification); (b) fibre distribution in the wall (×350 magnification) (Gribniak et al., 2021)

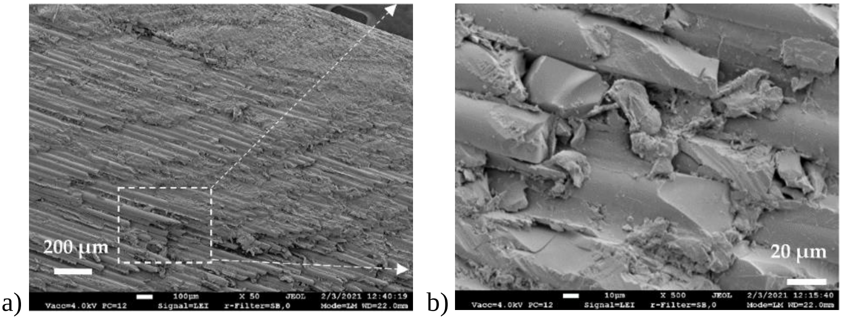

Fig. 3.2. Microstructure corresponding to the profile cut-side surface consistent with the pultrusion direction: (a) ×50 magnification; (b) ×500 magnification. Note: the rectangle indicates the location of the zoomed view in the image (b) (Gribniak et al., 2021)

The FE model verification employs the previous tests of SHS profiles of the same producer and the same internal structure (including the fibre content) (Gribniak et al., 2021). This research employs three FIBERLINE (50 × 50 × 5 mm) GFRP profile samples. All the test samples had a length of 1000 mm and were tested until failure. Steel rollers and bearing steel plates protected the GFRP profile from local damage. Fig. 3.3 shows the loading setup.

A 5 MN capacity servohydraulic machine LFV 5000 (W+B, Switzerland) loaded the profiles under displacement control. A 100 kN capacity cell measured the applied load; a digital image correlation (DIC) system captured surface deformation of the bending element; paired 100 mm range and 0.01 mm precision linear variable displacement transducers (LVDT) measured the mid-span vertical displacements. An ALMEMO 2890-9 data logger acquired the test data every second.

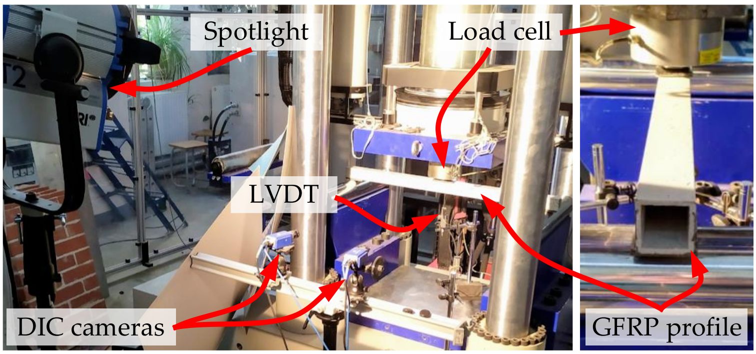

Fig. 3.3. Three-point bending test setup (Gribniak et al., 2021)

Fig. 2.8 in the Second Chapter shows the average mid-span displacements measured by the paired LVDTs (Fig. 2.7). The load-displacement diagrams of all specimens are almost linear until the ultimate load. The samples also revealed similar flexural stiffness and crushing failure mechanism of the compressive zone followed by cross-section integrity loss. The GFRP profile test results were in good agreement with the modelling results, which allowed the creation of a verified GFRP material model.

3.2.2. Verifying the constitutive model of the fibre-reinforced concrete

Wood formwork was cut out for casting the 550 × 550 × 40 mm PFRC plates (2 in total). After the formwork, a steel frame was welded to support the plate samples through the whole perimeter during testing. Then, the concrete mixture was cast into the forms (Fig. 3.4) and vibrated on a vibration table to densify the concrete. Finally, the plates were left to set for 28 days in laboratory conditions. The concrete mix used is given in Section 2.2.2 of this dissertation.

The punching shear test was carried out with a 5 MN servohydraulic press machine with the load applied in the displacement control manner with the 0.4 mm/min rate. A load cell was used to measure the applied load. An ALMEMO 2890-9 data logger recorded the reading of all LVDT devices and the load cell. The outputs were collected every second. Two LVDTs were used to measure the displacements on two sides of the servohydraulic presses plate (Fig. 3.5), and the vertical load was concentrated through a 100 × 100 mm steel plate in the middle of the PFRC plate. The steel frame was placed underneath the plate specimen, and rubber strips were put between the supports and frame to ensure the PFRC plate was not locally damaged during testing.

Fig. 3.4. Casted PFRC plate (made by the author)

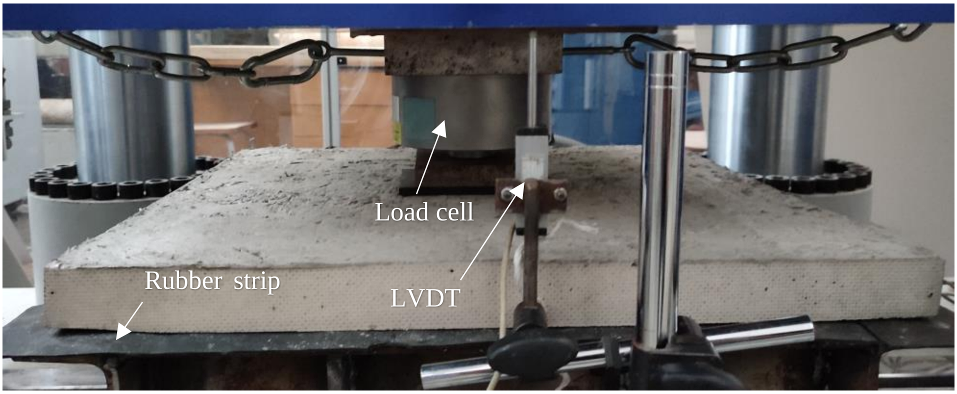

Fig. 3.5. Punching-shear test setup (made by author)

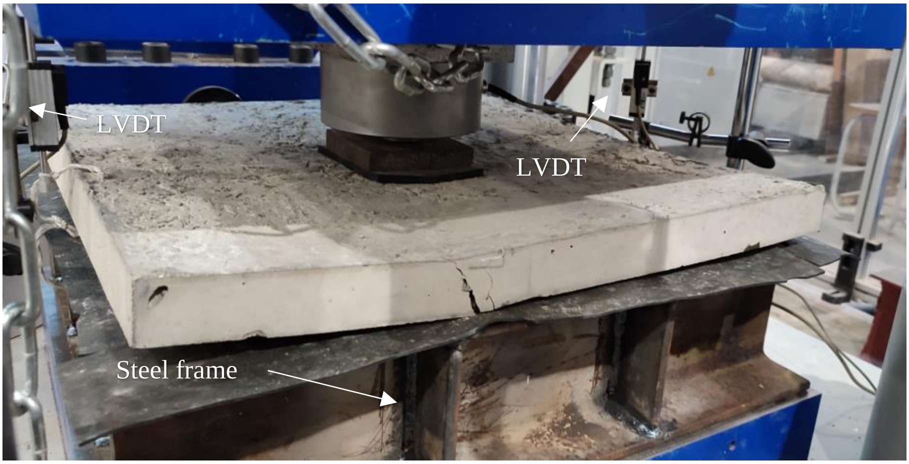

Fig. 3.6. PFRC plates specimen after failure (made by the author)

During the tests, the PFRC plates were tested until failure (Fig. 3.6). The load-bearing capacities of the plates were 9.5 kN and 10.5 kN, which agreed with the FE prediction discussed in Section 2.2.2. The modelling results of these tests are described in more detail in the Second Chapter. The cracking results were also very similar and are provided in Fig. 2.10.

The bond parameters of the synthetic macro-fibres needed to be determined to ensure an efficient bond with concrete. Previous studies conducted pull-out tests (Garnevičius et al., 2020, 2021a, 2021b) to determine bond parameters and optimise the proportions of polymeric fibre-reinforced concrete (PFRC) used for producing the hybrid beam. The modelling and results of these tests are provided in Section 2.2.2. This section will describe the experimental programe of the pull-out tests.

Garnevičius et al. (2020, 2021a, 2021b) considered two types of polymeric fibres. Still, this section includes only the fibres used in the hybrid beam prototype's polymeric fibre-reinforced concrete (PFRC) (Section 2.2.2). The selected fibres (Fig. 3.7a) had a length of 45 mm and an equivalent diameter of 0.9 mm; it had a tensile strength of 465 MPa and an elastic modulus of 3350 MPa. The selected fibre had a deep texture of surface embossment. The fibres were partially embedded in 100 mm cubes for pull-out testing; two bonding lengths (10 and 20 mm) were considered. The test campaign encompassed two sets of specimens from the two embedment lengths. Each group was experimentally investigated by testing with eight cubes. In total, 16 cube specimens were prepared. Expanded polystyrene was placed in the moulds (Fig. 3.7b) with fibres inserted before concreting to ensure the exact position of the "side" fibres (Fig. 3.7c).

All cube samples were produced from one concrete batch. The average compressive strength of the 100 mm concrete cubes was obtained at 28 days, and the testing date was at 153 days, equalling 39.14 and 46.16 MPa, respectively.

Fig. 3.8 shows the typical examples of the pull-out tests. The testing apparatus was a 75 kN capacity electromechanical machine H75KS (TINIUS OLSEN, Norway). The fibre under testing was loaded in a deformation-control manner with a 0.8 mm/min loading rate. A 2 kN load cell was employed to measure the applied load. Using such a relatively small capacity load cell could achieve higher measurement precision. Vertical displacements of the grips were monitored using linear variable differential transformers (LVDT), as shown in Fig. 3.9d; an additional LVDT was installed to monitor the vertical movements of the cube specimen. The unsuccessful results of the first trials motivated the development of a gripping system to protect the fibres from local damage. Plastic sleeves (Fig. 3.8a) were used to preserve the fibres' unbonded part from damage. The sleeves' mechanical properties (flexibility and friction coefficient) were chosen using the trial-and-error procedure. Adjustable steel clamps (Fig. 3.9a) were additionally introduced to fix the protected fibre, preventing the localisation of stresses induced by the gripping system of the tension apparatus (Fig. 3.9b–d).

After the testing was finished, it was clear that using two different types of fibres was beneficial to the performance of the concrete. Adding micro-fibres improved the bond performance of the macro-fibres, so these fibres and concrete mixture were chosen to verify the adequacy of the identified parameters of the bond model. After testing was completed, the results were compared to the modelling results. Both results were in good agreement, as shown in Fig. 2.13, and the prediction errors corresponding to the 1 cm and 2 cm simulation results do not exceed 4%, proving the adequacy of the PFRC model developed in Section 2.2.2.

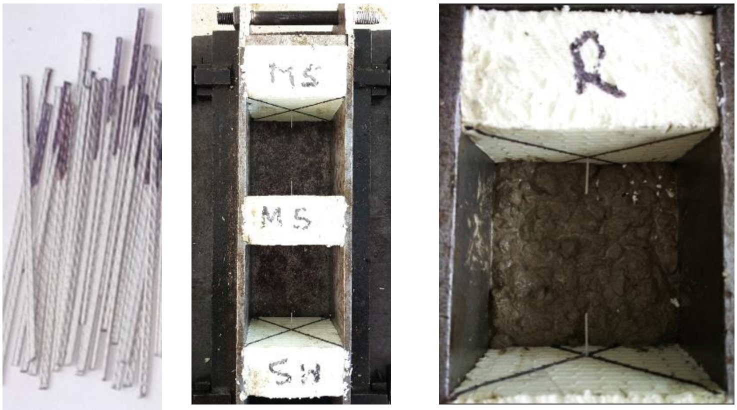

a) b) c)

Fig. 3.7. Preparing pull-out test specimens: (a) DURUS EASYFINISH polypropylene fibre; (b) steel moulds with expanded polystyrene; (c) mould partially filled with concrete (made by the author)

a) b) c)

Fig. 3.8. Preliminary pull-out tests of synthetic macro-fibre: (a) fibres protected with a plastic sleeve; (b) failure of the fibre samples due to slip of the protection sleeve; (c) loss of the cohesive contact with the grips (made by the author)

The results were used in developing the PFRC to withstand substantial deformations in the stress-ribbon deck. The polymeric fibres caused the crack closure after removing the load. Selecting an efficient type of fibre and concrete mixture is essential to ensure the required ductility, cracking resistance, and overall stiffness of the beam system. This research adopts this concrete mixture to develop the hybrid beam prototype.

a) b) c) d)

Fig. 3.9. Gripping system: (a) steel clamps; (b) inventory grips by testing machine; (c) the steel clamps in the grips; (d) electromechanical testing apparatus *H75KS* (made by the author)

3.3. First hybrid beam prototype tests

The first series produced the hybrid beam prototypes with nominal geometry, shown in Fig. 2.2. Beams of all series were poured into the inverted position. Two rectangular 550×550×40 mm slabs (Fig. 3.4) and eight 100 mm cubes (Fig. 3.10) were produced together with the hybrid beams of each series. The vibration table densified the concrete structure. Perforations were located in the middle of the support zone (Fig. 3.11a) and the top flange of the GFRP profile at the load application points and the centre of both support zones (Fig. 3.11b) to improve the contact performance with polymeric fibre reinforced concrete (PFRC).

Fig. 3.10. 100 mm cubes cast after every beam series (made by the author)

a)

b)

Fig. 3.11. Perforation in the beams: (a) in the web of the GFRP profile; (b) in the flange of the GFRP profile (made by the author)

a)

b)

Fig. 3.12. Foamed polystyrene and wood inserts used in the steel form: (a) forming the support blocks; (b) forming the extension of the support blocks (made by the author)

Foamed polystyrene and wood inserts were used to form the support blocks (Fig. 3.12a), fixing the GFRP profile. The concrete was poured into two layers. In the first layer, a 55 mm thickness concrete deck was formed and densified using the vibration table. After that, the concrete supports were formed using foamed polystyrene plugs and wooden extensions (Fig. 3.12b). The support blocks of the first beam series ensure the 20 mm cover of the profile on the beam support. Finally, the 95 mm monolithic concrete support blocks (Fig. 2.2) were densified by poking them with a metal rod.

The beams of all the series were de-moulded after two days and stored in laboratory conditions (average temperature 20 °C and 40% relative humidity) for

30 days before the tests. The measurement device's exact loading scheme and distribution were used for all beam series. Fig. 3.13 shows the characteristic views of the bending test setup. A digital image correlation system (Fig. 3.13a) was used to capture a sudden failure of the hybrid beam specimens. However, the dissertation does not include these results because of the gradual collapse of the beam samples. In addition, the uneven surface of the beams made the image correlation procedure inefficient for capturing deformation responses. Thus, this dissertation employs the linear variable displacement transducers (LVDT) to capture the vertical displacements at the beam mid-span and below the load application points (Fig. 3.13b). In addition, nine LVDT surface deformations were monitored in the pure bending zone. Then, they were applied to monitor longitudinal strains within the bending zone.

The bending tests were conducted using the same testing machine as the punching-shear tests. In addition, the servohydraulic machine press was used to apply the load at the same displacement control manner with the 0.4 mm/min rate.

Fig. 3.13b shows the longitudinal strain gauges' arrangement. It can be observed that the LVDT devices were distributed in three lines with a 50 mm offset of the bottom line regarding the bottom surface of the GFRP profile. Fig. 3.14 shows the deformation profiles corresponding to the beam reaction monitored with the load cell, i.e., the strain results from averaging three LVDT devices distributed in the row (Fig. 3.13b).

a)

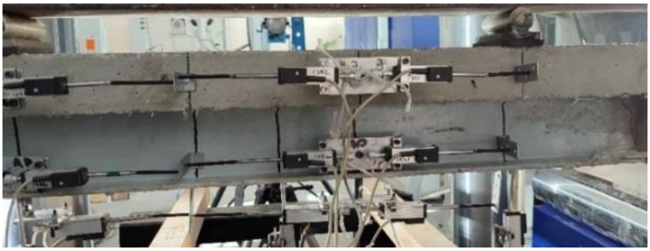

b)

Fig. 3.13. Examples of the bending test setup of the hybrid beam: (a) the surface exposed for digital image correlation; (b) distribution of linear variable displacement transducers, monitoring vertical and horizontal displacements (made by the author)

The 58 kN load defines the failure of the beams belonging to the first series. The beams' load-bearing capacity was 56 kN and 58 kN, and displacement at the mid-span was 14.2 mm and 10.7 mm, respectively. Longitudinal strain distribution was also measured to avoid slippage between the hybrid beam components.

The strain distribution in Fig. 3.14 is close to linear and is characteristic for all loading stages and both series of beams. This outcome substantiates the slip absence between the hybrid beam components, proving the adequacy of the perfect bond assumption in the numerical model. At the same time, considering the beam failure mechanisms, the inefficient behaviour of the first series of beams (Fig. 2.18) requires clarification.

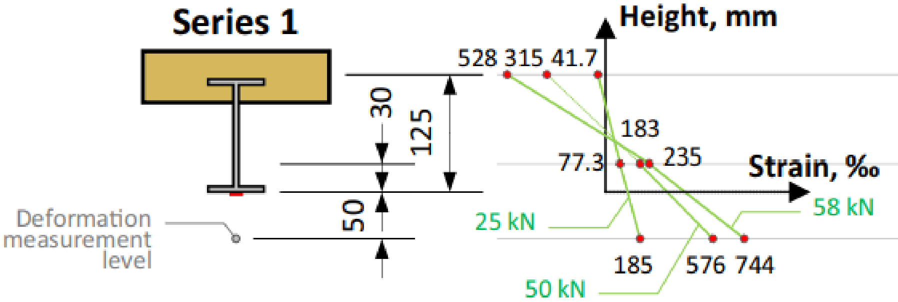

Fig. 3.14. Longitudinal strain distribution in the series one hybrid beams (made by the author)

Fig. 3.15. Typical failure of the support block of the first series beam (made by the author)

The crushing of the GFRP profile anchorage blocks results from the first series of tests. Fig. 3.15 shows a typical view of the beam support after the collapse. This outcome is a consequence of the insufficient resistance of the FRP materials to the transverse loads in the pultrusion direction. However, the FE model could not represent this failure mechanism because of the limited ability to simulate the transverse crushing of FRP materials (Fig. 2.17), resulting from the heterogeneity of the material structure (Gribniak et al., 2021).

After the first series of tests, the modelling was recalculated, and it was decided to modify the support blocks of the beams to connect PFRC and GFRP. A more detailed description of the results is provided in the Second Chapter.

3.4. Second test series of modified hybrid beams

After the lack of bonding in the support zones was identified as the problem (Fig. 2.18), a modified version of the beam design was created (Fig. 2.22). The preparation of forms, concrete casting, and testing were conducted. The beam specimens from the second series had improved anchorage blocks: a hollow-section steel 100×200 mm rectangular profile protected the GFRP profile at the supports. This modification increased the support block length from 95 to 250 mm, but the support distance remained unchanged. In addition, the width of the compressive concrete zone was decreased to simplify the beam production, preserving the flexural rigidity of the beam by increasing the compressive zone height. The remaining components of the hybrid system, i.e., GFRP profile, CFRP strip, and adhesive, remained the same. The second series profiles had no perforation on the top flange. Figs. 2.22 and 3.16 show the beam schematic and the anchorage block views.

a) b) c)

Fig. 3.16. Preparing the modified support blocks: (a) rectangular steel tube with drilled holes; (b) inserted 6 mm and 8 mm bars; (c) the steel tube inside the form (made by the author)

The vertical 6 mm and horizontal 8 mm steel bars prevented movements of the GFRP profile inside the steel tube (Fig. 3.16). The 8 mm bar went horizontally through the middle of the GFRP profile (Fig. 2.22). In the same way, as for the first series of beams, two beam prototypes, two 550×550×40 mm slabs, and eight 100 mm cubes were produced using identical concrete proportions (described in the Second Chapter). The beam samples were poured into two layers: the first layer, including the concrete slab, was densified using the vibrating table, and the second layer formed the support blocks. This concrete was carefully distributed and densified inside the protective steel shells using steel rods.

After the forms were filled with concrete, they were left to set for 30 days in laboratory conditions, identical to the first beam series. Then, the modified beams were tested (Fig. 3.17). The measurement device distribution and test setup were the same as in the first series. The longitudinal strain distribution in the bending zone was close to linear, just like in the first series of tests, showing no slip between the beam components (Fig. 3.18). The load-bearing capacity of this beam series was 110 kN and 78 kN. The corresponding vertical displacements at the mid-span were 13.6 mm and 12.2 mm, respectively.

Modifying the support joints simplified the failure prediction problem. Fig. 3.19 shows the failure localisation process predicted by ATENA that corresponds to the deformation results shown in Fig. 2.15. Remarkably, the PFRC had no additional reinforcement. This example provides insight for developing hybrid beam systems, which utilise advanced composite materials efficiently. More detailed results are given in the Second Chapter of this dissertation.

Fig. 3.17. Tested the second series hybrid beam prototype (made by the author)

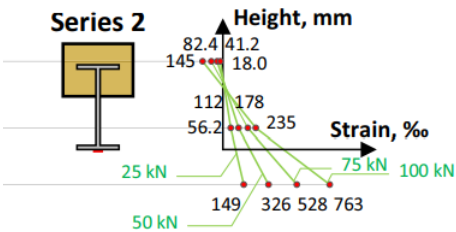

Fig. 3.18. Longitudinal strain distribution in the series of two hybrid beams (made by the author)

a) b)

Fig. 3.19. Failure mechanisms of the hybrid beams: (a) the predicted strain distribution in the FE model with the perfect bond (MPa) (**Fig. 2.15**); (b) shear failure of the concrete in the second series beam (made by the author)

3.5. Large-scale beam tests

This section will describe the preparations and testing of the large-scale beams. First, two beams are cast and tested like in the preliminary first two series. This requires preparing the casting forms and setting up the testing equipment. The concrete mixture used for this series is identical to the first two and is provided in the Second Chapter.

After the FE simulation was completed with the large-scale beam model, physical tests were conducted. Fig. 2.25 describes the geometry and cross-sections of the hybrid beam. The support zones were increased to 350 × 350 mm and protected with steel shells (the 350 mm long parts of the 150 × 350 mm rectangular profile). The 6 mm and 8 mm steel bars, placed in pre-drilled holes and poured with concrete, connected the GFRP profile on the supports. Figs. 3.20a and 3.20b show the support details of the physical beam element. The GFRP profile had no perforation to improve the contact with PFRC. The preliminary tests (first and second test series) employed the same methodology, demonstrating its efficiency in ensuring bond performance.

The beam sample was produced inverted and designated as S-5. The concrete slab over the span was densified at the vibrating table; the concrete inside the supports was poked with steel rods. Twelve 100 mm concrete cubes were produced with the beam sample for compressive tests. Thus, the concrete demonstrated 50 MPa compressive strength on the beam-testing day, which agreed well with the design compressive strength of PFRC; the test was conducted at the concrete's three-week age. Six linear variable displacement transducers (LVDT) measured vertical displacements under the load application points and mid-span (three by two LVDT, 3.20c); other 12 LVDT distributed in four continuous lines on the side surface of the beam in the pure bending zone captured longitudinal deformations of the concrete and GFRP profile (Fig. 3.20d). The remaining 2 LVDTs monitored the slip of the GFRP profile regarding the support joint. In total, there were 20 LVDTs.

a) b) c) d)

Fig. 3.20. Large-scale hybrid beam prototype: (a) and (b) the support joint; (c) and (d) the sample before the bending test (made by the author)

Fig. 3.21. Hybrid beam failure because of the concrete crushing (made by the author)

Fig. 3.22. Testing scheme (made by the author)

The beam sample was loaded in a 10 MN servohydraulic testing apparatus under 0.4 kN per second loading velocity until failure, resulting from the compressive concrete crushing at the beam mid-span (Fig. 3.21). The test scheme of the large-scale beam is shown in Fig. 3.22. The load-bearing capacity was 125 kN, and the corresponding vertical displacement at the mid-span was 34.7 mm.

Fig. 3.23 shows the longitudinal deformation monitoring results. It can be observed that the strains are distributed nearly linearly over the height of the hybrid beam in the pure bending zone. This tendency is valid almost until the ultimate bending moment: a nonlinearity corresponds to the 60 kNm load. At this load level, the maximum GFRP slip regarding the support blocks captured by LVDT did not reach 0.2 mm. In other words, the monitoring devices did not capture substantial deformation differences (bond slip) between the PFRC slab and GFRP profile. These results agree well with the previous series results that supported the fixation efficiency of the GFRP profile on the supports for ensuring the composite behaviour of the hybrid beam system (Fig. 3.18). In addition, the predicted failure (Fig. 2.27) agrees well with the observed response (Fig. 3.21). However, as described in the Second Chapter, the results did not coincide well.

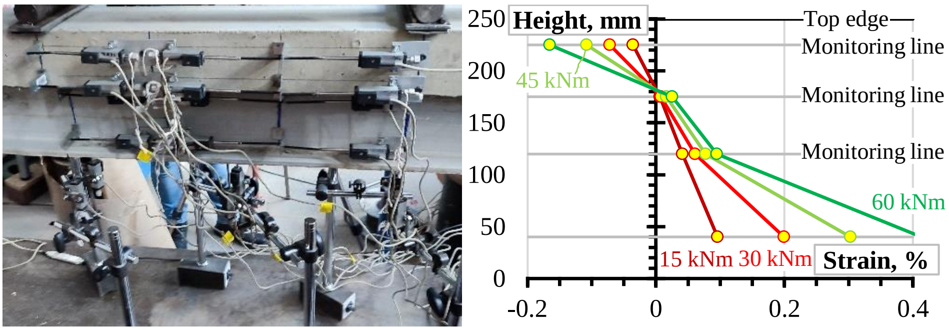

Fig. 3.23. Horizontal LVDT distribution and corresponding strain measurements (made by the author)

Fig. 3.24. Prestressing mechanism (made by the author)

Another beam (S-6) was produced with elongated support joints (+90 mm), increasing the concrete bond area with the GFRP. The CFRP strip was also glued to the GFRP while prestressed with metal weights (Fig. 3.24) to increase the bond strength between the CFRP and the GFRP profile. After the beam was produced, it was tested like beam S-5. The load-bearing capacity increased from 105 kN to 142.6 kN, bringing it closer to the modelled reference with the perfect connection between the CFRP and GFRP (165 kN); the difference was less than 14%.

3.6. Conclusions of the Third Chapter

This chapter describes the testing completed to verify the FE models and adaptive design concept created in the Second Chapter. The testing results and comparative analysis result in the following conclusions:

1. To verify the GFRP profile, heating tests were employed to determine the fibre volume fraction, and a bending test was used to verify the results of the heating tests. The fibre volume fraction required for the smeared reinforcement modelling was 63.4%.
2. To check the adequacy of the constitutive model of PFRC, a punching-shear test with PFRC slabs from the concrete was conducted. The load-bearing capacity of the plates was 9.5 kN and 10.5 kN, which agreed with the FE prediction as discussed in Section 2.2.2, and the error was below 10%. The cracking results were also very similar and are provided in Fig. 2.10.
3. The pull-out tests of individual fibres verified the bond model for the concrete and polymeric material. The bond parameters were acquired by modelling the tests in ATENA software using a trial-and-error procedure. After comparing the FE simulation of the pull-out tests with the completed experiments, the deformation prediction error did not exceed 4%. The polymeric fibres caused the crack closure after removing the load. Selecting an efficient type of fibre and concrete mixture is essential to ensure the required ductility, cracking resistance, and overall stiffness of the beam system. The polymeric fibre reinforcement makes the deformation capacity of the PFRC similar to the GFRP profiles. In other words, the PFRC can restore its initial shape without visible cracks after removing the mechanical load.
4. The preliminary tests of the hybrid beams (test series 1 and 2) checked the viability of the developed adaptive design, providing the engineer with an apparent solution to the support problem resulting from a low resistance of pultruded FRP profiles to transverse loads regarding the pultrusion direction.

5. After comparing the results of the first series test to the reference FE model solution, it was clear that modifications had to be made to the beam (improvement of the supports) to improve its performance. The supports' enhancement doubled the hybrid beam's flexural stiffness and load-bearing capacity (an increase of 107.5%) without the additional FRP bond improvement with concrete regarding the reference bridge (series 1) with typical weak supports. Still, the formal solution requires further tests to ensure the result's reliability and optimise the support blocks' geometry. However, the apparent effect of the adaptive design improvement proves the viability of the proposed design concept.

General Conclusions

The present research aims to develop a novel adaptive design concept when the numerically predicted outcome defines the design target. Then, an engineer can iteratively modify the solution (prototype), which becomes the subject of the physical tests to ensure the agreement of the test result with the predicted outcome. The hybrid beam structure is composed to test the adaptive design concept from a pultruded GFRP I profile, PFRC slab, and a CFRP strip for strengthening purposes. Connecting the polymeric fibre-reinforced concrete (PFRC) with the GFRP profile improves the general performance of hybrid beam structures. A series of physical tests verified the finite element (FE) model, which described the design reference. The research outcomes result in the following general conclusions:

1. A more systematic design approach is required for composite structures combining concrete and FRP components. Application of FRP components in long-span systems (e.g., 10–15 m long bridges) faces a significant challenge because of excessive deflections and vulnerability to dynamic loads. The research must focus on the shear resistance of FRP components and their bonding performance with concrete. Consequently, the existing design solutions are unreasonably conservative, with the safety factors reaching 18 times higher loads in found literature and articles, proportionally increasing the demands

for advanced materials. Thus, the identified literature gap motivated this dissertational work, in which a novel adaptive design concept was created, allowing the efficient development of hybrid systems. The modelling outcome for these advanced composite materials determined the desired mechanical performance because of a lack of design standards.

2. The conceptual example of the proposed adaptive philosophy demonstrated the design efficiency expressed as the differences between the alternative solutions: the supports' enhancement doubled the hybrid beam's flexural stiffness and load-bearing capacity regarding the reference bridge with typical weak supports without the additional GFRP bond improvements.
3. Fixing the FRP components at the rigid supports simplifies the numerical model, which is the perfect bond assumption that solves the modelling problems reported in the literature, making the FE approach acceptable for designing the hybrid systems considered in this research. In addition, it improves the FRP vulnerability to the loads acting in the transverse direction to the pultrusion pathway.
4. When an experimentally verified numerical model describes the structural design target, the considered adaptive design concept demonstrates room for practical applications, including advanced optimising algorithms, doubling the structure's flexural stiffness and load-bearing capacity regarding the weak concrete support system. However, additional tests are necessary to ensure the reliability of the outcomes and optimise the support blocks' geometry.
5. The comparison of the test results with the predicted load-bearing capacity and deformation response from the reference FE model pointed out a discrepancy. After receiving the first stage testing results, the FE simulation was performed again with a reduced bond strength in the support blocks. The simulation and test results (the load-bearing capacity and flexural stiffness) coincided, thus avoiding additional experiments. Therefore, it was decided to change the design solution (strengthen the support joints). After solving this problem, the FRP-PFRC hybrid beam outperformed the FE modelling reference by modifying the support structure. Thus, when there is a lack of design guidance, the developed finite element model determines the adequate reference for designing hybrid FRP-PFRC structural systems and efficiently utilising advanced composite materials.

References

ASCE. (1984). *Structural plastics design manual*. American Society of Civil Engineers. *https://ascelibrary.org/doi/10.1061/9780872624757*

ASCE (1985). *Structural plastics selection manual*. American Society of Civil Engineers. https://doi.org/10.1061/9780872624757

Ali, H. T., Akrami, R., Fotouhi, S., Bodaghi, M., Saeedifar, M., Yusuf, M., & Fotouhi, M. (2020). Fiber reinforced polymer composites in bridge industry. *Structures, 30*, 774–785. https://doi.org/10.1016/j.istruc.2020.12.092

Ascione, F., Mancusi, G., Spadea, S., Lamberti, M., Lebon, F., & Maurel-Pantel, A. (2015). On the flexural behaviour of GFRP beams obtained by bonding simple panels: An experimental investigation. *Composite Structures, 131*, 55–65. http://dx.doi.org/10.1016/j.compstruct.2015.04.039

Aydın, F., & Sarıbıyık, M. (2013). Investigation of flexural behaviors of hybrid beams formed with GFRP box section and concrete. *Construction and Building Materials, 41*, 563–569. http://dx.doi.org/10.1016/j.conbuildmat.2012.12.060

Bakis, C. E., Bank, L. C., Brown, V. L., Cosenza, E., Davalos, J. F., Lesko, J. J., Machida, A., S. H. Rizkalla, S. H., & Triantafillou, T. C. (2002). Fiber-Reinforced Polymer Composites for Construction—State-of-the-Art Review. *Journal of Composites for Construction*, *6*, 73–87. https://doi.org/10.1061/(ASCE)1090-0268(2002)6:2(73)

Brunton, J. J., Bank, L. C., & Oliva, M. G. (2016). Punching Shear Failure in Double-Layer Pultruded FRP Grid Reinforced Concrete Bridge Decks. *Advances in Structural Engineering, 15,* 601–613. https://doi.org/10.1260/1369-4332.15.4.601

Cai, J., Pan, J., & Zhou, X. (2017). Flexural behavior of basalt FRP reinforced ECC and concrete beams. *Construction and Building Materials, 142,* 423–430. http://dx.doi.org/10.1016/j.conbuildmat.2017.03.087

Canning, L., & Luke, S. (2016). Development of FRP Bridges in the UK — An Overview. *Advances in Structural Engineering, 13,* 823–835. https://doi.org/10.1260/1369-4332.13.5.823

Cervenka, V. (2002). Computer simulation of failure of concrete structures for practice. In *Proceedings of the First fib Congress Concrete Structures in 21 Century* (pp. 289–304). Semantic Scholar. https://www.semanticscholar.org/paper/COMPUTER-SIMULATION-OF-FAILURE-OF-CONCRETE-FOR-%C4%8Cervenka/88255cd50e2b64777945a8b5c5c6e52694b2afe6

Chaiyasarn, K., Ali, N., Phuphasuwan, P., Poovarodom, N., Joyklad, P., Mohamad, H., Zhou, M., & Hussain, Q. (2021). Flexural Behavior of Natural Hybrid FRP-Strengthened RC Beams and Strain Measurements Using BOTDA. *Polymers*, *13*(20), 3604. https://doi.org/10.3390/polym13203604

Chen, D., Sun, G., Meng, M., Jin X., & Li, Q. (2019). Flexural performance and cost efficiency of carbon/basalt/glass hybrid FRP composite laminates. *Thin-Walled Structures, 142,* 516–531. https://doi.org/10.1016/j.tws.2019.03.056

Chróścielewski, J., Miśkiewicz, M., Pyrzowski, L., Rucka, M., Sobczyk, B., & Wilde, K. (2018). Modal properties identification of a novel sandwich footbridge – Comparison of measured dynamic response and FEA. *Composites Part B, 151,* 245–255. https://doi.org/10.1016/j.compositesb.2018.06.016

Dang, H. V., & Phan, D. N. (2021). Experimental investigation and analysis of pure bending plastic hinge zone in hybrid beams reinforced with high reinforcement ratio under static loads. *European Journal of Environmental and Civil Engineering, 26*(13), 6188–6210. https://doi.org/10.1080/19648189.2021.1934553

Dongdong, Z., Yaru L., Qilin Z., & Feng L. (2019). Development of lightweight emergency bridge using GFRP–metal composite plate-truss girder. *Engineering Structures, 196,* 109291. https://doi.org/10.1016/j.engstruct.2019.109291

El-Wazery, M. S., El-Elamy, M. I., & Zoalfakar, S. H. (2017). Mechanical properties of glass fiber reinforced polyester composites. *International Journal of Applied Science and Engineering*, *14*(3), 121–131. https://doi.org/10.6703/IJASE.2017.14(3).121.

Eskandaria, S., Andrade Pires, F. M., Camanho, P.P., Cui, H., Petrinic, N., & Marques, A. T. (2019). Analyzing the failure and damage of FRP composite laminates under high strain rates considering visco-plasticity. *Engineering Failure Analysis, 101,* 257–273. https://doi.org/10.1016/j.engfailanal.2019.03.008

Fahmy, F. M. M., Sayed, H. A., Farghal, A. O., & Ahmed, M. A. (2019). Flexural behavior of new hybrid profiled steel-FRP T-beams filled with concrete: development and validation. *Journal of Composites for Construction, 24*(2), 1–18. https://doi.org/10.1061/(ASCE)CC.1943-5614.0001007

FIBERLINE. (2003). *GFRP Profiles – Design Manual*. Fiberline Composites A/S. https://fiberline.com/design-manual

FIBERLINE. (2021). *General Properties for P2600. FIBERLINE Datasheet*. FIBERLINE Building Profiles A/S. https://fiberline.com/media/zjgo4nia/fiberlinep2600_uk.pdf

Ghadimi, B., Russo, S., & Rosano, M. (2017). Predicted mechanical performance of pultruded FRP material under severe temperature duress. *Composite Structures, 176*, 673–683. https://doi.org/10.1016/j.compstruct.2017.05.061

Ghafoori, E., Hosseini, A., Al-Mahaidi, R., Zhao, X., Motavalli, M., & Koay, Y. (2019). CFRP strengthening and long-term monitoring of an old metallic roadway bridge in Melbourne. In *IABSE Symposium: Towards a Resilient Built Environment Risk and Asset Management*, (pp. 360–368). Structurae https://doi.org/10.2749/guimaraes.2019.0360

Goh, G. D., Yap, Y. L., Agarwala, S., & Yeong W. Y. (2018). Recent progress in additive manufacturing of fiber reinforced polymer composite. *Advanced Material Technologies*, *4*(1), 1800271. https://doi.org/10.1002/admt.201800271

Gribniak, V. (2009). *Shrinkage Influence on Tension-Stiffening of Concrete Structures* [Doctoral dissertation, Vilnius Gediminas technical university].Vilniustech elektroninė talpykla. https://etalpykla.vilniustech.lt/handle/123456789/111178

Gribniak, V. (2020). Advanced composites: From materials characterization to structural application. *Materials, 13*(24), 5820. https://doi.org/10.3390/ma13245820

Gribniak, V., Arnautov, A. K., & Rimkus, A. (2021). The development of nature-inspired gripping system of a flat CFRP strip for stress-ribbon structural layout. *Journal of Computational Design and Engineering, 8*(2), 788–798. https://doi.org/10.1093/jcde/qwab0 14

Gribniak, V., Kaklauskas, G., Kwan, A. K. H., Bacinskas, D., & Ulbinas, D. (2012). Deriving stress-strain relationships for steel fibre concrete in tension from tests of beams with ordinary reinforcement. *Engineering Structures*, *42*, 387–395. https://doi.org/10.1016/j.engstruct.2012.04.032

Gribniak, V., Sultani, H. A., Rimkus, A., Sokolov, A., & Torres, L. (2021). Standardised quantification of structural efficiency of hybrid reinforcement systems for developing concrete composites. *Composite Structures*, *274*, 114357. https://doi.org/10.1016/j.compstruct.2021.114357

He, J., Liu, Y., Chen, A., & Dai, L. (2012). Experimental investigation of movable hybrid GFRP and concrete bridge deck. *Construction and Building Materials*, *26*(1), 49–64. https://doi.org/10.1016/j.conbuildmat.2011.05.002

Hollaway, L. C., & Head, P. R. (2000). Composite materials and structures in civil engineering. *Comprehensive Composite Materials*, *6*, 489–527. https://doi.org/10.1016/b0-08-042993-9/00118-2

Hou, W., Wang, L., & Shi, D. (2022). Flexural behaviour of strengthened damaged steel beams using carbon fibre-reinforced polymer sheets. *Scientific reports*, *12*, 10134. https://doi.org/10.1038/s41598-022-14471-9

Issa, C. A., & Kmeid, Z. (2005). Advanced wood engineering: glulam beams. *Construction and Building Materials*, *19*(2), 99–106. https://doi.org/10.1016/j.conbuildmat.2004.05.013

Jaruševičiūtė, A. (2021). *Research of Composite Concrete and Polymer Profiles Slab Segment Deformation* [Master thesis, Vilnius Gediminas technical university]. Lietuvos akademinė elektroninė biblioteka. https://vb.vgtu.lt/object/elaba:97568384/

Juozapaitis, A., Sandovič, G., Jakubovskis, R., & Gribniak, V. (2021). Effects of flexural stiffness on deformation behaviour of steel and FRP stress-ribbon bridges. *Applied Sciences*, *11*(6), 2585. https://doi.org/10.3390/app11062585

Keller, T. (2018). Overview of fibre-reinforced polymers in bridge construction. Structural *Engineering International*, *12*(2), 66–70. https://doi.org/10.2749/101686602777965595

Keller, T., Schaumann, E., & Vallee, T. (2007). Flexural behaviuor of a hybrid FRP and lightweight concrete sandwich bridge deck. *Composites: Part A*, *38*(3), 879–889. https://doi.org/10.1016/j.compositesa.2006.07.007

Keller, T., & Schollmayer, M. (2004). Plate bending behavior of a pultruded GFRP bridge deck system. *Composite Structures*, *64*(3–4), 285–295. https://doi.org/10.1016/j.compstruct.2003.08.011

Kim, Y. J. (2018). State of the practice of FRP composites in highway bridges. *Engineering Structures, 179,* 1–8. https://doi.org/10.1016/j.engstruct.2018.10.067

Koaik, A., Bel, S., & Jurkiewiez, B. (2017). Experimental tests and analytical model of concrete-GFRP hybrid beams under flexure. *Composite Structures*, *180*, 192–210. http://dx.doi.org/10.1016/j.compstruct.2017.07.059

Lee, W. S., Hong, J. K., & Park, S. (2010). Current and future applications of glass-fibre-reinforced polymer decks in Korea. *Structural Engineering International*, *20*(4), 405–408. https://doi.org/10.2749/101686610793557672

Li, F., Li, W., Lu, S., & Shen, Y. (2019). Development of a Prestressing CFRP Laminate Anchorage System and Bridge Strengthening Application. *Advances in Materials Science and Engineering*, 2019, 3503898. https://doi.org/10.1155/2019/3503898

Li, F., Zhang, D. D., Zhao, Q. L., & Deng A. Z. (2015). A simple analytical solution for predicting the deflection of a hybrid FRP-aluminum modular space truss bridge. *Journal of Central South University*, *22*(11), 4414–4425. https://doi.org/10.1007/s11771-015-2989-5

Liu, T., Liu, X., & Feng, P. (2020). A comprehensive review on mechanical properties of pultruded FRP composites subjected to long-term environmental effects. *Composites Part B: Engineering*, *191*, 107958. https://doi.org/10.1016/j.compositesb.2020.107958

Liu, Y., Gu, M., Liu, X., & Tafsirojjaman, T. (2022). Life-Cycle Cost Analysis of Long-Span CFRP Cable-Stayed Bridges. *Polymers 14*(9), 1740. https://doi.org/10.3390/polym14091740

Mahboubi, S., & Shiravand, M. R. (2019). Failure assessment of skew RC bridges with FRP piers based on damage indices. *Engineering Failure Analysis*, *99*, 153–168. https://doi.org/10.1016/j.engfailanal.2019.02.010

Malakhov, A. V., Polilov, A. N., Li D., & Tian, X. (2021). Increasing the Bearing Capacity of Composite Plates in the Zone of Bolted Joints by Using Curvilinear Trajectories and a Variable Fiber Volume Fraction. *Mechanics of Composite Materials*, *57*, 287–300. https://doi.org/10.1007/s11029-021-09954-1

Mandal, B., & Chakrabarti, A. (2017). Numerical failure assessment of multi-bolt FRP composite joints with varying sizes and preloads of bolts. *Composite Structures*, *187,* 169–178. https://doi.org/10.1016/j.compstruct.2017.12.048

Mendes, P. J. D., Barros, J. A. O., Sena-Cruz, J. M., & Taheri, M. (2011). Development of a pedestrian bridge with GFRP profiles and fiber reinforced self-compacting concrete deck. *Composite Structures*, *93*(11), 2969–2982. https://doi.org/10.1016/j.compstruct.2011.05.005

Modak, N., Sivasankar, S., Sounthararajan, V. M., & Gunaselvi, S. (2020). Behaviour of hollow circular steel columns in compression retrofitted with aramid fibre reinforced polymer composites. *Materials Today: Proceedings*, *27*(2), 968–974. https://doi.org/10.1016/j.matpr.2020.01.290

Mosallam A. S. (2011). *Design guide for FRP composite connections*. American Society of Civil Engineers. https://ascelibrary.org/doi/book/10.1061/9780784406120

Muc, A., Stawiarski, A., & Chwal, M. (2020). Design of the hybrid FRP/concrete structures for bridge constructions. *Composite Structures*, *247,* 112490. https://doi.org/10.1016/j.compstruct.2020.112490

Muttashar, M., Manalo, A., Karunasena, W., & Lokuge, W. (2016). Influence of infill concrete strength on the flexural behaviour of pultruded GFRP square beams. *Composite Structures*, *145,* 58–67. http://dx.doi.org/10.1016/j.compstruct.2016.02.071

Naito, K. (2022). Static and fatigue tensile properties of carbon/glass hybrid fiber-reinforced epoxy composites. *Scientific Reports*, *12*, 6298. https://doi.org/10.1038/s41598-022-10245-5

Nerilli, F., & Vairo, G. (2018). Experimental investigation on the debonding failure mode of basalt-based FRP sheets from concrete. *Composites Part B*, *153,* 205–216. https://doi.org/10.1016/j.compositesb.2018.07.002

Obaidat, A. T. (2020). Flexural behavior of reinforced concrete beam using CFRP hybrid system. *European Journal of Environmental and Civil Engineering*, *26*(13), 6165–6187. https://doi.org/10.1080/19648189.2021.1934552

Papapetrou, V. S., Tamijani, A. Y., Brown, J., & Kim, D. (2018). Design optimization of hybrid FRP/RC bridge. *Applied Composite Materials*, *26,* 249–270. https://doi.org/10.1007/s10443-018-9691-3

Potyrala, B. P. (2011). *Use of fibre reinforced polymer composites in bridge construction. State of the art in hybrid and all-composite structures* [Doctoral dissertation; University of Catalonia]. AC Repository. https://core.ac.uk/download/pdf/41803742.pdf

Preinstorfer, P., Huber, T., Reichenbach, S., Lees, J. M., & Kromoser, B. (2022). Parametric Design Studies of Mass-Related Global Warming Potential and Construction Costs of FRP-Reinforced Concrete Infrastructure. *Polymers, 14*(12), 2383. https://doi.org/10.3390/polym14122383

Ramôa Correia, J. (2013). Pultrusion of advanced fibre-reinforced polymer (FRP) composites. *Advanced Fibre-Reinforced Polymer (FRP) Composites for Structural Applications*, 207–251. https://doi.org/10.1533/9780857098641.2.207

Robinson, M. J., & Melby, I. H. (2015). Effects of bonding in short-span rectangular concrete filled GFRP tubes. *Composite Structures, 133*, 131–139. http://dx.doi.org/10.1016/j.compstruct.2015.07.105

Rong, Y., Zhao, Z. L., Feng, X. Q., & Xie, Y. M. (2022). Structural topology optimization with an adaptive design domain. *Computer Methods in Applied Mechanics and Engineering*, *389*, 114382. https://doi.org/10.1016/j.cma.2021.114382

Rossini, M., Spadea, S., & Nanni, A. (2019). Pedestrian bridge as clarifying example of FRP-RC/PC design. *The Concrete Convention and Exposition*, *333*, 96–118. https://doi.org/10.14359/51720272

Salzano, P., Bonati, A., Ceroni, F., Crisci, G., Franco, A., & Occhiuzzi, A. (2019). Statistical analysis on mechanical properties of FRP materials for structural strengthening. In *7th ECCOMAS Thematic Conference on Computational Methods in Structural Dynamics and Earthquake Engineering* (pp. 5153–5168). ECCOMAS Proceedia.

Shi, Z. Y., Cui, P., & Li, X. (2019). A review on research progress of machining technologies of carbon fiber-reinforced polymer and aramid fiber-reinforced polymer. *Proc IMechE Part C: J Mechanical Engineering Science*, *233*(13) 1–13. https://doi.org/10.1177/0954406219830732

Siwowski, T., Kulpa, M., Rajchel, M., & Poneta, P. (2018). Design, manufacturing and structural testing of an all-composite FRP bridge girder. *Composite Structures, 206*, 814–827. https://doi.org/10.1016/j.compstruct.2018.08.048

Siwowski, T., Piątek, B., Siwowska, P., Wiater, A. (2020). Development and implementation of CFRP post-tensioning system for bridge strengthening. *Engineering Structures, 207*, 110266. https://doi.org/10.1016/j.engstruct.2020.110266

Siwowski, T., & Rajchel, M. (2019). Structural performance of a hybrid FRP composite – lightweight concrete bridge girder. *Composites Part B: Engineering*, *174*, 107055. https://doi.org/10.1016/j.compositesb.2019.107055

Siwowski, T., Rajchel, M., & Kulpa, M. (2019). Design and field evaluation of a hybrid FRP composite – Lightweight concrete road bridge. *Composite Structures, 230*, 111504. https://doi.org/10.1016/j.compstruct.2019.111504

Sun, W., Peng, X., & Yu, Y. (2017). Development of a simplified bond model used for simulating FRP strips bonded to concrete. *Composite Structures, 171*, 462–472. https://doi.org/10.1016/j.compstruct.2017.03.066

Tackitt, K. D., & Walsh, S. M. (2005). Experimental Study of Thickness Gradient Formation in the VARTM Process. *Materials and Manufacturing Processes, 20*(4), 607–627. https://doi.org/10.1081/AMP-200041896

Tamakuwala, V. R. (2020). Manufacturing of fiber reinforced polymer by using VARTM process: A review. *Materials Today: Proceedings, 44*(1), 987–993. https://doi.org/10.1016/j.matpr.2020.11.102

Thorhallsson, E. R., Hinriksson, G. I., & Snæbjörnsson, J. T. (2017). Strength and stiffness of glulam beams reinforced with glass and basalt fibres. *Composites Part B: Engineering, 115*, 300–307. https://doi.org/10.1016/j.compositesb.2016.09.074

Tuwair, H., Drury, J., & Volz, J. (2019). Experimental investigation of GFRP hybrid Full-scale bridge deck panels subjected to AASHTO design truck wheel load. *International Journal of Structural and Civil Engineering Research*, *8*(3), 280–283. https://doi.org/10.18178/ijscer.8.3.280-283

Votsis, R. A., Stratford, T. J., Chryssanthopoulos, M. K., & Tantele, E. A. (2017). Dynamic assessment of a FRP suspension footbridge through field testing and finite element modelling. *Steel and Composite Structures, 23*(2), 205–215. https://doi.org/10.12989/scs.2017.23.2.205

Xie, Y. M. (2022). Generalized topology optimization for architectural design. *Architectural Intelligence, 1*, 2. https://doi.org/10.1007/s44223-022-00003-y

Yang, Y., Wang, X., & Wu, Z. (2020). Long-span cable-stayed bridge with hybrid arrangement of FRP cables. *Composite Structures, 237*, 111966. https://doi.org/10.1016/j.compstruct.2020.111966

Yuana, Y., Yao, X., Niu, K., Liu, B., & Wuyun, Q. (2019). Compressive failure of fiber reinforced polymer composites by imperfection. *Composites Part A: Applied Science and Manufacturing, 118*, 106–116. https://doi.org/10.1016/j.compositesa.2018.12.017

Zhang, D., Li, F., Shao, F., & Fan, C. (2018). Evaluation of equivalent bending stiffness by simplified theoretical solution for an FRP-aluminum deck-truss structure. *KSCE Journal of Civil Engineering*, *23*, 367–375. https://doi.org/10.1007/s12205-018-1093-4

Zhang, P., Liu, X.Y., Li, Q., Deng, E., Gao, D., Zhang, Z., & Sheikh, S. A. (2020). Experimental and theoretical studies on the shear performance of innovative box-shape FRP profile-concrete hybrid beams. *Structures*, *28*, 2772–2784. https://doi.org/10.1016/j.istruc.2020.10.064

Zhang, P., Lv, X., Liu, Y., Zou, X., Li, Y., Wang, J., & Sheikh, S. A. (2021). Novel fiber reinforced polymers (FRP)-ultrahigh performance concrete (UHPC) hybrid beams with improved shear performance. *Construction and Building Materials*, *286*, 122720. https://doi.org/10.1016/j.conbuildmat.2021.122720

Zhu, Y., Zhu, H., & Gribniak, V. (2022). Analyzing the Sample Geometry Effect on Mechanical Performance of Drilled GFRP Connections. *Materials, 15*(8), 2901. https://doi.org/10.3390/ma15082901

Zou, X., Feng, P., Bao, Y., Wang, J., & Xin, H. (2020). Experimental and analytical studies on shear behaviors of FRP-concrete composite sections. *Engineering Structures*, *215*, 110649. https://doi.org/10.1016/j.engstruct.2020.110649

Zou, X., Lin, H., Feng, P., Bao, Y., & Wang, J. (2020). A review on FRP-concrete hybrid sections for bridge applications. *Composite Structures*, *262*, 113336. https://doi.org/10.1016/j.compstruct.2020.113336

List of scientific publications by the author on the topic of the dissertation

Papers in the reviewed scientific journals

Garnevičius, M., & Gribniak, V. (2022). Developing a hybrid FRP-concrete composite beam. *Scientific Reports, 12,* 1–9. https://doi.org/10.1038/s41598-022-20666-x

Garnevičius, M., Plioplys, L., Ng, P.-L., Chu, S., & Gribniak, V. (2020). Investigation and improvement of bond performance of synthetic macro-fibres in concrete. *Materials, 13*(24), 1–14. DOI: https://doi.org/10.3390/ma13245688

Gribniak, V., Rimkus, A., Plioplys, L., Misiunaite, I., Garnevičius, M., Boris, R., & Šapalas, A. (2021). An efficient approach to describe the fiber effect on mechanical performance of pultruded GFRP profiles. *Frontiers in Materials*, *8,* 1–17. https://doi.org/10.3389/fmats.2021.746376

Publications in other editions

Garnevičius, M., Plioplys, L., & Gribniak, V. (2021a). Determination and modelling of bond properties of synthetic macro-fibres in concrete. *Science – Future of Lithuania. Civil Engineering, 13,* 1–6. https://doi.org/10.3846/mla.2021.12807

Garnevičius, M., Plioplys, L., & Gribniak, V. (2021b). A bond model of synthetic macro-fibre in concrete. In *F. Gatuingt, J.-M. Torrenti (Eds.), Proc. of the 13th fib International Ph. D. Symposium in Civil Engineering*, (pp. 33–39). *fib* Proceedings. https://www.fib-international.org/publications/fib-proceedings/13th-phd-symposium-in-paris-france-2020-proceedings-em-pdf-em-detail.html

Sokolov, A., Gribniak, V., Rimkus, A., Hui, D., Garnevičius, M., & Plioplys, L. (2018). Experimental analysis of mechanical aspects of bond behavior of synthetic macro-fibers in concrete. In *Proc. of the 26th Annual International Conference on Composites/Nano Engineering (ICCE-26)*, 2 p. ICCE. https://www.google.lt/books/edtion/ICCE_26/WF0xygEACAAJ?hl=lt

Summary in Lithuanian

Įvadas

Problemos formulavimas

Nors įvairiose pramonės srityse, tokiose kaip medicina, aviacija, naudojamos patobulintų fizikinių savybių kompozitinės medžiagos, statybos sektoriuje vis dar vyrauja konservatyvūs konstrukcijų projektavimo principai. Inžinerinė praktika rodo, kad taikant pažangias statybos technologijas reikia naujų prototipavimo koncepcijų, pritaikytų naujai sukurtoms medžiagoms, kurių mechaninės savybės pritaikytos statybos tikslams. Toks požiūris prieštarauja dabartinei praktikai, pagal kurią standartizuoti inžineriniai sprendiniai siejami su esamomis medžiagomis, kurių fizikinės savybės nepritaikytos konstrukcijos keliamiems reikalavimams, todėl dėl saugios laikomosios galios užtikrinimo neracionaliai didinamas konstrukcinių medžiagų poreikis.

Pluoštu armuoti polimerai (angl. *fibre reinforced polymer*, FRP) vis plačiau pakeičia plieninius tiltų ir pastatų elementus, taip išsprendžiama korozijos problema, tačiau dėl FRP komponentų anistropinių medžiagų savybių kyla problemų, susijusių su jų jungtimis. Ilgalaikiai poveikiai (pvz., valkšnumas) mažina medžiagų mechaninį atsparumą. Dėl santykinai mažo tipinių FRP medžiagų tamprumo modulio (lyginant su plienu) padidėja šių konstrukcijų deformacijos. Šiai problemai išspręsti kuriamos kombinuotos kompozitinės konstrukcijos, sudarytos iš gniuždymui atsparaus betono ir tempimui atsparių pluoštu armuotų polimerų profiliuočių. Tokios kompozitinės sistemos taikomos tiltuose, tačiau šių pažangių konstrukcijų projektavimo metodų kūrimą apsunkina komponentų sukibimo savybių neapibrėžtumas. Įprastai šis klausimas sprendžiamas gerinant lokalų sukibimą. Šiame tyrime pateikiamas alternatyvus sprendinys –

kombinuotos sijos prototipo komponentai, sintetiniu plaušu armuoto betono plokštė ir pluoštu armuotas polimerinis profiliuotis, sujungiami juos įtvirtinant standžiose atramose.

Darbo aktualumas

Disertacijoje pateikiama kombinuotų kompozitinių sistemų adaptyvaus prototipavimo koncepcija. Šiai koncepcijai iliustruoti kuriamas sijos prototipas, sudarytas iš sintetiniu plaušu armuoto betono plokštės ir pluoštu armuoto polimero (FRP) profiliuočio, įtvirtinto atramose. Sujungus kompozitinės sijos komponentus išsprendžiama sijos sukibties problema ir supaprastinamas skaitinis modelis. Pagal šiame prototipavimo pavyzdyje pateiktus baigtinių elementų (BE) modeliavimo rezultatus nusakomas prototipavimo procedūros tikslas ir galima vertinti kuriamos kompozitinės sistemos efektyvumą. Mechaninių bandymų ir skaitinio modeliavimo rezultatų sutapimas atskleidžia fizinio prototipo tinkamumą. Dėl inovatyvių kompozitinių medžiagų projektavimo standartų trūkumo skaitinio modelio rezultatas yra tinkamas etalonas nustatyti siektiną konstrukcijos mechaninę elgseną. Iteracinis konstrukcinio sprendinio modifikavimas užtikrina fizinio prototipo (prototipinio sprendinio) priartėjimą prie etaloninio (tikslinio) skaitinio modeliavimo rezultato.

Siūlomas konstrukcinis sprendinys oponuoja tradicinei lokalaus sukibimo gerinimo idėjai. Disertacijos tyrimai rodo, jog vien išsprendus atramų mechaninio atsparumo problemą (dėl mažo pultruzijos būdu pagamintų FRP profiliuočių atsparumo šlyties apkrovoms) užtikrinamos tilto prototipo konstrukcinės charakteristikos – patobulintos konstrukcijos lenkiamasis standis ir laikomoji galia padvigubėja, lyginant su pradiniu kompozitinės sijos, turinčios silpnas atramas, atveju.

Tyrimo objektas

Tyrimo objektas – kombinuoto kompozitinio pėsčiųjų tilto sijos prototipo, veikiamo trumpalaike mechanine apkrova, mechaninės charakteristikos. Nagrinėjamą siją sudaro sintetiniu plaušu armuota betono plokštė ir pluoštu armuotas polimerinis (FRP) profiliuotis, sutvirtintas su plokšte standžiomis atramomis.

Darbo tikslas

Disertacijos tyrimų tikslas – sukurti adaptyvaus prototipavimo koncepciją.Tam tikslui sukuriamas kompozitinės sijos baigtinių elementų modelis, t. y. etaloninis sprendinys, fizinių bandymų rezultatams įvertinti (kai nėra standartinių sprendinių). Prototipinis sprendinys modifikuojamas, kol pasiekiamas skaitinio modeliavimo etaloninis rezultatas.

Darbo uždaviniai

Tyrimo tikslui pasiekti keliami šie uždaviniai:

1. Pluoštu armuoto polimero komponentus įtvirtinti standžiose atramose ir užtikrinti šių komponentų (polimeriniu plaušu armuoto betono ir pluoštu armuoto polimero) sukibtį.
2. Sukurti BE modelį taikant eksperimentiškai patikrintus medžiagų fizikinius modelius ir modeliavimo būdus.

3. Sukurti sisteminį metodą, leidžiantį eksperimentiškai patikrintam BE modeliui apibūdinti prototipavimo kriterijus, siektinas fizikines objekto savybes (pvz., laikomąją galią ir standumą), kai nėra atitinkamų projektavimo standartų.
4. Iliustruoti pasiūlytą adaptyvaus prototipavimo koncepciją, pritaikant ją kombinuotos kompozitinės pėsčiųjų tilto sijos kūrimo procese.

Tyrimo metodai

Objektui tirti pasirinkti šie *tyrimo metodai*:

1. Taikant teorinės literatūros analizę nustatomi veiksmingi kompozitinių konstrukcinių elementų komponavimo principai.
2. Suklasifikavus literatūros apžvalgos metu surinktą medžiagą, nustatomos nagrinėjamų FRP medžiagų gerosios bei blogosios savybės, taip pat įvertinama, kokių tyrimų trūksta, taip padedant suformuluoti disertacijos uždavinius.
3. Literatūros apžvalga, skaitinis modeliavimas ir fiziniai eksperimentai padeda suprasti, kaip komponuoti pažangias konstrukcines medžiagas, taip pat supaprastinamas teorinis modelis.
4. Atlikus fizinius sijų bandymus patikrinama disertacijos hipotezė ir pagerinama adaptyvaus prototipavimo koncepcija.
5. Skaitinio modeliavimo, fizinių bandymų, bei bandymų rastų literatūroje, rezultatų lyginamoji statistinė analizė užtikrina išvadų suformulavimą.

Darbo mokslinis naujumas

Pasiūlyta prototipavimo koncepcija leidžia susieti medžiagų inžineriją, konstrukcijų inžineriją ir skaitinį modeliavimą. Eksperimentiškai patikrintas skaitinis modelis užtikrina galimybę iteratyviai tobulinti prototipinį sprendinį. Kuriamame prototipe keičiamos medžiagos ir konstrukciniai sprendimai, atsižvelgiant į reikalingus (skaitiniu modeliavimu nustatytus) kompozitinės sistemos komponenčių fizikinius parametrus.

Darbo rezultatų praktinė reikšmė

Pasiūlytai naujai adaptyvaus prototipavimo koncepcijai taikomas eksperimentiškai patikrintas baigtinių elementų modelis, kurį galima pasitelkti įvairioms kombinuotoms konstrukcijoms prototipuoti.

Pasiūlyta prototipavimo metodologija leidžia efektyviai tobulinti kompozitines konstrukcijas dėl galimybės keisti patikimą skaitinį modelį, mažinant fizinių eksperimentų poreikį, kai nėra atitinkamų projektavimo dokumentų.

Sujungus sijos komponentus standžiose atramose supaprastinamas kompozitinės sijos teorinis modelis, nes pritaikoma prielaida, kad sijos komponentai yra sukibę idealiai.

Ginamieji teiginiai

1. Pritaikius kompozitinei konstrukcijai adaptyvaus prototipavimo koncepciją ir sukūrus eksperimentiškai patikrintą skaitinį modelį, kuris apibrėžia prototipavimo etaloną, galima atitinkamai pakeisti konstrukcinį sprendimą ir taip padidinti kompozitinės konstrukcijos lenkiamąjį standį ir laikomąją galią.

2. Eksperimentiškai patikrinto modelio ir fizinių bandymų rezultatų neatitikties nustatymas taikant skaitinį modeliavimą sumažina fizinių bandymų poreikį, nes kompiuterinis modeliavimas pakeičia dalį fizinių bandymų. Sukūrus patikimą skaitinį modelį fizinių bandymų bus galima atsisakyti.
3. Eksperimentiškai patikrintas baigtinių elementų modelis yra tinkamas etalonas pasiūlytam *adaptyviam* kombinuotų konstrukcinių sistemų prototipavimui, kai nėra standartinių sprendinių.
4. Disertacijoje pritaikytas inovatyvus konstrukcinis sprendimas, fiksuoti GFRP komponentes atramose, leido patobulinti kompozitinę siją ir užtikrinti sijos komponentų sukibtį bei jų kompozitinę elgseną.

Darbo rezultatų aprobavimas

Šio tyrimo tema buvo paskelbti keturi straipsniai mokslo žurnaluose, trys iš jų – žurnaluose *Clarivate Analytics Web o*f *Science* duomenų bazėse su cituojamumo rodikliu. Autorius pristatė tris pranešimus trijose skirtingose mokslinėse konferencijose:

1. *The First Olympiad in Engineering Science*, 2023, Olimpija, Graikija. Gribniak, V. ir Garnevičiaus, M. pristatymas, tema "Developing an adaptive design concept for structural composites" gavo "Olympiad Medal" apdovanojimą (https://www.uis.no/en/about-uis/olympiad-in-engineering-science-summed-up).
2. *The 13th fib International Ph. D. Symposium in Civil Engineering*, 2020, Paryžiuje, Prancūzijoje (Geriausio straipsnio apdovanojimas).
3. *The 26th Annual International Conference on Composites / Nano Engineering* (ICCE-26), 2018, Paryžiuje, Prancūzijoje.

Disertacijos struktūra

Disertaciją sudaro įvadas ir trys pagrindiniai skyriai. Įvade aprašomas tyrimo objektas, problema, aktualumas, tikslas ir metodai, pristatomas rezultatų naujumas ir suformuluojami ginamieji teiginiai.

Pirmame skyriuje apžvelgiama literatūra apie pluoštu armuotų polimerų medžiagų gamybos procesą, medžiagų tipus, fizines savybes ir konstrukcijų projektavimo principus. Daugiausia dėmesio skiriama sukurtoms eksperimentinėms procedūroms ir modeliavimo principams bei prielaidoms. Apžvelgus literatūrą atskleista, kaip efektyviai derinti kompozitines medžiagas ir kokius atlikti bandymus su sukurtu kompozitinės sijos prototipu. Pirmas skyrius baigiamas pagrindinio šio tyrimo tikslo ir uždavinių formuluotėmis.

Antrame skyriuje pristatoma nauja kompozitinių sijų prototipavimo koncepcija, pagal kurią skaitiniu modeliu prognozuojami eksperimentinio bandymo rezultatai. Naudojant komercinį programinės įrangos paketą ATENA buvo sukurtas kompozitinės polimeriniu plaušu armuoto betono (PFRC) ir pluoštu armuoto polimero (FRP) sijos netiesinis baigtinių elementų modelis. Buvo daroma prielaida, kad tarp kompozitinės sijos komponentų sukibtis yra ideali. Ši prielaida supaprastino skaitinį modelį. Anksčiau atliktų bandymų rezultatai patvirtino gautą modeliavimo rezultatą, todėl šio modeliavimo rezultatas buvo laikomas etaloniniu (tiksliniu).

Trečiame skyriuje pateikiami eksperimentiniai tyrimai ir šių tyrimų eiga, taip pat rezultatai, kuriais patvirtinama ankstesniame skyriuje pateikta adaptyvaus prototipavimo koncepcija. Atlikti kompozitinės sijos prototipo keturių taškų lenkimo bandymai. Skaitinio modeliavimo ir pirmojo bandymų etapo rezultatų neatitiktis leido daryti prielaidą, kad sijos atramų neužtenka pakankamai GFRP profiliuočio ir dispersiškai armuoto betono plokštės sukibčiai užtikrinti. Modifikavus atraminę konstrukciją, prototipo bandymų rezultatas sutapo su modeliavimo rezultatu, tai įrodė adaptyvaus prototipavimo koncepcijos patikimumą.

Darbo pabaigoje formuluojamos bendrosios išvados ir rekomendacijos dėl tolesnių tyrimų. Po jų pateikiamas literatūros šaltinių ir autoriaus publikacijų disertacijos tema sąrašas. Disertacijoje taip pat pateikiamas su ja susijusių autoriaus publikacijų sąrašas. Disertacijos apimtis – 113 puslapių, 65 iliustracijos, 8 lentelės ir 83 moksliniai šaltiniai.

Padėka

Autorius dėkoja už Europos regioninės plėtros fondo finansinę paramą (projekto Nr. 01.2.2-LMT-K-718-03-0010), suteiktą pagal dotacijos sutartį su Lietuvos mokslo taryba.

Taip pat Autorius norėtų padėkoti VILNIUS TECH už suteiktą jaunojo mokslininko poziciją.

1. Pluoštu armuotų polimerų kompozitai statyboje

Šiame skyriuje aprašytas pluoštu armuotų polimerų (FRP) medžiagų naudojimas statyboje ir jų gamybos būdai. Dėmesys skiriamas naujiems konstrukciniams sprendiniams, atitinkamų kompozitinių medžiagų ir jų derinių nustatymui. Rasti sprendiniai pritaikyti kombinuotos kompozitinės sijos prototipui kurti pagal adaptyvaus prototipavimo koncepciją. Literatūros apžvalgoje taip pat nagrinėjami eksperimentinių bandymų ir skaitinio modeliavimo metodai bei FRP ir betono kombinuotų konstrukcijų projektavimo principai.

Projektavimo standartų trūkumas komplikuoja inovatyvių konstrukcijų kūrimą. Dėl šių priežasčių disertacijoje išplečiama adaptyvaus prototipavimo koncepcija (Rong, Zhao, Feng, & Xie, 2022). Ši koncepcija būdinga teorinėms analizėms (Rong et al., 2022) ir architektūriniam projektavimui (Xie, 2022). Tačiau, autoriaus žiniomis, ji nebuvo taikoma konstrukcinėms problemoms spręsti.

Literatūros analizė parodė, kad FRP elementai nuolat tobulinami ir taikomi įvairioms konstrukcijoms. Čekijoje, Šveicarijoje, Amerikoje, Lenkijoje, Pietų Korėjoje ir kitose šalyse statomi ir renovuojami tiltai, kurių elementai pagaminti iš FRP medžiagų; taip pat anglies pluošto lakštai, lynai ir juostos plačiai naudojamos esamoms konstrukcijoms stiprinti. FRP elementai pasižymi mažesniu svoriu nei tradicinės medžiagos (pvz., plienas ir betonas), bet yra panašaus stiprumo, todėl dažnai naudojami laikinų tiltų konstrukcijoms.

1. Rinkoje vyrauja trys FRP rūšys: stiklo, anglies ir aramido pluoštais armuoti polimerai. Egzistuoja didelis kiekis kompozitų, kurie sudaryti kombinuojant skirtingas medžiagas: stiklo, aramido, anglies pluoštą. Stiklo pluošto polimeras (GFRP) naudojamas tiltų paklotams, laikantiesiems elementams, sijoms, kolonoms, lynams,

vantiniams ir kabamiesiems tiltams projektuoti. Aramido ir anglies pluošto polimerai naudojami konstrukcijoms sustiprinti. Iš šių medžiagų taip pat gali būti gaminama armatūra konstrukciniam betonui armuoti.

2. Pultruzija yra dažniausiai taikomas aptariamųjų medžiagų gamybos būdas. Šis gamybos būdas užtikrina tikslius FRP komponentų matmenis, greitą pramoninę gamybą ir didelį pluošto kiekį matricoje (apie 75 %). Pultruzijos gamybos būdas efektyviausias, lyginant su kitais gamybos būdais (tokiais kaip rankinis liejimas, apvyniojimas pluoštu, dervos perpilamasis formavimas, įpurškiamasis formavimas).
3. Kuriami įvairūs skaitiniai modeliai su skirtingomis FRP medžiagomis ir komponentais, įskaitant sijų, santvarų, vantinių ir kabamųjų tiltų modelius, tačiau dėl FRP fizikinių savybių anizotropijos (skirtumų skirtingomis kryptimis) kyla problemų aprašant medžiagų ir jungimo (sukibimo) modelius. Sukurti tokius modelius taip pat nėra paprasta, nes ne visose baigtinių elementų (BE) programose, skirtose tradicinėms medžiagoms, minėtos savybės vertinamos.
4. Pluoštu armuotų polimerų komponentus naudoti santykinai ilgo tarpatramio konstrukcijoms (pvz., 10–15 m ilgio tiltuose) problemiška dėl pernelyg didelių deformacijų ir jautrumo dinaminėms apkrovoms. Be to, anglies pluošto panaudojimą riboja didelė kaina. Vykdant mokslinius tyrimus daug dėmesio turėtų būti skiriama pluoštu armuotų komponentų atsparumui šlyčiai ir jų sukibčiai su betonu vertinti. Trūksta žinių apie pluoštu armuotų polimerų komponentų dinamiką, nuovargį ir atsparumą ugniai. Todėl jau pastatytų tiltų bandymai rodo nepagrįstai didelį laikomosios galios rezervą, kai kurios konstrukcijos atlaiko iki 20 kartų didesnes apkrovas, nei numatyta projekte.
5. Kadangi nėra bendrai pripažintų projektavimo ir gamybos standartų, pluoštu armuotų polimerų elementai dažniau naudojami pėsčiųjų tiltams, platformoms, architektūrinėms detalėms, fasadams, vamzdynams ir cheminių medžiagų talpykloms statyti.
6. Plačiausiai pritaikytas bandymas yra keturių taškų lenkimo. Šiuo bandymu nustatoma sijos mechaninė elgsena. Fizinė sija turi būti pagaminta ir išbandyta po to, kai sukurtas BE modelis, kad būtų galima patikrinti atitiktį skaitinio modeliavimo rezultatams.

Disertacijoje atliekamu tyrimu siekiama sukurti adaptyvaus prototipavimo koncepciją, pagal kurią eksperimentiškai patikrintas skaitinis modelis apibrėžia prototipavimo etaloną. Remiantis išanalizuotomis mokslinėmis publikacijomis suformuluotos šios tyrimo gairės:

1. Kombinuota kompozitinė sijos konstrukcija yra adaptyvaus prototipavimo objektas. Šią siją sudaro pultruzijos būdu pagamintas GFRP dvitėjis profiliuotis, anglies pluošto juostelė (CFRP), skirta sijos atsparumui tempimo įtempiams padidinti ir deformacijoms apriboti, bei polimeriniu plaušu armuoto betono (PFRC) plokštė, skirta gniuždymo įtempiams atlaikyti, su pagerintu plastiškumu, atsparumu pleišėjimui, taip pat užtikrinanti bendrą sistemos standumą. Šiame darbe FRP komponentai įtvirtinami santykinai standžiose atramose; plokštės sujungimas su GFRP profiliuočiu taip pat padidins konstrukcijos atsparumą šlyčiai.
2. Medžiagų modeliai (parametrai), panaudoti sukurtame BE modelyje, buvo nustatyti eksperimentiškai. Literatūroje rastos modeliavimo prielaidos dėl idealios sijos FRP ir

PFRC komponentų sukibties ir tiesinės-elastinės medžiagų savybės buvo pritaikytos skaitiniame modelyje.

3. Kompozitinių konstrukcijų iš betono ir FRP komponentų projektavimas reikalauja sisteminio požiūrio. Efektyvią kompozitinę konstrukciją galima sukurti tik tada, kai ištiriama kombinuojamų elementų sandara, nustatomos jų mechaninės ir sukibties savybės. Esami projektavimo metodai yra pernelyg konservatyvūs dėl patikimų medžiagų modelių ir projektavimo standartų trūkumo. Šių projektavimo metodų saugos koeficientai gali nepagrįstai (iki 20 kartų) padidinti konstrukcinių medžiagų poreikį. Dėl šių priežasčių šiame tyrime sukurti skaitiniai modeliai ir prototipai nusako pasiūlyto adaptyvaus prototipavimo metodo efektyvumą.
4. Pėsčiųjų tiltui skirta kompozitinė sija buvo sukurta, kad būtų galima išbandyti pasiūlytą adaptyvaus prototipavimo koncepciją. Ši sija buvo palyginta su eksperimentiškai patikrintu baigtinių elementų modeliu. Jei reikia, kompozitinė sija modifikuojama, kad jos elgsena sutaptų su modeliavime gautu rezultatu.

2. Adaptyvus kompozitinių konstrukcinių sistemų prototipavimas

Šiame skyriuje pristatoma adaptyvaus prototipavimo koncepcija. Pateikiama pavyzdinė kompozitinės sijos prototipavimo eiga (1S pav.). Šį konstrukcinį elementą sudaro polimeriniu plaušu armuoto betono (PFRC) plokštė, stiklo pluoštu armuoto polimero (GFRP) profiliuotis bei anglies pluoštu armuoto polimero (CFRP) juostelė.

Pirmoje skyriaus dalyje aprašoma adaptyvaus prototipavimo koncepcija. Nagrinėjamos sistemos taikomos tiltų konstrukcijose, nes plieno pakeitimas GFRP komponentais išsprendžia korozijos problemą, tačiau kompozitinės sistemos veikimą apsunkina stiklo pluošto profiliuočio sukibties su betonu neapibrėžtumas (Mendes et al., 2011; Zhang et al., 2021).

Suprojektuotą siją sudaro polimeriniu plaušu armuoto betono (PFRC) plokštė, atlaikanti gniuždymą ir įtvirtinanti stiklo pluoštu armuotą profiliuotį (GFRP, 120×60/6/6 mm I profiliuotis, gamintojas FIBERLINE, Danija) atramose. Atlikus preliminarų modeliavimą (Jaruševičiūtė, 2021) nustatyta atraminio bloko geometrija. Be to, labiausiai įtemptą stiklo pluoštu armuoto profiliuočio paviršių sutvirtina anglies pluoštu armuoto polimero (CFRP, 10 × 1,4 mm, gamintojas „S&P C-Laminate“, Jungtinė Karalystė) juostelė. Šiam konstrukciniam elementui komponuoti taikoma vienajuosčių tiltų koncepcija (Juozapaitis et al., 2021; Gribniak et al., 2021). Plokštė užtikrina patikimą jungtį su GFRP profiliuočiu. Baigtinių elementų modelyje pluoštu armuotų polimerų komponentų mechanines charakteristikas nusako išskirstytojo armavimo (angl. *smeared reinforcement*) metodas (Gribniak et al., 2021), fiziškai netiesinis medžiagos modelis (Garnevičius et al., 2020) apibrėžia plaušu armuoto betono elgseną, o idealios sukibties modelis pritaikytas kontaktui aprašyti. Kai buvo parinkta kompozitinės sijos geometrija, ji buvo sumodeliuota komercinės programinės įrangos paketu ATENA.

Kaip pavaizduota S2.1 pav., sąveika tarp konceptualaus sprendimo („1“) ir patikrinto BE modelio („2“) sukuria preliminarų sprendimą pagal nustatytus prototipavimo kriterijus (laikomoji galia ir lenkiamasis standis). Pagal sumodeliuotą rezultatą nustatomas prototipavimo etalonas tolesniems fiziniams bandymams („3“), kuriais patikrinamas koncepcijos „1“ efektyvumas (t. y. „patikrinimas 1“). Nepasiekęs nurodyto rezultato, inžinierius modifikuoja prototipinę koncepciją („4“). Iteracinis koregavimas tęsiamas tol, kol pasiekiama priimtina fizikinių bandymų ir skaitinio modeliavimo rezultatų sutaptis (t. y. „patikrinimas 2“).

Pažangios modeliavimo procedūros gali pakeisti ekspertų nuomone pagrįstą optimizavimo procesą, todėl siūloma koncepcija yra veiksminga kompiuterizuoto prototipavimo srityje. Be to, BE rezultatai gali suteikti daug informacijos, naudingos siekiant tobulinti medžiagų parametrus ir konstrukcinius sprendinius. Ši analizė susideda iš trijų dalių: eksperimentinis medžiagų modelių ir modeliavimo procedūrų patikrinimas, etaloninio kompozitinės sistemos skaitinio modelio sukūrimas ir fizinio prototipo sprendinio bei gamybos technologijos pritaikymas BE modeliui. Eksperimentinė pirmo etapo medžiagų modelių patikra garantuoja etaloninio skaitinio modelio patikimumą. Antrame skyriuje daroma prielaida, kad skaitinis modelis yra eksperimentiškai patikrintas siekiant supaprastinti disertacijos struktūrą. Trečiame skyriuje pateiktas šios prielaidos įrodymas.

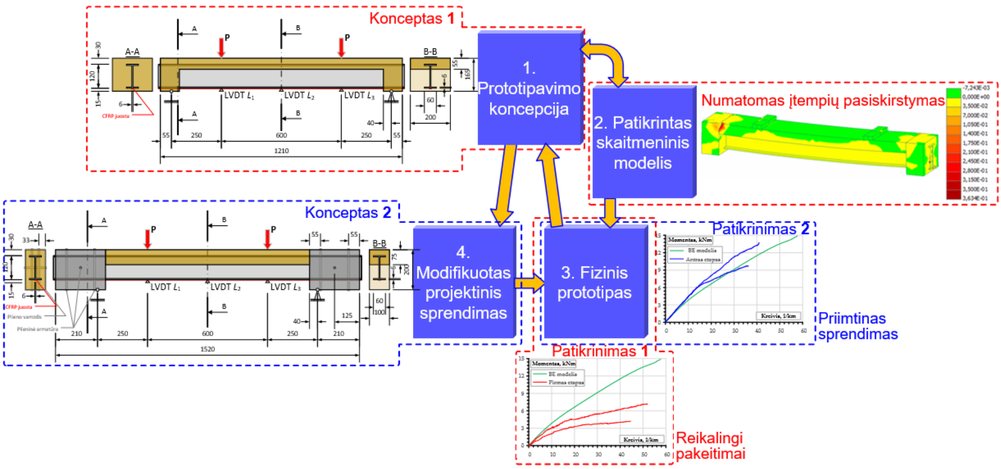

S2.1 pav. Adaptyvaus prototipavimo koncepcija

Antroje skyriaus dalyje aprašoma BE modelio kūrimo eiga ir atraminių blokų modifikavimo eiga. Sumodeliavus siją programinės įrangos paketu ATENA buvo nustatytos šios sijos deformacijos ir jos laikomoji galia. Sumodeliuotas keturių taškų lenkimo bandymas. Ankstesniuose tyrimuose (Gribniak et al., 2021a, Gribniak et al., 2021b; Garnevičius et al., 2020) patikrinti medžiagų modeliai nusako polimero plaušu armuoto betono ir FRP komponentų mechaninę elgseną modeliavimo programoje. Iš tetraedrinio tinklelio sudarytas BE modelis pavaizduotas S2.2 paveiksle. Idealiai tamprios plieninės plokštelės apsaugo betoną apkrovos pridėjimo TAŠKUOSE (S2.2 pav., a). Šių plokštelių BE tinklelio elementų dydis yra 15 mm. Monolitinių betoninių atramų (S2.2 pav., b) tinklelio elemento dydis – 30 mm; CFRP juostos ir GFRP profiliuočio baigtinių elementų dydis – 7,5 mm. Šio tinklelio tankumo užteko skaičiavimų tikslumui užtikrinti. Iš modelio paimti rezultatai – vertikalieji poslinkiai tarpatramio viduryje ir poslinkiai GFRP profiliuočio apačioje po apkrovos pridėjimo taškais.

Skaitiniame modelyje panaudotas netiesinis cementinės medžiagos, turinčios 55 MPa gniuždomąjį stiprį, modelis (Garnevičius et al., 2020), pateiktas 2.2.2 skirsnyje (disertacijos dalyje anglų kalba). Šis modelis nustato plaušu armuoto betono plokštės deformatyvumo savybes ir suirimo mechanizmą. CFRP (10 × 1,4 mm) juostelės medžiagos elgsena aprašyta elastiniu-plastiniu medžiagos modeliu (tamprumo modulis = 170 GPa ir tempiamasis stipris = 2,8 GPa) (Gribniak et al., 2021). Gavus rezultatus iš BE modeliavimo metu parinktų stebėjimo taškų, buvo sudaryta momentų ir kreivių diagrama. Momentų ir kreivių priklausomybė puikiai tinka kompozitinių sijų deformacijoms nusakyti (Gribniak, 2009; Gribniak et al., 2021, 2021). Kreivis buvo apskaičiuotas grynojo lenkimo zonoje pagal įlinkius, padarius prielaidą, kad sijos deformacijos yra apskritimo formos:

$$\kappa = \frac{8 \cdot \delta}{l_b^2 + 4 \cdot \delta^2}, \delta = L_2 - (L_1 + L_3)/2, \tag{S2.1}$$

čia l_b grynojo lenkimo zonos ilgis (= 600 mm); L_1, L_2 ir L_3 yra stebėjimo taško rodikliai. Čia δ stebėjimo taškų rodiklių skirtumas.

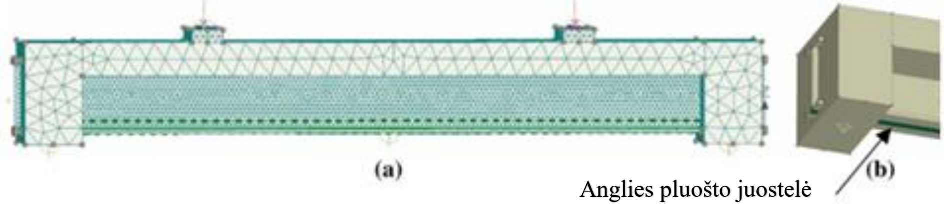

S2.2 pav. Kompozitinės sijos baigtinių elementų modelis: a) BE diskretizacija; b) atramos vaizdas

Apskaičiavus kreivį, buvo sudaryta momentų ir kreivių diagrama. Šis grafikas bus lyginamas su fizinių bandymų rezultatais ir naudojamas kaip etalonas. Fiziniais bandymais, aprašytais 3.3 ir 3.4 poskyriuose (disertacijos dalyje anglų kalba), patikrinama modelio rezultatų atitiktis (S2.3 pav.).

Gavus pirmojo bandymų etapo rezultatus buvo dar kartą atliktas modeliavimas esant sumažintam GFRP profiliuočio sukibimo su betonu stipriui atraminiuose mazguose, po šio sumažinimo, modeliavimo ir bandymo rezultatai sutapo. Taip buvo išvengta papildomų eksperimentinių bandymų ir buvo nuspręsta keisti prototipavimo sprendimą (stiprinti atraminius mazgus). Todėl buvo pakeista sijos schema ir buvo pagamintos antros grupės sijos, kurios vėliau buvo išbandytos. Antrasis bandymų etapas aprašytas 3.4 poskyryje (disertacijos dalyje anglų kalba). Mėlynos linijos S2.3 pav. rodo antrojo etapo sijų deformacijas. Bandymų rezultatai sutampa su BE modelio rezultatu, kuriame padaryta prielaida, kad visos kombinuotos sijos kompozitinės dalys yra idealiai sujungtos. Antrojo etapo kompozitinių sijų laikomoji galia padidėjo 107,5%, lyginant su pirmojo etapo sijomis. Antrojo etapo sijų GFRP profiliuočio ir PFRC plokštės sukibtis nebuvo papildomai gerinama, naudojant profiliuočio perforaciją ar kitas priemones.

Trečioje skyriaus dalyje sukurta prototipų prototipavimo koncepcija (S2.1 pav.) išplečiama iki konstrukcinio dydžio kompozitinės sijos. Pasirengimo ir bandymų detalės pateikiamos 3.5 poskyryje (disertacijos dalyje anglų kalba). Preliminari 3 m ilgio sija pateikta S2.4 paveiksle, kuriame atsižvelgta į modifikuotą antrojo etapo sijų atraminių jungčių konstrukciją. Kaip matyti iš S2.4 pav., stiklo pluošto profiliuočio aukštis nuo 120 mm padidėjo iki 200 mm (dvitėjis profiliuotis, FIBERLINE, Danija), palyginti su antrojo etapo prototipais. Dėl šio pasikeitimo padidėjo ir betoninė dalis bei atramų konstrukcija. Išliko tokie patys anglies pluošto armuotų juostelių matmenys (10 mm × 1,4 mm, S&P C-LAMINATE, Jungtinė Karalystė) ir betono mišinio proporcijos. Modeliavimui naudojamas programinės įrangos paketas ATENA ir tie patys medžiagų modeliai, kurie buvo naudojami preliminarių bandymų metu (2.3 poskyris) (disertacijos dalyje anglų kalba). Apkrovų dydis padidėdavo po 0,5 kN po kiekvieno žingsnio.

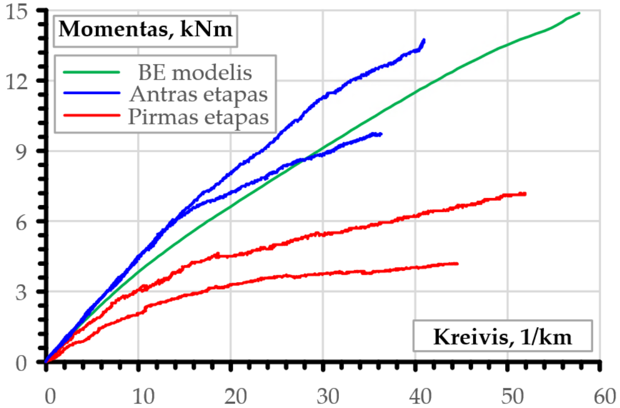

S2.3 pav. Skaitinio modelio ir prototipinių sijų (abiejų etapų) eksperimentų momentų ir kreivių grafikų palyginimas

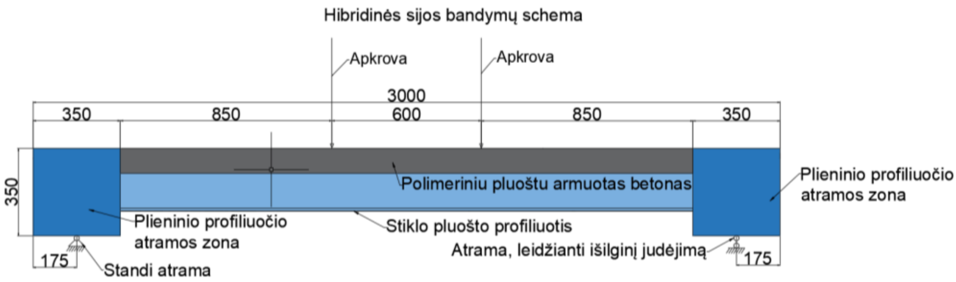

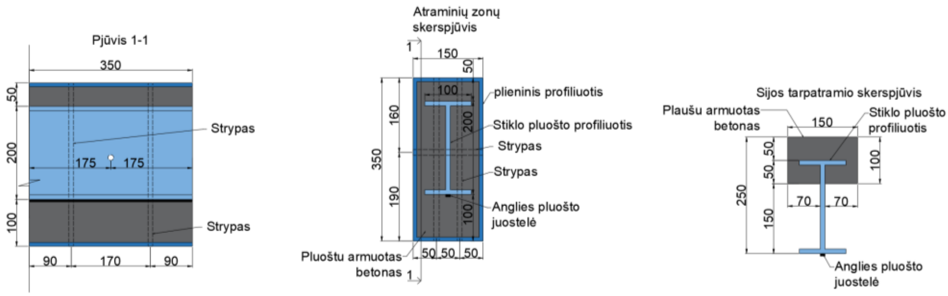

S2.4 pav. Kompozitinės 3 m sijos schema ir atramos bei tarpatramio skerspjūviai (matmenys mm)

Šiame skyriuje sukurta adaptyvaus prototipavimo koncepcija, pagal kurią skaitiniu modeliavimu nustatytas rezultatas apibrėžia prototipavimo tikslą. Kadangi šios pažangios kompozitinės medžiagos (FRP) neturi joms pritaikytų projektavimo standartų, šiame tyrime BE modeliavimu gautas rezultatas laikomas siekiamu ir nurodo, kokia fizinės sijos mechaninė elgsena priimtina. Eksperimentiniais bandymais patikrintos BE modelio komponentų medžiagų savybės, t. y. stiklo pluoštu armuoto polimerinio profiliuočio (GFRP), polimeriniu plaušu armuotos betoninės plokštės (PFRC) ir polimerinio plaušo sukibimo su betonu. Kombinuotos GFRP ir PFRC kompozitinės sijos prototipas pasirinktas adaptyvaus prototipavimo koncepcijos taikymui iliustruoti. Siekiant pagerinti nagrinėjamos sijos eksploatacines savybes, GFRP profiliuotis ir PFRC plokštė fiksuojama atramose. Gauti rezultatai leido suformuluoti šias išvadas:

1. Patobulinto sijos prototipo atramų modifikavimas padvigubino lenkiamąjį standį ir laikomąją galią, palyginti su pirmo etapo išbandyta sija, turinčią silpnas atramas. Prototipų su modifikuotomis atramomis bandymų rezultatai pasiekė etaloninio skaitinio modeliavimo rezultatą (standį ir laikomąją galią), taip pat sumažino poreikį atlikti daugiau fizinių bandymų. Todėl eksperimentiškai patikrintas BE modelis gali būti laikomas tinkamu etalonu adaptyvioms kombinuotoms konstrukcinėms sistemoms prototipuoti, atramų modifikavimas padvigubino sijos lenkiamąjį standį ir laikomąją galią, lyginant su sija su silpnomis atramomis ir be papildomo GFRP sukibties gerinimo.
2. Kompozitinės sijos pluoštu armuoti polimeriniai komponentai įtvirtinami standžiose atramose. Taikant šį metodą supaprastinamas skaitinis sijos modelis. Idealios sukibties prielaida leidžia išspręsti literatūroje aprašytas modeliavimo problemas. Sukurta adaptyvaus prototipavimo koncepcija kartu su BE modeliavimo metodu yra tinkama tyrime nagrinėjamoms kombinuotoms sistemoms prototipuoti. Norint patikrinti prielaidos dėl idealios sukibties tarp skaitinio modelio komponentų priimtinumą, buvo matuojamas išilginių deformacijų pasiskirstymas sijose eksperimentinių bandymų metu. Šių bandymų metu nebuvo rasta jokio pastebimo praslydimo. Šis rezultatas patvirtina idealios sukibties prielaidos tinkamumą skaitiniam modeliui.

3. Adaptyvaus prototipavimo koncepcija gali būti pritaikoma, kai eksperimentiškai patikrintas skaitinis modelis apibūdina pageidaujamą FRP-betoninės sijos konstrukcijos rezultatą. Ši koncepcija gali apimti pažangius optimizavimo algoritmus, kurie gali padvigubinti konstrukcijos lenkiamąjį standį ir laikomąją galią. Nepaisant to, būtina atlikti papildomus bandymus, siekiant užtikrinti rezultatų patikimumą ir optimizuoti atraminių blokų geometriją.
4. Kompozitinės sijos skaitinio modeliavimo rezultatai palyginti su plieno ir betono sijos ir gelžbetoninės sijos teoriniais modeliais. Nustatyta, kad kompozitinė GFRP ir PFRC sija buvo 25,8% lengvesnė už gelžbetoninę siją. Plieno ir betono sija buvo tokio paties svorio ir standumo kaip ir siūloma GFRP bei PFRC kombinuota sija, bet jos mechaninis atsparumas pasiekė tik pusę kombinuotos sijos laikomosios galios.

3. Adaptyvaus prototipavimo koncepcijos eksperimentinė programa

Šiame skyriuje aprašyta eksperimentinė programa, įvykdyta siekiant nustatyti GFRP ir CFRP medžiagų parametrus, kompozitinių sijų prototipų fiziniai bandymai ir konstrukcinio dydžio sijų bandymai. Šiame skyriuje taip pat aptariamas išilginių deformacijų pasiskirstymas kompozitinėse sijose, atskleidžiantis sukombinuotų skerspjūvio komponentų suderinamumą. Kiekvienam kompozitinės sijos bandymų etapui buvo pagamintos dvi sijos. Iš viso buvo pagamintos šešios sijos.

Šiame skyriuje pateikti stiklo pluošto profiliuotį įtvirtinančių betoninių atramų sugniuždymo rezultatai, gauti atlikus pirmąjį bandymų etapą. Tipinis suirusios sijos atramos vaizdas pateiktas S3.1 pav. Toks rezultatas yra nepakankamo pluoštu armuotų polimerų medžiagų atsparumo skersinėms apkrovoms pasekmė. Tačiau BE modelis negalėjo atspindėti šio irties mechanizmo, nes pluoštu armuotų medžiagų skersinio gniuždymo modeliavimo galimybės yra ribotos.

Atlikus BE modeliavimą su konstrukcinio dydžio sijos modeliu, buvo atlikti fiziniai bandymai. Sijos bandinys buvo apkrautas 10 MN servohidrauliniu apkrovos aparatu, 0,4 kN per sekundę apkrovos greičiu, kol įvyko suirimas, atsiradęs dėl gniuždymo įtempių betono grynojo lenkimo zonos viduryje (S3.2 pav.).

Šiame skyriuje aprašomi bandymai, atlikti siekiant patikrinti 2 skyriuje sukurtus BE modelius ir adaptyvios konstrukcijos koncepciją. Bandymų rezultatai ir lyginamoji analizė leidžia daryti šias išvadas:

1. Stiklo pluoštu armuotam profiliuočiui patikrinti buvo atlikti kaitinimo bandymai, siekiant nustatyti pluošto procentinę tūrio dalį profiliuotyje, o rezultatams patikrinti atliktas lenkimo bandymas. Pluošto tūrio dalis, reikalinga išskirstytojo armavimo modeliavimui, buvo nustatyta 63,4%.
2. Siekiant patikrinti pluoštu armuoto betono medžiagos modelio patikimumą, buvo atliktas praspaudimo bandymas su 2 plokštėmis iš šio betono. Plokščių laikomoji galia buvo 9,5 kN ir 10,5 kN, ji atitiko 2.2.2 skirsnyje (disertacijos

dalyje anglų kalba) aptartą BE modeliavimo rezultatą, o paklaida neviršijo 10%. Supleišėjimo rezultatai (modelio ir bandymo) taip pat buvo labai panašūs.

3. Atskirų plaušų ištraukimo bandymai patvirtino betono ir polimerinės medžiagos sukibties modelį. Sukibties parametrai buvo gauti modeliuojant bandymus ATENA programinės įrangos paketu. Palyginus ištraukimo bandymų BE modeliavimą su atliktais eksperimentais, gauta, kad deformacijų sutapimo paklaida neviršijo 4%. Polimerinis plaušas leido plyšiams užsiverti, kai buvo nuimta apkrova. Tinkamo plaušo ir tinkamos betono sudėties parinkimas yra svarbus norint užtikrinti reikiamą betono plastiškumą, atsparumą pleišėjimui ir bendrą kompozitinės sijos sistemos standumą. Sintetinio plaušo panaudojimas leido sugretinti PFRC ir GFRP profiliuočių deformacines savybes. Kitaip sakant, PFRC plokštė gali atgauti pradinę geometrinę formą, kuri buvo prieš ją apkraunant, kartu užveriami visi susidarę plyšiai.

S3.1 pav. Tipinė pirmojo etapo sijos atraminio bloko irtis

S3.2 pav. Kompozitinės 3 m sijos irtis dėl betono sugniuždymo grynojo lenkimo zonoje

4. Atlikus preliminarius kompozitinių sijų bandymus (1 ir 2 bandymų etapų) buvo patikrintos sukurto adaptyvios konstrukcijos koncepcijos pritaikymo galimybės. Buvo išspręsta atramų problema, kuri kildavo dėl mažo pultruzijos būdu pagamintų FRP profiliuočių atsparumo skersinėms apkrovoms.

5. Kai buvo palyginti pirmos bandymų serijos ir baigtinių elementų etaloninio modelio rezultatai, pasidarė aišku, jog reikia modifikuoti siją (atramų modifikavimas), kad būtų galima pagerinti jos mechaninę elgseną. Sustiprinus atramas dvigubai padidėjo antro etapo kompozitinių sijų lenkiamasis standis ir laikomoji galia (padidėjo 107,5%), lyginant su pirmojo etapo sijomis, turinčiomis tipines silpnas atramas (pirma serija). Nebuvo taikytas joks papildomas FRP sukibties su betonu gerinimo būdas. Vis dėlto formaliam sprendimui reikia papildomų bandymų, kad būtų užtikrintas rezultatų patikimumas ir optimizuota atraminių blokų geometrija. Tačiau pasiektas akivaizdžiai geresnis kompozitinės sijos rezultatas (laikomoji galia ir lenkiamasis standis) įrodo siūlomos prototipavimo koncepcijos veiksmingumą.

Bendrosios išvados

Šiuo tyrimu buvo siekiama sukurti adaptyvaus prototipavimo koncepciją, pagal kurią skaitiniu modeliavimu nustatytas rezultatas apibrėžia prototipavimo etaloną. Iteracinis konstrukcinio sprendinio modifikavimas, skaitiniu būdu nustatant eksperimentiškai patikrinto modelio ir fizinių bandymų rezultatų nesutaptis, skatina fizinio prototipo (prototipinio sprendinio) priartėjimą prie etaloninio skaitinio modeliavimo rezultato. Kompozitinės sijos prototipas pasirinktas siekiant iliustruoti adaptyvaus prototipavimo koncepciją. Nagrinėjama sija sudaryta iš pluoštu armuoto polimero (GFRP) dvitėjo profiliuočio, polimeriniu plaušu armuoto betono (PFRC) plokštės ir anglies pluoštu armuoto polimero (CFRP) juostos, skirtos konstrukcijos tempiamajai zonai sustiprinti. Siekiant pagerinti kompozitinės sijos eksploatacines savybes, kompozitinės konstrukcijos PFRC plokštė ir GFRP profiliuotis sujungiami standžiose atramose. Sukurtas baigtinių elementų (BE) modelis, kuris buvo nustatytas kaip prototipavimo etalonas, buvo patikrintas keliais eksperimentinių bandymų etapais. Tyrimų rezultatai leido padaryti šias pagrindines išvadas:

1. Kompozitinių konstrukcijų iš betono ir FRP komponentų prototipavimas reikalauja sisteminio požiūrio: efektyvią kompozitinę konstrukciją galima sukurti tik ištyrus kombinuojamų elementų sandarą ir nustačius jų mechanines bei sukibties savybes. FRP komponentų taikymas didelio tarpatramio konstrukcijoms (pvz., 10–15 m ilgio tiltams) gali būti problemiškas dėl didelių deformacijų ir jautrumo dinaminėms apkrovoms. Taip pat FRP komponentai nėra atsparūs šlyčiai, o jų sukibties su betonu stipris gali būti nepakankamas bendrai kompozito elgsenai užtikrinti. Esami projektavimo metodai yra pernelyg konservatyvūs, o jų saugos koeficientai gali nepagrįstai (iki 18 kartų rastoje literatūroje ir straipsniuose) padidinti konstrukcinių medžiagų poreikį. Pagal pažangių kompozitinių medžiagų skaitinio modeliavimo rezultatą buvo nustatyta etaloninė mechaninė elgsena, kai nėra kitų projektavimo gairių ir standartų.
2. Pateiktas adaptyvaus prototipavimo pavyzdys parodė siūlomos koncepcijos veiksmingumą didinant prototipinių kompozitinių elementų lenkiamąjį standį ir gerinant komponentų sukibties savybes. Skirtumas tarp alternatyvių sprendinių

akivaizdus – atramų modifikavimas padvigubino kompozitinės sijos lenkiamąjį standį ir laikomąją galią, palyginti su pirmo etapo sija, turinčia silpnas atramas. Pažymėtina, kad šis rezultatas pasiektas netaikant jokio papildomo GFRP profiliuočio ir PFRC plokštės sukibties gerinimo būdo.

3. Įtvirtinus FRP komponentus standžiose atramose, supaprastinamas skaitinis modelis – idealios sukibties prielaida (sujungus GFRP ir PFRC) padeda išspręsti literatūroje aprašytas modeliavimo problemas. Taip pat šio sprendinio pritaikymas išsprendžia FRP atsparumo šlyčiai problemą.
4. Kompozitinei konstrukcijai pritaikius adaptyvaus prototipavimo koncepciją ir sukūrus eksperimentiškai patikrintą skaitinį modelį, kuris apibrėžia prototipavimo etaloną, konstrukcijai galima taikyti pažangius optimizavimo algoritmus, tačiau, norint užtikrinti rezultatų patikimumą ir optimizuoti konstrukcijos geometriją, būtina atlikti papildomus bandymus.
5. Palyginus gautus kuriamos sijos prototipo eksperimentinių bandymų rezultatus su BE modeliavimo rezultatais gautas laikomosios galios ir deformacijų nesutapimas. Dar kartą atliktas modeliavimas su sumažintu GFRP profiliuočio sukibties stipriu su betonu atraminiuose mazguose ir modeliavimo bei bandymo rezultatai sutapo. Taip buvo nustatytas projektinio sprendinio trūkumas ir išvengta papildomų eksperimentinių bandymų. Atitinkamai nuspręsta keisti prototipavimo sprendimą (stiprinti atraminius mazgus). Kai ši problema buvo išspręsta, FRP ir PFRC kompozitinė sija pasiekė etaloninio BE modelio rezultatą, modifikavus atramas. Kai nėra jokių standartinių projektavimo metodų, sukurtas BE modelis yra tinkamas etalonas kurti efektyvias kompozitines konstrukcijas, kuriose naudojamos pažangios medžiagos.

Mantas GARNEVIČIUS

ADAPTIVE DEVELOPMENT OF A LIGHTWEIGHT COMPOSITE PEDESTRIAN BRIDGE PROTOTYPE

Doctoral Dissertation

Technological Sciences,
Civil Engineering (T 002)

LENGVOS KOMPOZITINIO PĖSČIŲJŲ TILTO SIJOS PROTOTIPO ADAPTYVUSIS KŪRIMAS

Daktaro disertacija

Technologijos mokslai,
statybos inžinerija (T 002)

Lietuvių kalbos redaktorė Dalia Markevičiūtė
Anglų kalbos redaktorė Jūratė Griškėnaitė

2023 12 14. 10 sp. l. Tiražas 20 egz.
Leidinio el. versija *https://doi.org/10.20334/2023-051-M*
Vilniaus Gedimino technikos universitetas
Saulėtekio al. 11, 10223 Vilnius
Spausdino UAB „Ciklonas“,
Žirmūnų g. 68, 09124 Vilnius